

University of Louisville

ThinkIR: The University of Louisville's Institutional Repository

Electronic Theses and Dissertations

12-2015

Functional characterization of *Aggregatibacter actinomycetemcomitans* QSEBC : a bacterial adrenergic receptor and global regulator of virulence.

Whitney Weigel

Follow this and additional works at: <https://ir.library.louisville.edu/etd>



Part of the [Bacteriology Commons](#)

Recommended Citation

Weigel, Whitney, "Functional characterization of *Aggregatibacter actinomycetemcomitans* QSEBC : a bacterial adrenergic receptor and global regulator of virulence." (2015). *Electronic Theses and Dissertations*. Paper 2296.
<https://doi.org/10.18297/etd/2296>

This Doctoral Dissertation is brought to you for free and open access by ThinkIR: The University of Louisville's Institutional Repository. It has been accepted for inclusion in Electronic Theses and Dissertations by an authorized administrator of ThinkIR: The University of Louisville's Institutional Repository. This title appears here courtesy of the author, who has retained all other copyrights. For more information, please contact thinkir@louisville.edu.

FUNCTIONAL CHARACTERIZATION OF *AGGREGATIBACTER ACTINOMYCETEMCOMITANS* QSEBC: A
BACTERIAL ADRENERGIC RECEPTOR AND GLOBAL REGULATOR OF VIRULENCE

Whitney Weigel

A Dissertation Submitted to the Faculty of the School of Medicine of the University of
Louisville in Partial Fulfillment of the Requirement for the Degree of

Doctor of Philosophy

In Microbiology & Immunology

Department of Microbiology and Immunology

University of Louisville

Louisville, Kentucky

December 2015

FUNCTIONAL CHARACTERIZATION OF *AGGREGATIBACTER ACTINOMYCETEMCOMITANS* QSEBC: A
BACTERIAL ADRENERGIC RECEPTOR AND GLOBAL REGULATOR OF VIRULENCE

By

Whitney Weigel

A Dissertation approved on

October 29, 2015

by the following Dissertation Committee:

Donald Demuth (Dissertation Director) _____

Pascal Alard (Co-mentor) _____

David Scott _____

James Graham _____

Matthew Lawrenz _____

ACKNOWLEDGEMENTS

There are so many people who made this possible without which I would not be in the position I am today, and for all these people I am grateful. First and foremost, I want to thank Dr. Don Demuth for all of his support, kindness and understanding. I can't imagine having had as wonderful an experience nor learning as much as I have under a different mentor. I have always appreciated your patience and openness in helping students and really look up to your abilities as a scientist and mentor. Whenever I think of how I can try to be a better scientist and writer, I try to think of what you would do.

I'd also like to thank all my committee: Dr. Pascale Alard, Dr. James Graham, Dr. David Scott and Dr. Matt Lawrenz. Thank you Dr. Alard for being my co-mentor, giving me an appreciation for immunology, and for the experience of working briefly in your laboratory. Dr. Graham, thank you for the advice on working with RNA, especially, but for other technical issues as well. Thank you Dr. Scott for teaching me to be more detailed in my work, for looking out for me and also for all the times hanging out at the bar. Dr. Lawrenz, I wish I would have had time to work with you more particularly on the luciferase experiments I wanted to do. Thank you also for getting me in touch with Dr. Guo and Dr. Dersch. I have enjoyed my conversations with all of you on both a professional and personal level.

Besides Dr. Demuth, the two people who had the greatest impact in shaping me as a scientist are Drs Ascension Torres-Escobar and Maria Delores Juarez-Rodriguez. You were always so patient and helpful to me, and I hope one day to have even a fraction of your talent, precision and dedication. I'd also like to thank Liz Novak who was my student mentor when I started the Ph.D. program in Dr. Demuth's lab. Thank you for being so patient. Even though you were always so busy, you took the time to help me. Thank you also to all the members of lab, both former

and current. Particularly, thank you to Blair Schneider who was always willing to help me, answer my questions or even just talk and hang out. Thank you also to Julie Tan. You always work so hard on your own project, but at the same time you make sure all of our stuff is ordered and the lab runs smoothly. Taylor Johnston, thank you for being my first student to train and for having patience with me while I try to figure out this whole mentor thing. My experience in lab would have been so different without all of you.

To the Microbiology and Immunology department, I'd like to thank you for taking a risk on a student with very little science background and admitting into the program and for making this department an amazing one. To the Oral Immunology and Infectious Diseases department, I don't think any other department is as close knit and friendly as this one. Thank you to every one of the PI's, the lab members, and the staff for being so friendly and also encouraging each other to be better scientists. Thank you especially to Barbara Potempa for always looking out for me. You were like my mom at work and always made my day.

To the former members of the department, Jeremy Camp, Iris Zeller and Justin Hutcherson, thank you for helping me to be a better scientist, listening to my rants, and being really good friends. I miss you all.

I probably would not be here today if it wasn't for you Dr. Quin Chipley. You are true professional and great at what you do. Thank you for just listening. I will miss you.

On a personal note, I'd like to thank my mother for inspiring and showing me that a woman can be independent and smart. Thank you also to all my friends and family. I'd also like to thank my partner, Kwame Hagan, who has stood by me and supported me through very trying times while I finish this. Your love and patience has given me the strength to do something I didn't know I was capable of doing.

Lastly, to all the groups we have collaborated with: the UofL sequencing core, the

microarray core, the metabolomics core, and Dr. Guo, thank you for sharing your expertise and skills to make these studies possible.

Thank you everyone, listed and unlisted who supported me. I wouldn't be here today without you.

-Whitney

ABSTRACT

FUNCTIONAL CHARACTERIZATION OF *AGGREGATIBACTER ACTINOMYCETEMCOMITANS* QSEBC: A BACTERIAL ADRENERGIC RECEPTOR AND GLOBAL REGULATOR OF VIRULENCE

Whitney Weigel

October 29, 2015

In order for a pathogen to successfully colonize the host, it must be able to acquire essential nutrients and regulate gene expression to respond to environmental fluctuations. One mechanism bacteria have evolved in order to detect these fluctuations and respond is the two component signal transduction systems (TCS). *Aggregatibacter actinomycetemcomitans*, a dental commensal associated with localized aggressive periodontitis, contains a TCS designated QseBC that was previously shown to regulate expression of several iron acquisition genes, biofilm formation and virulence, but the activating signal was unknown [1]. QseBC is a conserved TCS in the *Enterobacteriaceae* and *Pasteurellaceae*, but the activating signal for QseC varies for each species [125]. The QseC in *Escherichia coli* responds to catecholamines whereas the QseC homolog (FirS) in *Haemophilus influenzae* responds to ferrous iron. Here we show that the activating signal for the *A. actinomycetemcomitans* QseC is a combination of iron and catecholamines (CAT-Fe). The sensing of the CAT-Fe complex leads to a significant stimulation of biofilm and planktonic growth, as well as induction of genes involved in anaerobic metabolism, electron transport and oxidative stress while down-regulating expression of genes involved in iron acquisition and fatty acid and LPS biosynthesis. Using a combination of RNA analysis and metabolomics, we identified an increased flux through the TCA cycle to pyruvate and then to anaerobic respiration and metabolism with exposure to CAT-Fe. Cells exposed to Cat-Fe also expressed higher levels of catalase and were more resistant than untreated cells to oxidative

stress.

Finally, QseB also appears to play a role in regulating the general stress response in *A. actinomycetemcomitans* since a $\Delta qseB$ mutant exhibits increased transcription of several stress response genes, including the Lon protease. Ectopic expression of *lon* resulted in an increase in transcription of *ygiW-qseBC*. Lon is involved in activating type II toxin/anti-toxin (TA) systems, one of which (D11S_2133-2134) was shown to be highly up-regulated during iron starvation. Further, it was found that ectopic expression of the putative anti-toxin D11S_2134 resulted in a significant increase in transcription of *qseBC*. Based on this data, it is likely that D11S_2133-2134 regulates expression of *qseBC* allowing QseBC and D11S_2133-2134 to tightly control iron acquisition and regulate adaptation to the host.

TABLE OF CONTENTS

Acknowledgements	iii
Abstract	vi
List of Figures	xi
List of Tables	xii
Chapter One: Introduction	
Periodontal Diseases.....	2
Biofilms.....	5
<i>A.actinomycetemcomitans</i>	6
Two-Component Systems.....	8
QseBC.....	9
Microbial Endocrinology.....	11
Toxin/Anti-toxin Systems.....	14
Significance.....	16
Chapter Two: Materials and Methods	
Bacterial Strains and Culture Conditions.....	18
Growth Kinetics.....	19
Construction of TA System and Lon Ectopic Expression Plasmids.....	22
B-galactosidase Assay.....	26
Formate Assay.....	27
Oxidative Stress Assay.....	27
RNA Isolation.....	27
Microarray.....	32

cDNA Synthesis and qRT-PCR.....	33
cDNA RACE.....	34
Biofilms.....	34
Metabolomics.....	35
Catalase Assay.....	36
Protein Gels.....	37
Construction of TonB Dependent Receptor Mutant.....	37
Construction of TonB Dependent Receptor Complement.....	38
Statistics.....	39
Chapter Three: QseBC is Activated by Catecholamine Stress Hormones and Iron	
Introduction.....	40
Results	41
Discussion.....	54
Chapter Four: QseBC is a Global Regulator of <i>A. actinomycetemcomitans</i> Metabolism, Oxidative Stress, and Iron Acquisition	
Introduction.....	52
Results.....	54
Discussion.....	60
Chapter Five: CAT-Fe Exposure Stimulates Biofilm Formation and Planktonic Growth of <i>A. actinomycetemcomitans</i>	
Introduction.....	79
Results.....	79
Discussion.....	82

Chapter Six: The Iron-Responsive Toxin/Anti-toxin (TA) System D11S_2133-2134 and Its Role in *ygiW/qseBC* Regulation

Introduction.....	93
Results.....	95
Discussion.....	99
Chapter Seven: Summary.....	115
Chapter Eight: Future Directions.....	120
References.....	125
Appendix.....	132
Curriculum vitae.....	151

LIST OF FIGURES

Chapter 3	
Figure 1:	Expression of the <i>ygiW-qseBC</i> operon in <i>A. actinomycetemcomitans</i> exposed to catecholamines, zinc, cold temperatures.....47
Figure 2:	Expression of the <i>ygiW-qseBC</i> operon in <i>A. actinomycetemcomitans</i> exposed to CAT-Fe.....48
Figure 3:	The CAT-Fe induction of <i>ygiW-qseBC</i> is dependent on a functional QseB binding domain.....49
Figure 4:	The CAT-Fe induction of <i>ygiW-qseBC</i> is dependent on a putative conserved iron responsive motif, EYRDD50
Figure 5:	Expression of <i>ygiW-qseBC</i> operon in response to adrenergic receptor antagonists.....51
Chapter 4	
Figure 6:	Leukotoxin Expression in Response to CAT-Fe.....64
Figure 7:	Extracellular Formate Concentration in Response to CAT-Fe.....65
Figure 8:	Changes in Metabolic Flux in Response to CAT-Fe.....66
Figure 9:	The Oxidative Stress Response.....67
Chapter 5	
Figure 10:	Biofilm Formation in the Wt Strain Exposed to CAT-Fe.....86
Figure 11:	Biofilm Formation in the <i>qseCΔp</i> Strain Exposed to CAT-Fe.....87
Figure 12:	Schematic of the Enterobactin Transport and Receptor Operon.....88
Figure 13:	Biofilm Formation in the TonB Receptor Mutant Strain Exposed to CAT-Fe.....89
Figure 14:	Planktonic Growth in Response to CAT-Fe.....90
Figure 15:	Planktonic Growth in the TonB Dependent Receptor Mutant.....91
Figure 16:	Planktonic Growth in Response to Adrenergic Receptor Antagonists...92
Chapter 6	
Figure 17:	Expression of <i>lon</i>103
Figure 18:	Expression of <i>ygiW</i> in Response to Ectopic Expression of <i>lon</i>104
Figure 19:	Planktonic Growth in Strain Ectopically Expressing <i>lon</i>105
Figure 20:	Expression of D11S_2133-2134.....106
Figure 21:	The D11S_2133-2134 Operon.....107
Figure 22:	Growth in Strains Ectopically Expressing D11S_2133-2134 in <i>E. coli</i>108
Figure 23:	Growth in Strains Ectopically Expressing D11S_2133-2134 in <i>A. actinomycetemcomitans</i>109
Figure 24:	Expression of <i>ygiW-qseBC</i> in strains Ectopically Expressing D11S_2133-2134 on the Trc Promoter.....110
Figure 25:	Confirmation of Ectopic Expression of D11S_2133-2134.....111
Figure 26:	Expression of <i>ygiW-qseBC</i> in Strains Ectopically Expressing D11S_2133-2134 on <i>lrrA</i> Promoter.....112
Figure 27:	Schematic of QseBC activation by CAT-Fe and regulation by D11S_2134113

LIST OF TABLES

Chapter 2	
Table 1:	Strains and plasmids.....19-20
Table 2:	Composition of CDM.....22-25
Table 3:	Primers used in this study.....28-31
Chapter 4	
Table 4:	Genes Involved in Anaerobic Metabolism68-70
Table 5:	Water Soluble Metabolites.....71-73
Table 6:	Genes Involved in Iron Acquisition.....74
Table 7:	Genes Involved in Fatty Acid, LPS and Lipis
Biosynthesis.....	75-76
Table 8:	Lipid soluble metabolites.....77
Chapter 5	
Table 9:	Stress response genes.....114

CHAPTER ONE: INTRODUCTION

As awareness of germ theory gained acceptance in the early 1900's, the idea that systemic and chronic diseases, such as atherosclerosis, mental illness and cancer, were caused by the systemic spread of microbes and their toxins through the body also gained traction. The idea behind the theory of focal infection was that the root cause of these systemic diseases could eventually be traced back to some sort of infectious origin [1]. In the 1890's W.D. Miller and later in 1911 William Hunter, were the earliest to make the link between oral infections and systemic health issues [2, 3]. As a result, one of the methods that was employed to treat and prevent systemic disease included the therapeutic extraction of teeth, sometimes even healthy teeth [1]. One piece of evidence given to support this therapy is the claim that Hippocrates cured arthritis in 400 B.C. by extracting infected teeth [2]. This led to widespread extraction of infected and sometimes even healthy teeth as a way to treat and prevent disease although much of the evidence given in support of the theory was anecdotal [4]. The theory was discredited as additional studies were conducted that showed the extraction of teeth did not on a whole lead to or prevent disease and there was no proof of a direct cause and effect between oral infections and some systemic diseases [2, 4]. The problem of cause and effect was difficult to solve at this time since the molecular technology was not advanced enough to prove pathogens isolated from other sites had an oral origin [3]. Recently, some of the ideas of focal infection have started to regain popularity as people have done epidemiological studies looking at the association between periodontal disease and systemic inflammatory diseases such as atherosclerosis [5], diabetes [1], and rheumatoid arthritis [6]. Numerous case studies have shown systemic issues such as urinary tract infections [7], brain abscesses [8] and pneumonia [8] can occur from oral infections or after routine dental procedures. One of the strongest links is data suggesting a

strong correlation to periodontal disease and endocarditis [9]. Evidence exists of the presence of oral pathogens in numerous extra-oral tissues including the heart [10] and brain [11] suggesting that oral bacteria can use the oral cavity as a reservoir from which to disperse, most likely after dental procedures where small cuts in the gum allow the bacteria access to the bloodstream [2]. It has also been suggested that depending on the oral hygiene, activities as innocuous as chewing could cause cuts from which the bacteria can enter the blood stream and travel throughout the body [3]. From there, depending on the health of the patient, the bacteria can travel and potentially colonize other sites in the body.

Periodontal Diseases

There are two types of periodontal diseases: periodontitis, a chronic inflammatory disease of the periodontium characterized by massive soft tissue destruction, irreparable bone and tooth loss, and bleeding upon probing. Gingivitis is a milder inflammation of the gingiva that with proper treatment can be reversed, but if left untreated can result in periodontitis [12]. In clinical terms, gingivitis is characterized as a subgingival pocket depth of 4-5 mm with bleeding of the gums, while periodontitis is characterized by a subgingival pocket depth greater than 6 mm, and severe periodontitis giving a subgingival pocket depth greater than 7mm [12].

Forty six percent of the adult population of the United States have some form of periodontitis and 8.9% have severe periodontitis, making it the most common chronic inflammatory disease [13]. The prevalence of periodontitis varies with race with Hispanics having the highest percentage (63.5%) and non-Hispanic whites having the lowest percentage (40.8%) [13]. \$14.3 billion was spent on treating periodontal disease in the US alone in 1999 [14]. This amount has undoubtedly increased since then. In addition, research correlating periodontal disease to the development of other potentially life-threatening and costly diseases

such as atherosclerosis [5], arthritis, diabetes, pulmonary disease and adverse pregnancy outcomes means that the cost of periodontal disease in terms of dollar amounts and in terms of morbidity/mortality is much higher. This suggests that there is a high need for innovative treatments and preventative therapies.

Numerous risk factors can influence the onset of periodontitis including age, race, gender, oral hygiene, diet, socio-economic status, education status, smoking, and stress [13, 15]. Hispanics, males, people over the age of 30, and smokers are much more likely to develop disease, with 63% of current smokers having periodontal disease and 18.9% of current smokers having severe periodontal disease compared to 5.5% of non-smokers with severe periodontal disease [13]. The bias towards males developing periodontal disease is interesting since more often it is females that are more likely to develop inflammatory diseases, which is thought to be due to the influence of hormones on immune cell development [16]. The reasons for the increase incidence of periodontal disease in males is still not well known, since female mice in lab settings are more likely to develop periodontal disease [17]. This could be explained by differences in oral hygiene between males and females since when age and oral hygiene are taking into account, incidence of disease between males and females, females are more likely to have periodontal disease [117]. The impact of socio-economic and education status can be explained in these populations due to reduced access to oral healthcare. In addition, the association between race, in particular Hispanics, with the development of periodontal disease could have a two-fold explanation. One explanation is that Hispanics may be less likely to receive proper oral healthcare [18]. Several of these risk factors (i.e. smoking and diet) are due to the direct impact on the microbiome, whereas other risk factors (i.e. smoking, age, sex and stress) may have indirect influences on the microbiome by modulating the immune response. These impacts on the microbiome can cause significant population shifts resulting in the presence of

more pathogenic bacteria. For example, several studies have shown an increase in the prevalence of pathogenic bacteria such as *Tannerella forsythia*, *Aggregatibacter actinomycetemcomitans*, *Porphyromonas gingivalis*, and *Treponema denticola* in the oral cavity of smokers [19, 20]. In addition, smoking has been shown to cause a dampening of the immune response and causes also changes in the oral biofilm [21] by increasing the incidence of pathogenic bacteria such as *F. nucleatum*, *P. intermedia*, and *Actinomyces* spp [22]. It can also promote colonization by *P. gingivalis* by causing an increase in fimbriae expression which augments the immune response [23].

In healthy gums, the teeth are connected to the soft tissue via gingival fibers and the alveolar bone via the periodontal ligament fibers. Colonization with pathogenic bacteria triggers inflammation resulting in a massive influx of infiltrating neutrophils, macrophages, and lymphocytes and eventually leads to deterioration of the supporting soft tissue around the teeth, destruction of the periodontal ligaments and gingival fibers, and loss of attachment to the tooth. Ultimately the activation of bone-resorbing osteoclasts, over the bone-forming osteoblasts, results in alveolar bone loss that causes a reduction in the height of the alveolar bone crest and an increase in vertical bone loss. The pro-inflammatory cytokines released by invading immune cells and leading to the activation of osteoclasts include IL-1B, IL-6, TNF- α , IL-8, and RANKL [24]. Osteoclast activation leads to bone resorption and alveolar bone loss [24]. In addition, infiltrating neutrophils can release a whole host of chemicals from their granules (e.g. defensins, proteases, lactoferrin, and catecholamines [25]) when triggered by pro-inflammatory signals.

A second form of periodontitis differs from the typical chronic periodontitis. Localized aggressive periodontitis (LAP) is a rapid onset periodontal disease, and when left untreated

results in rapid alveolar bone loss and destruction of the supporting tissues around the teeth, particularly in the incisors and first molars. LAP has significant differences in geographic burden with people from Moroccan descent more likely to have LAP suggesting that geographic location, socio-economic factors and race play an important role in its development [26]. It is more often seen in juveniles compared to chronic periodontitis and is strongly associated with colonization with *A. actinomycetemcomitans* [26], and in particular, a hyper-leukotoxic strain of the organism [37].

Biofilms

Periodontitis is an inflammatory response triggered by certain oral bacteria that form biofilms, structured communities of bacteria in a self-generated matrix of proteins, nucleic acids, and carbohydrates, in the subgingival pocket. The plaque deposited on the teeth (hard tissue) and in the subgingival pocket (soft tissue) is comprised of a microbial biofilm. The presence of plaque is the most important risk factor for the development of periodontitis. The development of biofilms is advantageous to the bacteria since the structured community allow them to more tightly adhere to the salivary pellicle or each other, making them more difficult to remove by chemical or physical means. Biofilms also help bacteria to resist antibiotic mediated killing and can promote slow-growing persister cell formation [122]. These are cells that are physiologically dormant and more resistant to anti-bacterial treatment. The oral biofilm is extremely complex, containing both pathogens and commensals, and usually exists in homeostasis with the host. However, a variety of environmental stimuli can induce populational changes in the biofilm that disrupt homeostasis and initiate disease. Development of biofilms on the teeth starts within hours of tooth eruption from the gingiva [123]. In addition, routine cleanings can clear the biofilm, but it will start to reform soon after [123]. Formation begins with the deposition of the

salivary pellicle and initial colonizers such as *Streptococci* spp. and *Actinomycetes* spp. attaching to these immobilized salivary components [27]. Early (i.e. *Neisseria*, *Prevotella*, *Eikenella*, *Rothia*, *Porphyromonas*, and *Veillonella*), middle (i.e. *Fusobacterium nucleatum*) and late colonizers (i.e. those most associated with disease, such as *P. gingivalis*, *T. denticola*, *T. forsythia*, and *A. actinomycetemcomitans* [28]) will then attach to the established biofilm making it more complex and diverse.

The oral biofilm consists of around 700 species, but only some of these bacteria have been associated with the progression from health to disease. A shift of mostly Gram-positive aerobes to Gram-negative anaerobes is associated with the development of disease [27]. Some of the better characterized bacteria that have been associated with periodontitis include bacteria of the “red complex” (*T. denticola*, *T. forsythia*, and *P. gingivalis*), *Filifactor alocis*, *Prevotella intermedia*, and *A. actinomycetemcomitans* [26, 28]. The colonization of the subgingiva by these pathogens is aided by several virulence factors that help in evading the immune response. Biofilm development depends on the interaction of not only bacteria to the surface of the tissues of the host, but also on bacteria-bacteria interactions [27].

Aggregatibacter actinomycetemcomitans

A. actinomycetemcomitans is gram-negative, non-motile, facultative anaerobe of the *Pasteurellaceae* family. Other members of the *Pasteurellaceae* family include *Haemophilus influenzae* and *Actinobacillus pleuropneumoniae*. There are five serotypes (a-e), with variation in the global population in serotype burden, with a, b, and c being globally dominant, while d and e are rare [29, 30]. This study utilizes the smooth strain D11S c serotype of *A. actinomycetemcomitans* due to its role in pathogenesis of localized aggressive periodontitis.

Although *A. actinomycetemcomitans* is now considered to be an oral opportunistic

pathogen, it wasn't recognized as being a member of the oral microbiota until 1975, 63 years after it was first isolated [31]. It is associated with a particular type of periodontitis called localized aggressive periodontitis (LAP) [26]. Geographic and race disparities have been reported in terms of incidence of LAP, but *A. actinomycetemcomitans* remains prevalent in the overall population and is commonly present in the subgingival plaque. *A. actinomycetemcomitans* has also been shown to cause extra-oral infections and complications such as infective endocarditis [10], soft-tissue abscesses [8], reactive arthritis [32], urinary tract infections [7], pneumonia [8] and has been associated with atherosclerosis [33].

A. actinomycetemcomitans has a variety of virulence factors including a 116 kDa leukotoxin, a member of the repeats-in-toxin (RTX) family of pore-forming toxins that specifically kills polymorphonuclear leukocytes, monocytes and T-cells in humans, apes and Old-World monkeys [34, 35]. Previous studies have shown that people harboring an *A. actinomycetemcomitans* strain JP2 that expresses higher levels of leukotoxin due to a deletion in the toxin promoter have earlier onset of periodontitis than patients colonized with a non-JP2 strains [36, 37]. In addition, *A. actinomycetemcomitans* produces other virulence factors such as a cytolethal distending toxin that causes apoptosis of lymphocytes [38], lipopolysaccharide (LPS) [39], collagenase [39], a capsular polysaccharide that has been shown to inhibit IL-6 and IL-8 production [40], an IgA protease [41], an adhesin associated with infective endocarditis EmaA [42], and fimbriae that allows it to form robust biofilms [43]. The fimbriae play an important role in the ability of *A. actinomycetemcomitans* to attach to itself or to other surfaces and resist salivary flow when forming biofilms [44].

A. actinomycetemcomitans is also resistant to complement mediated phagocytosis and killing by neutrophils [45] although the exact mechanism by which it resists neutrophil killing is

unknown. The b serotype of *A. actinomycetemcomitans* is capable of resisting phagocytosis via serotype b-specific polysaccharide antigen [46]. However, it's also able to invade epithelial [47] and endothelial cells [48]. The ability to invade into these cells may be an important mechanism by which the bacteria shields itself from immune killing or a way for the bacteria to disseminate through the host [39].

Since a virulence factor can be defined as anything that helps a pathogen to successfully colonize a host, the definition of virulence factors has started to be expanded to include things that would have been considered house-keeping genes before, such as essential metabolic genes. Recent research now suggests that metabolites and changes in metabolism itself can be considered a virulence factor since many virulence factors and quorum sensing systems are under metabolite control, for example, the regulation of carbon metabolism via the cAMP regulatory protein [49-51]. Further, successful colonization of the host requires correct expression of metabolic pathways. For example, Jorth *et al* showed that when *A. actinomycetemcomitans* grown in *in vitro* biofilms was compared to *A. actinomycetemcomitans* cultured in a mouse abscess model, the largest changes in gene transcription revolved around genes involved in anaerobic respiration and metabolism [52]. In addition, deletion mutants of some of the genes that were up-regulated in *in vivo* conditions (e.g. fumarate reductase and formate dehydrogenase) were attenuated compared to wild type strains [52].

Two-component Regulatory Systems and QseBC

Successfully colonizing a host requires that a pathogen respond quickly to environmental fluctuations. One way that bacteria respond to changes in their environments is through the activity of two component signal transduction systems. These systems have evolved to respond to a variety of stimuli including pH, temperature, salinity, and concentrations of ions such as zinc

and iron [59, 62, 60]. They are usually comprised of a membrane bound histidine kinase sensor and a cytosolic, DNA-binding response regulator that are often co-transcribed in an operon. When the inner membrane bound sensor senses its cognate stimulus, it becomes activated and auto-phosphorylates at a highly conserved histidine residue. The histidine kinase sensor will then transfer the phosphate to the cognate response regulator causing it to change conformation and become activated. The activated response regulator can then bind to DNA to either promote or repress expression of certain genes, sometimes including its own operon [60, 101]. There has also been evidence that some sensors can activate response regulators other than its own cognate response regulator [60]. This suggests that a large and complex signaling cascade can occur in order to change gene transcription in response to environmental stimuli.

QseBC is a two-component system that is highly conserved in the *Enterobacteriaceae* and the *Pasteurellaceae*. In *A. actinomycetemcomitans*, the operon is transcribed with a gene encoding a small putative periplasmic solute binding protein of the OB-fold family designated *ygiW* [53]. The *ygiW* gene is present in *Escherichia coli*, but it is divergently transcribed from the *qseBC* operon.

Work done in *E. coli* and *Salmonella enterica* have shown that this two component system responds to catecholamines in iron-limiting environments [54-57]. This response is also dependent on the presence of a functional synthesis and transport system for the enterobactin siderophore [58]. The *E. coli* QseBC can also become activated with increased levels of ferric iron, but it is not directly activated by the iron. Iron activates another TCS, PmrAB [59], and PmrA binds to the promoter region of *qseBC* to induce its expression [60]. Further, PmrB will phosphorylate QseB which in turn auto-regulates expression of the *qseBC* operon [60]. In addition, the *E. coli* QseBC is able to respond to a quorum sensing molecule designated as AI-3

[55, 61]. It was shown that exposure to catecholamines regulates the production of AI-3 by the bacteria, and AI-3 goes on to further activate QseBC on its own. Contrary to this, the QseBC homolog in *H. influenzae* (FirRS) did not appear to respond to catecholamines, and instead responded to ferrous, and not ferric, iron [62]. This response to iron was dependent on an iron-responsive motif in FirS, DYRED [62].

Some of the reported changes in response to QseC activation by catecholamines in *E. coli* include the activation of genes involved in the formation of the attaching and effacing lesion [63], the Type Three Secretion System (TTSS) contained on the locus of enterocyte effacement (LEE) [54], and flagella and motility genes [64, 65]. Other effects of catecholamine exposure include increase in planktonic growth [66], biofilm formation [65], as well as virulence [65]. This effect has also been seen in *P. gingivalis* and *A. plueropneumoniae*, where catecholamines have been shown to cause an up-regulation of certain virulence factors [67, 68]. It is not known if catecholamines cause changes in gene transcription and growth in *A. actinomycetemcomitans*, but since the *A. actinomycetemcomitans* genome lacks many of the QseBC-regulated gene of *E. coli*, the potential impact of catecholamines on *A. actinomycetemcomitans* will likely be novel and species specific.

Although the activating signal for the *A. actinomycetemcomitans* QseBC has not been identified, previous work has shown that QseC plays an essential role in two important and complex phenotypes. The first phenotype is virulence, since a $\Delta qseC$ mutant is attenuated in a mouse model of periodontitis, and a *qseC* complemented strain restores the virulence phenotype, as measured by alveolar bone loss [44]. The other phenotype that QseBC plays a role in is biofilm formation [44, 53].

The ability of *A. actinomycetemcomitans* to form biofilms is contingent on its ability to

sense the quorum sensing molecule AI-2 by the receptors LsrB and RbsB [70]. In an AI-2 synthase mutant ($\Delta luxS$) biofilm formation is reduced. QseBC is activated downstream of AI-2 detection, but QseBC is not directly activated by AI-2 [44]. The mechanism linking AI-2 detection to QseBC activation is unknown, but in *E. coli* it was shown that *qseBC* is regulated by the toxin MqsR, which is activated by AI-2 [71]. Biofilm formation was significantly reduced in a MqsR deletion mutant in the presence of AI-2 and MqsR was found to positively regulate *qseBC* expression [71].

Microbial Endocrinology

Microbial endocrinology refers to the rapidly growing field dedicated to understanding the impact of host hormones on pathogens in terms of virulence and growth. Hormones play an important and varied role within the host. One process that is controlled by hormones in humans is the stress response. High catecholamine (i.e. norepinephrine, epinephrine and dopamine) hormones are associated with stress [15, 72]. When the host encounters some sort of stressor, the sympathetic nervous system becomes activated causing signaling through the hypothalamic-pituitary-adrenal axis [73]. This activation triggers the response of the catecholamine neurotransmitters in order to put the body into a “fight-or-flight” response mode. Effects of catecholamines include increased heart rate, blood pressure, and glucose levels [73].

Catecholamines are mainly produced in the adrenal glands by chromaffin cells and in the post-ganglionic fibers of the sympathetic nervous system. Recent research has shown that norepinephrine can also be produced and released by activated phagocytes (including activated neutrophils which migrate into the tissue during periodontitis) in response to inflammatory signals [25, 74]. The concentration of released catecholamines can reach up to millimolar amounts and work to activate other immune cells, ramping up the immune response [25, 57].

The synthesis of catecholamines begins with L-phenylalanine, which is converted into L-

tyrosine by aromatic amino acid hydroxylase (AAAH). Using the same enzyme, L-tyrosine is converted into L-DOPA with tetrahydrobiopterin, O₂, and ferrous iron acting as cofactors. L-DOPA is converted by aromatic L-amino acid decarboxylase (AADC) to dopamine with pyridoxal phosphate as the cofactor. Dopamine can then act as a precursor for the synthesis of the other catecholamines: epinephrine and norepinephrine. Dopamine is first converted to norepinephrine by dopamine β-hydroxylase (DBH) using O₂ and L-ascorbic acid as cofactors and is then converted into epinephrine by phenylethanolamine N-methyltransferase (PMNT) with S-adenosyl-L-methionine acting as the cofactor [75]. There are two enzymes which can degrade catecholamines: catechol-O-methyltransferase (COMT) and by monoamine oxidases (MAO) [75].

The original studies done on the effect of catecholamines on bacteria began with work on *E. coli* and *S. enterica*. It had been widely reported that animals exposed to stressful conditions were more susceptible to disease [57, 76]. These reports contradict evidence showing that catecholamine stress hormones can activate immune cells [25] which would be expected to decrease susceptibility to disease. It was hypothesized that catecholamines had a direct impact on pathogens leading to an increase in virulence. This was confirmed with work showing that catecholamines result in increased growth in minimal, iron-restricted media [57].

Catecholamines can also act as pseudo-siderophores and can scavenge iron from host iron-binding proteins [77]. This ability of catecholamines to scavenge iron was suggested to contribute to the growth phenotype in response to catecholamines, suggesting that bacteria can exploit the production of host hormones to acquire the essential nutrient iron. Catecholamines have been shown to scavenge iron through their catechol moiety by forming a complex with the iron-loaded lactoferrin [77]. This complex causes reduction of the iron, which destabilizes the bond between the iron and lactoferrin, allowing iron to be released [77]. Both catecholamines and lactoferrin can be released by neutrophils in response to pro-inflammatory signals [78, 79],

so the bacteria may not only exploit the systemic production of hormones, but also the inflammatory response designed to combat infection.

Normally, free iron is very limited in the host due to host iron-binding proteins that ensure bacteria cannot easily acquire this essential nutrient [124]. Bacteria have in turn evolved mechanisms to counter iron sequestration, most notably through the secretion of siderophores such as enterobactin, which is able to bind iron via a catechol moiety [58]. However, in bacteria that do not produce siderophores, e.g., *A. actinomycetemcomitans*, the use of catecholamines to scavenge iron may represent a novel mechanism for nutrient acquisition [57]. Several different proteins have been suggested to function as bacterial adrenergic receptors and interact with catecholamines but the best characterized protein is QseC [55]. The ability of bacteria to sense catecholamines through bacterial adrenergic receptors like QseC demonstrates the ability of these organisms to take part in inter-kingdom signaling.

As previously mentioned, stress is a risk factor for the development of periodontitis [15]. In addition, it has been shown that activated polymorphonuclear cells can release up to millimolar concentrations of catecholamine stress hormones in response to inflammatory signals [78, 79]. Although macrophages have been shown to release higher amounts of catecholamines, infiltrating neutrophils are in a higher abundance during periodontitis [95, 96] and are more likely to have an effect on periodontal microbes like *A. actinomycetemcomitans* due to their release of catecholamines. Therefore, a better understanding of how oral bacteria, specifically *A. actinomycetemcomitans*, respond to catecholamines and the impact on virulence may provide insight for understanding the connection between stress and pathogenesis. Understanding the impact of catecholamines on the pathogenesis of *A. actinomycetemcomitans* may allow us to use different therapies to block the recognition of catecholamines by *A.*

actinomycetemcomitans. There are already drugs on the market (i.e. alpha blockers and beta blockers) that block the recognition of catecholamine hormones by adrenergic receptors [80]. If QseC is functioning as an adrenergic receptor, then these receptor antagonists could potentially block the recognition of catecholamines by the bacteria and therefore could modulate pathogenesis and reduce the damage caused by periodontitis. In addition, understanding the link between catecholamines and periodontitis and the effect on *A. actinomycetemcomitans* may allow dentists in the clinical setting to look at which patients will need to be targeted for more aggressive treatment. Ultimately, this information could also be used to determine patients that are at higher risk to develop more virulent bacterial infections leading to periodontitis due to increased catecholamines and target them with more aggressive dental care and potentially therapeutic agents such as adrenergic receptor antagonists.

Toxin/Anti-toxin (TA) Systems:

Previous work done on *E. coli* has shown that QseBC activation is directly controlled by the toxin MqsR, which is directly downstream of AI-2 detection [71]. MqsR is the toxin in the *mqsRA* type II toxin/anti-toxin (TA) system. Type II TA systems are comprised of a labile protein anti-toxin that is co-transcribed in a small operon with its cognate protein toxin [81]. Under normal conditions, the anti-toxin binds to the toxin to negate its effects. TA systems can be activated by the Lon [82] or Clp [83] proteases which more readily degrades the labile anti-toxin, releasing the toxin [85, 83]. Most toxins act as endoribonucleases [84], but some toxins can target other factors such as DNA gyrase, elongation factors, or uridine diphosphate-N-acetylglucosamine [81]. TA systems are activated by a signaling mechanism involving RelA/SpoT, the signaling nucleotide (p)ppGpp, and polyphosphate (PolyP) [85]. RelA/SpoT synthesizes ppGpp which causes an inhibition of exopolyphosphatase (PPX), which is an enzyme that

degrades PolyP [85]. PolyP is produced by polyphosphate kinase (PPK), and since PPK is inhibited, the concentration of PolyP within the cell increases, which activates Lon [85]. This signaling mechanism can be activated stochastically at very low levels [85], or conversely, when the bacterium is stressed or goes through metabolic transitions [86]. In addition, the Clp protease can also degrade anti-toxins [83], but it has not been determined if it responds to the same mechanisms as Lon. *A. actinomycetemcomitans* contains both the Lon (D11S_1522) and Clp (D11S_2042-2043) proteases. The activation of TA systems through this signaling mechanism is hypothesized to be a way for the bacterium to form a persister state in response to stress [81, 84]. TA systems can respond to a variety of stressors, and they can be functionally redundant. For *E.coli*, all 10 TA systems had to be knocked out in order to see a phenotype of decreased persistence [84].

As mentioned previously, *qseBC* is part of the AI-2 regulon in *A. actinomycetemcomitans*, but it is not directly activated by AI-2 detection [44]. The mechanism that links AI-2 and *qseBC* remains unknown. There are 10 putative TA systems in *A. actinomycetemcomitans*, and it is possible that one of these TA systems plays a role in *qseBC* expression. The stimuli that activates these TA systems in *A. actinomycetemcomitans*, their mechanism of action, and their targets for regulation are unknown. Previous work done in *E. coli* has shown that certain TA systems can have a wide range of targets, for example, the MazF toxin acts as an endoribonuclease that targets the sequence ACA, which is present in almost all mRNA's [87]. The targets for TA systems allow the bacteria to down-regulate processes such as transcription and translation, processes that require a significant amount of energy and are required for a metabolically active cell. By down-regulating these processes, the cell can go into a persister state and persist under conditions of environmental stress [125]. Therefore, understanding how TA systems regulate cell activities could elucidate targets for therapeutics that could be employed as a way to prevent

persist cell formation and make the bacteria more susceptible to antibiotics.

Significance

QseBC has been previously shown to be essential for the pathogenesis of *A. actinomycetemcomitans* and from these studies seem to regulate many key cellular processes like metabolism, biofilm formation and the stress response. The data presented in this dissertation demonstrates that the *A. actinomycetemcomitans* QseBC responds to both iron and catecholamines (CAT-Fe) and to high concentrations of the adrenergic receptor antagonists propranolol and phentolamine. CAT-Fe stimulates both planktonic growth and biofilm formation in a TonB dependent manner. In addition, CAT-Fe significantly alters the metabolic flux of *A. actinomycetemcomitans* and results in an up-regulation of genes involved in oxidative stress which protects the bacteria after exposure to H₂O₂. The ability of *A. actinomycetemcomitans* to respond to CAT-Fe and exploit it as a nutritional niche may provide insight about the connection between stress and periodontitis. Further, the loss of QseB results in an up-regulation of the stress response. Ectopic expression of *lon*, one of the proteases involved in the stress response, induces increased transcription of *ygiW-qseBC*. In addition, ectopic expression of the iron-responsive D11S_2133-2134 TA system was shown to modulate expression of *ygiW-qseBC*. These results suggest that the D11S_2133-2134 TA system and QseB might be involved in a regulatory circuit that fine-tunes the response of *A. actinomycetemcomitans* to changes in iron in the environment and might represent a target for therapeutics. In addition, our results potentially provide insights into the structure and nature of QseC that could facilitate the development of novel therapeutics.

CHAPTER TWO: MATERIALS AND METHODS

Bacterial strains and culture conditions: All strains used are listed in Table 1. LB (Luria–Bertani) broth, LB agar (LB broth with 1.5 % agar) and brain–heart infusion (BHI) broth, BHI agar, and a chemically defined media (CDM) was used to propagate and plate bacteria. *A. actinomycetemcomitans* 652 serotype c was grown at 37°C in 5.0% CO₂ in either Brain Heart Infusion (BHI) supplemented with 40 mg of NaHCO₃ per liter or CDM supplemented when required with 100uM of ferrous or ferric iron or 50uM of epinephrine or norepinephrine or 50-400uM of phentolamine or propranolol. The components of CDM are essentially described by Socransky *et al* [88] listed in Table 2. Cultures grown in CDM for CAT-Fe studies were first inoculated into BHI and cultured overnight to an O.D._{600nm} of 0.3-0.4. The overnight culture was then passaged into fresh BHI at a 1:30 dilution until growth reached an O.D._{600nm} of 0.5-0.6. The culture was then passaged into CDM at a 1:30 dilution. The $\Delta qseC$ complemented strain and strains carrying the pDJR29 plasmid were grown as described above but supplemented with kanamycin (25ug/mL). The *A. actinomycetemcomitans* strain carrying pWAW28 was grown in BHI supplemented with kanamycin while the strains carrying pWAW17, pWAW19, pWAW20, and pWAW31 were grown with kanamycin in BHI with or without 1mM IPTG supplementation. The *A. actinomycetemcomitans* strains carrying pWAW14 or pWAW16 were grown in LB with kanamycin with or without supplementation with 0.2% glucose. XL Blue *Escherichia coli* cultures containing the plasmids pWAW17, pWAW19, and pWAW21 were cultured in Luria Broth (LB) supplemented with tetracycline (50ug/mL), kanamycin (25ug/mL) or with 1mM IPTG. XL Blue *Escherichia coli* strains carrying pWAW14 and pWAW16 were grown in LB supplemented with tetracycline and kanamycin. *A. actinomycetemcomitans* cultures harboring the suicide plasmid

pWAW23 were grown in BHI with spectinomycin (25ug/mL) or TYE with 1mM IPTG and 10% sucrose.

Growth Kinetics: For determining the effect of CAT-Fe on growth, a frozen glycerol stock of *A. actinomycetemcomitans* was inoculated into BHI and allowed to grow to an O.D._{600nm} of 0.3-0.4. Cells were then transferred to fresh BHI at a dilution of 1:30 until an O.D._{600nm} of 0.5-0.6 was achieved. The cells were then inoculated into fresh CDM at 1:30 dilution with or without CAT-Fe supplementation or adrenergic receptor antagonist supplementation. At various time points, aliquots were removed from triplicate cultures and the O.D._{600nm} measured using a BioRad SmartSpec Plus UV-vis spectrophotometer. Growth kinetics for *XL* strains or *A. actinomycetemcomitans* strains containing plasmids for the ectopic expression of the Lon protease or the TA systems were done in triplicate using aliquots taken a various times and the O.D._{600nm} measured. For all other growth curves, cultures were inoculated from an overnight stock at a 1:30 dilution into fresh media with the appropriate supplementations. At various time points, aliquots were removed from triplicate cultures and measured for the O.D._{600nm}.

Table 1: Strains and plasmids

Strain or plasmid	Derived, relevant genotype or characteristics	Source or reference
<i>Escherichia coli</i>		
XL1-Blue MRF'	$\Delta(mcrA)183$ $\Delta(mcrCB-hsdSMR-mrr)173$ endA1 supE44 thi-1 recA1 gyrA96 relA1 lac [F' proAB. lacIqZ Δ M15 Tn10 (Tcr)]	Stratagene
<i>Aggregatibacter actinomycetemcomitans</i>		
652 WT	Wild type, serotype c	Laboratory stock
652-JR23	652 <i>qseC</i> Δ p	Juárez-Rodríguez <i>et al.</i> (2013a)
652-JR36	652 Δ <i>ygiW</i>	Juárez-Rodríguez <i>et al.</i> (2013a)
652-JR37	652 Δ <i>qseB</i>	Juárez-Rodríguez <i>et al.</i> (2013a)
652-JR38	652 Δ <i>qseC</i>	Juárez-Rodríguez <i>et al.</i> (2013a)
652-JR39	652 Δ <i>qseBC</i>	Juárez-Rodríguez <i>et al.</i> (2013a)
652-JR39-46	652 Δ <i>qseBC</i> ::46 (YgiW QseBQseC)	Juárez-Rodríguez <i>et al.</i> (2014)
652-JR39-61	652 Δ <i>qseBC</i> ::61 (YgiW QseBQseC _{Y155A, R156A})	Weigel <i>et al.</i> (2015)
652-WW1	652 Δ D11S_1352	This study
Plasmids		
pJT1	Sp ^r , suicide vector	Juárez-Rodríguez <i>et al.</i> (2013b)
pJT3	Km ^r , <i>lacZ</i> promoterless	Juárez-Rodríguez <i>et al.</i> (2013b)

Strain or plasmid	Derived, relevant genotype or characteristics	Source or reference
Derived from pJT1		
pWAW4	Sp ^r , D11S_1352	This study
Derived from pJT3		
pWAW17	Km ^r , pTRC promoter -1 to -87, Lon -87 to -2505	This study
pWAW19	Km ^r , pTRC promoter -1 to -87, D11S_2134 -87 to -2505	This study
pWAW20	Km ^r , pTRC promoter -1 to -87, D11S_2133 -87 to -2505	This study
pDJR29	Km ^r , <i>ygiW-qseBC</i> promoter -1 to -372- <i>lacZ</i>	Juárez-Rodríguez <i>et al.</i> (2013a)
pWAW31	Km ^r , pTRC promoter -1 to -87, D11S_1354-1352	This study
pWAW16	87 to -2305	
	Km ^r , <i>lsrA</i> promoter -441 to +182 D11S_2134 +182 to +338	This study
pWAW14	Km ^r , <i>lsrA</i> promoter -441 to +182 D11S_2133 +182 to +464	This study
pATE33	Km ^r , <i>lsrA</i> promoter -441 to +182 <i>lacZ</i>	Juárez-Rodríguez <i>et al.</i> (2013a)

Construction of TA system and Lon ectopic expression plasmids: pWAW17, pWAW19, and pWAW20, were constructed from the *lacZ*-reporter strain pJT3. Using *A. actinomycetemcomitans* chromosomal DNA as a template, fragments representing *lon*, D11S_2133, or D11S_2134 were PCR amplified using a high fidelity Taq polymerase (Invitrogen) and primer sets: WW64&WW75, WW76&WW68, and WW70&WW77, respectively. The primers were flanked with restriction sites as shown in Table 3. The 2.4kb, 156bp, or 282 bp products were digested with *Bam*HI-*Xba*I and ligated into the *Bam*HI-*Xba*I digested pJT3 to make pWAW17A, pWAW19A, and pWAW20A. Using pJT1 plasmid DNA, primer set WW86&WW87 was used to PCR amplify the pTRC promoter. The 150 bp product was then digested with *Bam*HI-*Kpn*I and ligated together with *Bam*HI-*Kpn*I digested pWAW17A, pWAW19A, or pWAW20A to create pWAW17, pWAW19, or pWAW20, respectively. To make pWAW14 or pWAW16, the reporter plasmid containing the *lcrA* promoter, pATE33 [49] was digested with *Kpn*I/*Bam*HI and ligated together with *Kpn*I/*Bam*HI digested products from the PCR amplification of WW76&WW68 and WW70&WW77, respectively. The ligation reaction was then transformed into *E. coli* XL gold electrocompetent cells. Electroporated cells were incubated for 1 hour in SOC (2% tryptone, 0.5% yeast extract, 10 mM NaCl, 2.5 mM KCl, 10 mM MgCl₂, 10 mM MgSO₄, and 20 mM glucose) media with shaking then plated on LB plates supplemented with 50ug/mL of tetracycline and 25ug/mL kanamycin and incubated overnight. Colonies were chosen and grown in LB with tetracycline and kanamycin overnight. Plasmid was extracted from cultures using the Plasmid Miniprep Kit (Qiagen) and confirmed by sequencing using the University of Louisville Sequencing Core to confirm correct insertion. 25ug of plasmid was then used to transform *A. actinomycetemcomitans* by electroporation. Transformed cells were then cultured on BHI plates supplemented with kanamycin and resulting colonies were selected for plasmid purification and confirmed again by sequencing.

Table 2: Composition of CDM

1L CDM	
10mL	CaCl ₂ (10mg/mL)
50mL	Amino Acid Stock
50mL	Inorganic Salt Stock
1mL	Vitamin Stock
50mL	NaHCO ₃ (20mg/mL)
10mL	Cysteine (65mg/mL)
10mL	MgSO ₄ (70mg/mL)
1mL	Pimelic acid/Biotin
10mL	Riboflavin (0.1mg/mL)
1mL	Lipoamide
1mL	Folic Acid

Amino Acid Stock	
Hydrophilic Amino Acids	
10mL	H ₂ O
2.5mL	2M NaOH
499.2mg	L-glutamic Acid
200mg	Glycine
200mg	L-Threonine
200mg	L-Serine
200mg	L-lysine hydrochloride
242mg	L-arginine hydrochloride
270.2mg	L-histidine hydrochloride
200mg	L-glutamine
227.2mg	L-asparagine
200mg	L-proline
200mg	L-aspartic acid
40mg	L-ornithine hydrochloride
40mg	L-hydroxyproline

Hydrophobic Amino Acids	
--------------------------------	--

15mL	H ₂ O
3.125mL	2M NaOH
200mg	L-alanine
200mg	D-alanine
200mg	L-leucine
200mg	L-valine
200mg	L-Tryptophan
200mg	L-methionine
200mg	L-isoleucine
200mg	L-phenylalanine
40mg	L-tyrosine

Purine/Pyrimidine	
--------------------------	--

10mL	H ₂ O
1.25mL	2M NaOH
25mg	Adenine
20mg	Guanine
27mg	Cytosine hydrochloride
20mg	Thymine
20mg	Xanthine
20mg	Hypoxanthine
20mg	Uracil

L-cystine

5mL	H ₂ O
0.625mL	2M NaOH
10mg	L-cystine

Combine hydrophobic, hydrophilic, purine & pyrimidine and cystine to make amino acid stock.

Inorganic Salt Stock	
-----------------------------	--

99.5mL	H ₂ O
10mg	MnSO ₄
200mg	NaCl
400mg	K ₂ HPO ₄
2000mg	KH ₂ PO ₄
200mg	KNO ₃
0.1mg	KI
0.065mg	CuSO ₄ :5H ₂ O
0.5mg	Boric Acid
0.7mg	ZnSO ₄ :7H ₂ O
0.5mg	Sodium molybdate

Vitamin Stock	
----------------------	--

20mL	H ₂ O
1000mg	Choline chloride
200mg	β-alanine
20mg	Pyridoxal
20mg	Pyridoxine-HCl
20mg	Pyridoxamine-di-HCl
20mg	Spermidine-tri-HCl
20mg	Nicotinic Acid
20mg	Calcium pantothenate
20mg	Spermine-tetra-HCl
20mg	Thiamine-HCl
200mg	Myo-Inositol
20mg	NAD
2mg	<i>p</i> -aminobenzoic acid
.00005mg	Vitamin B12

Pimelic Acid/Biotin	
----------------------------	--

5mL	H ₂ O
5mL	Ethanol
1mg	Pimelic Acid
1mg	D-Biotin

Folic Acid

9.975mL	H ₂ O
25uL	NH ₄ OH
10mg	Folic Acid

β -Galactosidase Assay: *A. actinomycetemcomitans* containing the *lacZ* reporter plasmid pDJR29 were grown in CDM with or without supplementation of catecholamines, iron, and/or adrenergic receptor antagonists. Quantitative evaluation of β -galactosidase was carried out using permeabilized cells incubated with *o*-nitrophenyl- β -d-galactopyranoside (ONPG) substrate (Sigma-Aldrich) as previously described by Miller. Briefly, at 24 hours, 1mL of culture was taken to measure the O.D._{600nm} and 100uL of culture was taken for a β -Galactosidase assay. 700uL of Buffer Z (0.06M Na₂PO₄·7H₂O, 0.04M NaH₂PO₄·H₂O, 0.01M KCl, 0.001M MgSO₄·7H₂O, 0.05M 2-mercaptoethanol, pH7.0) was added to the 100uL of culture. Cells were then permeabilized using 20 μ L of chloroform and 0.5% SDS. 200uL of *o*-nitrophenyl- β -galactoside (ONPG) (4ug/mL) in Buffer Z was added to initiate the reaction. The reaction was stopped by the addition of 500uL of Na₂CO₃ after a color change was observed. The absorbance at 420nm and 550nm was read using a BioRad SmartSpec Plus UV-vis spectrophotometer.

Formate Assay: Formate concentration was calculated by the conversion of formate and NAD⁺ to bicarbonate and NADH via formate dehydrogenase using a Formic Acid Kit (r-Biopharm). *A. actinomycetemcomitans* was grown in CDM with or without supplementation with catecholamines and/or iron until 16 hours. Cells were then pelleted and the supernatant was harvested. The supernatant was then treated with 30mM trichloroacetic acid (TCA) at a 2:1 ratio of TCA to supernatant. The solution was then neutralized with 2M sodium hydroxide and filtered to remove all proteins. The filtered product added to the assay was adjusted based on growth rates of the bacteria and used in the Formic Acid Assay (r-Biopharm) as per manufacturer's instructions.

Oxidative Stress: *A. actinomycetemcomitans* was cultured in CDM with or without supplementation with iron and/or Ne for 16 hours. At this time, the growth was measured at O.D._{600nm} and the culture was split into two equal volumes in separate conical tubes. One half of

the culture was incubated at 37°C for 15 minutes while the other half of the culture was then stressed for 15 minutes using 0.3% H₂O₂ at 37°C. The hydrogen peroxide was quenched after 15 minutes with 50mM sodium pyruvate. Growth was measured 5 hours after culture at 37°C and compared to the pre-stress levels of growth.

RNA Isolation: Total RNA was harvested from mid-log growing cells using the RNA Lipid Tissue Minikit (Qiagen) as per manufacturer's instructions. To ensure that the RNA was free from any contaminating genomic DNA, the sample was digested by the Rnase-Free Dnase Set. The concentration and purity of each RNA sample were measured via spectrophotometry (ND-1000 Spectrophotometer, NanoDrop Technologies, Inc, Wilmington, DE). The RNA was tested for any genomic DNA contamination using qRT-PCR with primers specific for the 5S rRNA (Table 3) of *A. actinomycetemcomitans* and the SYBR Green FastMix (Quanta). RNA samples were considered free of significant genomic DNA if no amplification product was detected by qRT-PCR after at least 30 cycles of amplification.

Table 3		
Primers		
Primer	Description	Sequence
5sF	5s	GCGGGATCCTGGCGGTGACCTACT
5sR	5s	GCGATCTAGACCACCTGAAACCATACC
MDJR- 263F	pJT1 sequencing	GTTAGCAGTTCGTAGTTATCTTGGAGAGAATATTGAATGGAC
ww 26	D11S_2135 real-time	GGTATGCGCGAAAAAGCCACCAACGCG
ww 27	D11S_2135 real-time	CGCCTTTGATTTTATCGACCACATCCATGCC
ww 28	2134-2135 intergenic real-time	CCGAATGAGGATGTGGTGATTACTTCGGTTAC
ww 29	2134-2135 intergenic real-time	CTTTAGCTTTTACCGCCGCTTGAATCACGC
ww 36	D11S_2134 real-time	GATGACACAGGAATATAAGCAGTTTTTGCAACAAAAG
ww 37	D11S_2134 real-time	CATTCCTTCTTTAGCTTTTACCGC
ww 38	D11S_2133 real-time	CGAATATGCCGATTTAGCAGTGC
ww 39	D11s_2133 real-time	CAATTCGATAGCCTCTGACATAAATTTCA
ww 42	D11S_2134 5'RACE	CATTCCTTCTTTAGCTTTTACCGCCGCTTGAATCAC
ww 64	Lon R pjt4	GCTTTTGAAAAACTGAA <u>TCTAGA</u> TTAATTGACCGCAC
ww 65	Lon real-time	GGATGTTACAAGTGCTTGGCACAAACGTAGTAAAG
ww 66	Lon real-time	CGCCACAAACATTACGTCCGATAAATCATAATCC
ww 68	2134 pWAW19	CTGAATAAATAATT <u>TCTAGA</u> TTATGCAACGTCTTCATTCC
ww 70	2133 pWAW20	GGTATCAAAAAAAGGCATGA <u>TCTAGA</u> TTAGAAATTGG
ww 75	lon pWAW17	GGAATTTAGATAAGAGAGTACATG <u>GGATCC</u> ATGAGAGC
ww 76	2134 pWAW19	GGAGGTTATGATG <u>GGATCC</u> ATGACACAGG
ww 77	2133 pWAW20	GAAGGACGTTG <u>GGATCC</u> CATAAAATTATTTATTCAG
ww 80	<i>qseC</i> real-time	GATAATTTAACCCAAGGTATCGACCGTGCGACG
ww 81	<i>qseC</i> real-time	CATGAAAATACAGGTCGCCGATAAGGGACGGAAC
ww 82	<i>qseB</i> real-time	GAAATTGCCCTGACCACCCGTGAATATAAACTG
ww 83	<i>qseB</i> real-time	CACTTCCAGCGGTTACTGCTCACTTC
ww 84	<i>ygiw</i> real-time	CACAAGGCGGTTTTCAAGACCCGAATGC

ww 85	<i>ygiW</i> real-time	CGGCCAGGCTTTGCGTTCGATTC
ww 86	pTrc	GCGCTT ATTGCT <u>GGTACC</u> ATTCTG AAATGAGCTG
ww 87	pTrc	CATAGATCT <u>GGATCC</u> CATTTCCTGTGTGAAATTGTTATCC
ww142	Formate Dehydrogenase real-time	GGACTATTCTGCCGTTCTATGACAG
ww143	Formate Dehydrogenase real-time	CAAACCAAGTCGTTGTTTTAATACCCAGTGC
ww138	Formate Acetyltransferase real-time	GCAATGAATATGATCAATTGTTCTCCGGCG
ww139	Formate Acetyltransferase real-time	CGGAAGCTGTTTTGGTCACGAGAGTAC
ww 149	<i>focA</i> real-time	CATTATGGTAGTGGTGTGCGGCTCC
ww 150	<i>focA</i> real-time	CTAAAACAATAAAAATTGCGCCGACGAAATTACCAC

29

ww123	Nitrate Reductase real-time	GCGTGCCGAAAGATGTGTTGGAAAATTTGG
ww124	Nitrate Reductase real-time	GGTCAGCAAATGGATGTTATAAATGAGGTGG
ww109	Nitrite Reductase <i>nrfD</i> real-time	GACAAAAAATGGTCGCCATGCACAACGCCCTAAG
ww110	Nitrite Reductase <i>nrfD</i> real-time	CGGGATGAGGATGCCGATAAGCATGAC
ww113	<i>hypF</i> real-time	GTGTTACACCACCACGCCACATCGTCAG
ww114	<i>hypF</i> real-time	CCTAAATAGTACGCGGCTTTTTCATCTGCCAGC
ww 147	Catalase real-time	GGTCATAAATTTTAACCAACGCAGAAGCGG
ww 148	Catalase real-time	GATTTGAATTCGCACGTTCCAACGGGG
ww129	<i>arcA</i> real-time	GAGTTCCGCGCCATGTTACATTTCTG
ww130	<i>arcA</i> real-time	CGTGATGATCTTCAAATGTTTACGAATTTCGAC
ww131	<i>arcB</i> real-time	GCAGACAGCAGAGGAAGAATTTGCGTTG
ww132	<i>arcB</i> real-time	CACTTCGCTACTGACGGTTAAATCGCC
ww133	<i>oxyR</i> real-time	GGACCTTATCTAATGCCTCATATCGTACC

ww134	<i>oxyR</i> real-time	CGGTACGGACGCTACAATAGCACAATC
ww127	<i>ahpD</i> real-time	GAGGTCGCCGCCGCACTTGCTATG
ww128	<i>ahpD</i> real-time	GTCTTTTTGTGATTGTAAGCTTCTAATGCGCGTAATG
ww151	Ferritin real-time	GGTTAAACTATTAACGACCAAATGAATTTAGAG
ww 152	Ferritin real-time	GCATATGTTGCATTTCTTCACCTGCGTG
ww88	<i>fepA</i> real-time	GGAAAATTAATGATCATTGGGACATTAATACG
ww89	<i>fepA</i> real-time	CTGCATTACGATAAATACGTTTATCTAAAATATTATTCACACCC
ww96	<i>FecCD</i> family permease real-time	GGCGTTTAAATTTGCTTTCTTTAGAGGAAGAAG
ww97	<i>FecCD</i> family permease real-time	CAATAAGCCGACCCAACCGATAATGC
ww111	<i>ccmF</i> real-time	GGGTATCGGACCGCTGGTAAAGTGGCG
ww112	<i>ccmF</i> real-time	CGACATCATGGTGCCGAGTACGGCGC
ww117	Fumarate Reductase real-time	GGTGTTGCTTTACGGTGTGATTTGTTGGG
ww118	Fumarate Reductase real-time	CGGTCATGTCAAATAATGTCACGGCGTG
ww119	Fumarate Hydratase real-time	GGTGAAAATCGGTTCGTACGCATTTAATGG
ww120	Fumarate Hydratase real-time	GCCGAGGGCTAATTGACGCAAATG
ww121	Oxaloacetate Decarboxylase real-time	CCATCGTGGCAACTTTGCAAGGCAC
ww122	Oxaloacetate Decarboxylase real-time	GCACTTGCGCCACCAAATTCGGCTG
ww125	Ammonia Aspartate Lyase real-time	GGCGCACCAATTGCAAGATGCGG
ww126	Ammonia Aspartate Lyase real-time	CGGTGCGACCTAAGTTCACTTCAAGC
ww136	2133 reverse sequencing	GAAATTGGGATAAAGTCTTTTACAATGAATGATGG
ww137	2134 reverse sequencing	GCAACGTCCTTCATTCTTTCTTTAGC
ww 154	D11S_1352 mutant upstream fragment 5'	GATTTATTTG <u>GCGGCCGC</u> CACCTACCCATTTATG
ww 155	D11S_1352 mutant upstream fragment 3'	GGCATCATCC <u>CTCGAG</u> AAGAATGGCAAG
ww 156	D11S_1352 mutant downstream fragment 5'	GCTAATCTGAAATACAGTTTCTAA <u>CTCGAG</u> TGAATGATATAAGAAAG
ww 157	D11S_1352 mutant downstream fragment 3'	GCGCGCTGTTTT <u>CTGCAG</u> TTACCTGCCTAG
ww 158	D11S_1352 deletion confirmation	CCGTTTACCTTGGGCAGTACCGGCC
ww159	D11S_1352 deletion confirmation	CGGCGGCGGAAACGTGATTTCTTCCAC

ww175 TonB dependent receptor complement 5'
ww176 TonB dependent receptor complement 3'

CAAGGACGTACCATGGGATCCAAAAAACTC
GCACTTTCTTATATCATTCATCTAGATTAGAAACTGTATTCAG

Microarray: A custom *A. actinomycetemcomitans* gene expression microarray (GE 8 X 15k per slide, 60-mer oligonucleotide probes) was printed by Agilent Technologies using oligonucleotide probes obtained from the OligoArray Database for *A. actinomycetemcomitans* D11S-1 at the University of Michigan

(<http://berry.engin.umich.edu/oligoarraydb/organismPage.php?ORG=Aggregatibacter%20actinomycetemcomitans%20D11S-1>). This database comprises 5638 oligonucleotides representing 2062 transcripts encoded by the *A. actinomycetemcomitans* D11S-1 genome. Of the 2062 transcripts, 1552 are represented by three independent oligonucleotide probes, 215 are represented by two probes and 221 by a single specific oligonucleotide. Each oligonucleotide was printed twice on the array; thus the majority of genes are represented by six separate spots on the array and no transcript is represented by fewer than two spots. Seventy two putative transcripts of *A. actinomycetemcomitans* D11S-1 are not represented in the oligonucleotide database; these mostly comprise hypothetical proteins (37) and transposases/integrases of mobile genetic elements (11).

A. actinomycetemcomitans 652 was cultured in CDM or in CDM supplemented with 50 μ M Ne and 100 μ M FeCl₂ to mid-log phase (roughly 16 hours after inoculation) as described previously. Labeling of RNA, microarray hybridization, array scanning and data analysis was carried out by the MicroArray Core Facility at the University of Louisville. Briefly, RNA was isolated using the Lipid Tissue Minikit (Qiagen) following the protocols supplied by the manufacturer. The quality of the isolated RNA was assessed using an Agilent 2100 Bioanalyzer (Agilent Technologies, Inc.). RNA samples were considered to have little or no degradation if they exhibited an RNA integrity number (RIN) greater than 9 [89]. Total RNA (100ng) was labeled with Cyanine 3-CTP using the Low Input Quick Amplification WT Labeling Kit for one color (Agilent Technologies). This kit uses random nucleotide-based T7 promoter primers to first

synthesize cDNA which is then reacted with T7 RNA polymerase in the presence of NTPs and Cyanine 3-CTP to generate labeled cRNA. The labeled cRNA was purified using the RNeasy Mini Elute kit (Qiagen) and total yield and Cy3 incorporation efficiency was determined using a NanoDrop Technologies spectrophotometer.

Array hybridizations were carried out using the Agilent Gene Expression Hybridization kit as described by the manufacturer. Briefly, 600ng of each labeled cRNA sample was incubated at 60°C for 30 min and then hybridized to the custom *A. actinomycetemcomitans* gene expression array at 65°C for 17 hours. After hybridization, the microarray slides were washed with Agilent gene expression wash buffer 1 at 37°C for 5 minutes followed by wash buffer 2 at 37°C for 1 minute. After hybridization and washing, the slides were scanned using an Agilent microarray scanner (Model G2505C) set for one-color using the green channel and 5 µm resolution. The one-color microarray images (.tif) were extracted with the aid of Feature Extraction software (v 9.5.1, Agilent Technologies). The raw data files (.txt) were imported into GeneSpring (GX 11.1) and the data were transformed to bring any negative or value <0.01 to 0.01. Normalization was then performed using a per-chip 75 percentile method that normalizes each chip on its 75 percentile to facilitate comparison among chips. A per-gene on median normalization was then performed to normalize the expression of every gene on its median among samples. An expression threshold of ≥2-fold was applied and the differentially expressed genes were evaluated using a pair-wise t-test and genes with p-values <0.05 were considered to be significantly up- or down-regulated.

cDNA synthesis & qRT-PCR: cDNA synthesis was carried out using the cDNA Synthesis Kit (Quanta) as per manufacturer's instructions. qRT-PCR was then carried out with the Applied Bioscience using 50ng of cDNA, 250nM specific primer (Table 3) and PerfeCTa SYBR Green Fastmix Low Rox (Quanta). The protocol was as follows: 95°C for 3 minutes for 1 cycle, 95°C for

15 seconds and 60°C for 30 seconds for 45 cycles, with extension and annealing occurring at 60°C. The threshold cycle for each qRT-PCR was determined from a second derivative plot of total fluorescence as a function of cycle number by using the software package supplied with the. All gene-specific threshold values were normalized against the values measured from primers specific to the 5S rRNA. qRT-PCR was carried out in triplicate with two independent measurements.

cDNA RACE: The Rapid Amplification of cDNA Ends (RACE) allows for the amplification of messenger RNA and its subsequent sequencing. Primers were designed to specifically amplify the 5' end of cDNA for identification of the promoter region of the TA system, D11S_2133-2134. The GeneRacer kit (Invitrogen) was used as per manufacturer's instructions. Briefly, RNA from the *ΔqseB* mutant was harvested as previously described and the 5' phosphate of truncated mRNA's or non-mRNA's was removed using calf intestinal phosphatase (CIP). The mRNA's were then treated with tobacco acid pyrophosphatase to remove the 5' cap. An RNA oligo of known sequence was then ligated on to the 5' end of the mRNA's and the mRNA is reverse transcribed. Primers specific for the ligated cDNA oligo and the gene of interest are then used to amplify a specific product. The resulting product is then gel purified and cloned into the pCR4-TOPO vector and transformed into Top10 competent cells. Transformed cells were then plated on LB agar plates supplemented with ampicillin (50ug/mL). Ten colonies were chosen and plasmid was purified using the Qiagen Plasmid Miniprep kit. The plasmids were digested with *EcoRI* to confirm insertion and also sequenced to determine the promoter region of the genes of interest.

Biofilms: *A. actinomycetemcomitans* was grown on saliva-coated coverglass in a polycarbonate flow chamber (model FC81; Biosurface Technologies Corp., Bozeman, MT). Chamber dimensions are 50.5 mm by 12.7 mm by 2.54 mm) at 25°C. Saliva was harvested, diluted 1:2 with ddH₂O, and filter sterilized. 50uL was then incubated for 30 min at 37°C on a coverglass (60 mm by 24 mm).

The saliva-coated coverglass was then washed with 1X phosphate-buffered saline (PBS) for 10 min at a flow rate of 5.8mL per hr using a multichannel peristaltic pump (ManoStat Sarah cassette; Fisher Scientific Co.). The flow cells were inoculated with a 40mL culture of *A. actinomycetemcomitans* (O.D._{600nm} 0.5-0.6) then allowed to incubate for one hour. Biofilms were fed with fresh media for 62 hours and then stained with 40mL of 0.2 mg/ml fluorescein isothiocyanate (FITC) in the dark and then washed with 1X PBS for 2 hours. Biofilms were visualized by using a Leica TCS SP8. Confocal images were captured from 5 randomly chosen frames from each flow chamber with each biofilm done in triplicate independently. Biofilm depth was determined by performing z-plane scans from 0 to 100 µm above the glass surface, and total biomass was determined by integrating fluorescence intensity across the z-stack using the Volocity software.

Metabolomics: Each cell sample was mixed in a glass vial with 500 µL CH₃CN, 375 µL H₂O and 250 µL CHCl₃. The mixture was grounded with 2 beads at 30 Hz for 2 min, followed by centrifugation at 4 °C and 13,000 rpm for 20 min. The bottom layer (lipid layer) was dried in speedvac after removing the liquid layer. Each dried sample was re-dissolved in 100 µL solution of chloroform:methanol (2:1, v:v) containing 1 mM butylated hydroxytoluene (BHT). The mixture was then split into two aliquots. One aliquot was diluted 10-fold using a methanol solution containing 0.1% acetate, 1 mM BHT and 1 µg/mL reserpine. This diluted sample was then analyzed on FTIRC-MS in positive mode. The other aliquot was also diluted 10 times using a methanol solution containing 5 mM ammonium acetate, 1 mM BHT and 1 µg/mL reserpine. This sample was analyzed on FTICR-MS in negative mode.

FTICR-MS experiment was performed on an FT-MS instrument (LTQ-FT; Thermo Electron Corporation, Bremen, Germany) equipped with a chip-based nanoelectrospray ionization (nESI) ion source (Triversa NanoMate) (Advion Biosciences, Ithaca, NY, USA). Each sample was

measured for 15 min and covered the $m/z = 150-1,600$ range. The mass spectra were recorded using Fourier Transform Ion Cyclotron Resonance (FTICR) in the profile mode, and the resolving power (RP) was set at 400,000 at $m/z = 400$. The maximum ion accumulation time was set at 1,000 ms. The ion optics was tuned for a typical precursor ion mass (taurocholic, m/z 514) in MS/MS mode with a normalized collision energy of 34 using the linear ion trap (LIT). The two most important nESI parameters were as follows: the spray voltage = -1.6 kV and the nitrogen gas pressure = 0.7 psi.

The FTICR-MS data was processed with a software package MetSign. For the metabolite quantification, the instrument data was first reduced into a peak list using second-order polynomial fitting (SPF) and Gaussian mixture model (GMM). For metabolite identification, each peak detected in the FTICR-MS data was first assigned to metabolite(s) recorded in LIPID MAPS, by matching the experimentally measured metabolite ion m/z value and the profile of the isotopic peaks with the corresponding theoretical data calculated from the chemical formula of database metabolites. The threshold for m/z variation was set as ≤ 3 ppm. After cross sample alignment, contrast normalization was performed to make the abundance of metabolites in all samples comparable. Pairwise two-tail t -test with up to 1,000 sample permutation was used to recognize metabolites with significant abundance difference between sample groups by setting p -value ≤ 0.05 .

Catalase Assay: Catalase activity was measured using the Catalase Assay Kit (Cayman Chemical, 707002). Briefly, *A. actinomycetemcomitans* was cultured in 35mLs of CDM with or without Ne, ferrous iron, or both for 24 hours. Cells were pelleted at 4,000g for 10 minutes at 4°C. Pelleted cells were homogenized by sonication in 800 ml of 1X Sample Buffer and then centrifuged at 16,000xg for 5 min at 4°C. A standard curve was constructed using the Catalase Formaldehyde Standard provided with the kit for different concentrations (0, 5, 15, 30, 45, 60, 75 mM) diluted

in 1X Sample Buffer. Assays were performed in a 96 well plate and the catalase positive control, standards, and samples were done in triplicates. Each well contained 1X Assay Buffer, methanol, and one of the following: catalase positive control, standard or sample of interest. The catalase reaction was initiated by the addition of 0.035 M hydrogen peroxide, followed by incubation and shaking at room temperature for 20 minutes. The reaction was terminated by the addition of 10 M Potassium Hydroxide and Catalase Purpald. Covered plates were incubated with shaking at room temperature for 10 minutes. Finally, Catalase Potassium Periodate was added, and the covered plates were incubated shaking at room temperature for 5 minutes. Absorbance was read at 570 nm.

Protein Gels: At 8 hours post-inoculation, 1mL aliquots of *A. actinomycetemcomitans* cultures were used to measure the O.D._{600nm}. 30mL cultures were diluted to similar densities and then pelleted by centrifugation. The cell pellet was re-suspended in 1mL of phosphate buffer (0.5M KH₂PO₄) pH 8 and homogenized by sonication. The cell lysate was centrifuged at 4°C for 5 minutes at 13,000xg to separate the soluble and non-soluble fractions. The soluble fraction was removed to a clean tube and the non-soluble fraction was re-suspended in 1mL of phosphate buffer containing 8M urea. Protein concentration of cell extracts was determined using a BCA assay. 1X of LDS 5X Sample Buffer (141mM Trizma base, 2% lithium dodecyl sulfate, 10% glycerol, 0.51mM EDTA, 0.22M Serva Blue G, 0.175mM Phenol Red, pH 8.5) (LifeTechnologies) was added to roughly 1ug of protein and then loaded on a NuPAGE Novex 4-12% Bis-Tris Protein gel (LifeTechnologies). The gel was run for 50 minutes at 200V. The gel was stained for one hour with shaking with AquaStain (Bulldog Bio) and then washed with water and visualized.

Construction of TonB Dependent Receptor Mutant: *A. actinomycetemcomitans* 652 deletion mutants (Table 1) used in this study were constructed by allelic replacement of the target gene by double homologous recombination using a suicide vector pJT1 [\[90\]](#). Briefly, the flanking

regions of a fragment of the TonB dependent receptor were amplified by PCR using *A. actinomycetemcomitans* chromosomal DNA as a template with two primer sets: ww154/155 & ww156/157. Each primer was flanked with a restriction site as stated above (Table 1). The 1.8kb and the 393 base pair PCR products were digested with *NotI*-*XhoI* and *XhoI*-*PstI* respectively, and both PCR fragments were cloned adjacent to each other (joined by the *XhoI* restriction site) into *NotI*-*PstI*-digested pJT1 suicide vector to create pWAW23. The recombinant suicide plasmid was introduced into *A. actinomycetemcomitans* by electroporation. The cells were incubated for 5 h at 37 °C and plated onto BHI agar containing 50 µg spectinomycin (Sp) ml⁻¹ to select for cells with single recombinant crossover events. Sp-resistant (Sp^r) colonies were selected and grown statically in BHI broth for 24 hr at 37 °C. On the next day, each culture was diluted 1: 200 in tryptone–yeast-extract (TYE) broth and grown for 24 h at 37 °C. This step was repeated for 3 consecutive days, except that the cultures on day 3 were grown in the presence of 1 mM IPTG. Afterwards, to select bacteria with a second recombination event resulting in the deletion of the target gene, cells were diluted 10-fold and spread onto TYE agar supplemented with 1 mM IPTG and 10% sucrose and grown for 24 h at 37 °C. Sucrose-resistant (Suc^r) colonies were selected and replica plated onto TYE agar supplemented with sucrose and onto BHI agar supplemented with spectinomycin. Spectinomycin-sensitive (Sp^S) colonies were selected to perform PCR to confirm the deletion of the target gene. Sp^S colonies that were PCR-positive for the appropriate gene deletion were chosen for further analysis. Primer sets used to verify by PCR amplification the expected fragment and nucleotide sequence for each isogenic mutant were: ww158 & ww159.

Construction of TonB Dependent Receptor Complemented Strains:

For construction of the TonB dependent receptor, complement primers amplifying the entire

TonB dependent receptor were PCR-amplified from *A. actinomycetemcomitans* chromosomal DNA using the primer set: ww175 & ww176. The resulting 2.1kb base pair PCR product was digested with *BamHI-XbaI* and cloned with *BamHI-XbaI* digested pWAW17 resulting in pWAW31.

Statistics:

All experiments were conducted in triplicates for at least three independent experiments. Data was analyzed by either two-tailed t-test or ANOVA using the InStat program (Graphpad).

Statistical differences were considered significant at the level of $p < 0.05$.

CHAPTER THREE: *A. ACTINOMYCETEMCOMITANS* QSEBC IS ACTIVATED BY CATECHOLAMINES
STRESS HORMONES AND IRON

Introduction:

Bacteria have evolved a specialized signaling transduction mechanism called the two-component regulatory system (TCS) as a way to quickly sense changes to the environment and adapt by changing gene transcription. QseBC is a TCS that is conserved in the *Enterobacteriaceae* and the *Pasteurellaceae* [126]. The *A. actinomycetemcomitans* QseC sensor kinase contains a highly conserved acidic motif (EYRDD) [69] and a similar motif (DYRED) in the *H. influenzae* QseC homolog (FirS) was shown to be essential for the response to ferrous iron [62]. *A. actinomycetemcomitans* QseBC shares 70% sequence similarity to the *E.coli* QseBC, but differs in the organization of the operon. In many of the *Enterobacteriaceae* and *Pasteurellaceae*, the *qseBC* locus is associated with a gene, designated *ygiW*, that encodes a putative periplasmic protein in the OB fold family [91], but transcription and genetic organization of *ygiW* relative to the *qseBC* operon varies. In many of the *Pasteurellaceae*, including *A. actinomycetemcomitans*, *ygiW* is co-transcribed with *qseBC* but there exists an attenuator region between them [53, 62]. *ygiW* also resides upstream of *qseBC* in many of the available *Enterobacteriaceae* sequences but in these organisms, it is transcribed from the opposite strand.

The signal that activates the QseC in *A. actinomycetemcomitans* has not yet been determined, but it has been shown that QseC regulates virulence and biofilm formation [44, 53]. The expression of *qseBC* is also regulated by AI-2, but the sensor is not directly activated by AI-2 [44]. *qseBC* is also part of the AI-2 regulon in *E.coli*, but quorum sensing-mediated regulation requires the toxin MqsR of the MqsAR TA system [71].

In this chapter we show that QseBC is activated by the combination of both catecholamines and iron (CAT-Fe). In addition, adrenergic receptor antagonists that functioned to block catecholamine mediated growth responses and QseC activation in *E. coli* are inactive against QseC in *A. actinomycetemcomitans* and at higher concentrations may function as QseC agonists. These results suggest that there may be significant differences in the structure of the *A. actinomycetemcomitans* QseC compared to either eukaryotic adrenergic receptors or the QseC in *E. coli*.

Results:

QseC is Not Activated by Catecholamines, Iron, Zinc, or Cold Temperatures

In order to determine the activating signal for QseBC, a *lacZ* reporter plasmid was constructed to take advantage of the fact that QseB auto-regulates the operon. The reporter plasmid, pDJR29, was created by fusing the promoter region for *ygiW-qseBC* to the *lacZ* gene. The strain was then tested in a chemically defined media (CDM) with a variety of conditions that were reported to activate the QseBC in other bacterial species. Increasing concentrations of the catecholamine norepinephrine (0-300 μ M) (Figure 1A), ZnCl₂ (Figure 1B), as well as temperatures down to 4°C (Figure 1C) failed to significantly stimulate QseC compared to the control condition of *A. actinomycetemcomitans* grown in CDM at 37°C. Supplementation of 100 μ M of ferrous or ferric iron failed to significantly stimulate the operon (Figure 2A). In addition, previous attempts to isolate AI-3 from *A. actinomycetemcomitans* failed suggesting that the bacteria does not make that particular quorum sensing molecule [69].

QseC is Activated by a Combination of Iron and Catecholamines

The combination of both ferrous and ferric iron and different catecholamines (i.e.

norepinephrine or epinephrine) were then tested for the ability to stimulate the QseBC operon since the individual components failed to do so (Figure 2A). Chemically Defined Media (CDM) supplemented with either 100 μ M ferrous or ferric chloride, 50 μ M of norepinephrine (Ne) or epinephrine (Ep), or a combination of both (CAT-Fe). Supplementation with either single component, iron or catecholamines, resulted in no significant induction of the operon as shown previously (Figure 2A).

In contrast, the combination of CAT-Fe resulted in a robust, significant induction of operon expression suggesting that both signals are required in activating QseBC in *A. actinomycetemcomitans* (Figure 2A). The activation of QseC occurred with either norepinephrine or epinephrine and with either ferrous or ferric iron, in contrast to the *qseBC* homolog in *H. influenza* which responds only to ferrous iron.

To determine if CAT-Fe activation of the QseC sensor was autoinduced and dependent on a functional QseBC, pJDR29 was transformed into non-polar gene deletion mutants of *A. actinomycetemcomitans* that lacked *ygiW*, *qseC* or *qseB* ($\Delta ygiW$, $\Delta qseC$ and $\Delta qseB$, respectively), or into a strain in which *qseC* was replaced by a copy of the *qseC* gene that did not encode the periplasmic region of the sensor kinase (*qseC* Δ p). As shown in Figure 2B, *lacZ* expression in CDM alone was reduced by approximately 4-fold in the $\Delta ygiW$, $\Delta qseC$ and $\Delta qseB$ strains and no induction of *lacZ* expression occurred in the presence of Ep/FeCl₂. These results are consistent with our previous finding that *ygiW-qseBC* is auto-regulated by QseC-mediated activation of QseB [53]. Importantly, no Ep/FeCl₂-dependent induction of *lacZ* occurred in *A. actinomycetemcomitans* that expressed a QseC protein that lacked the periplasmic domain (Figure 2B). These results suggest that Ep and Fe⁺² function as signals that activate the QseC sensor and require its periplasmic domain.

To confirm that Ep/FeCl₂-dependent induction of *lacZ* was mediated by QseB, a family of reporter plasmids containing a nested series of *ygiW-qseBC* promoter deletions were tested (Figure 3A). These constructs were previously described and were used to map the -10, -35 and QseB binding sites in the *ygiW-qseBC* promoter [53]. As shown in Figure 3B, *ygiW-qseBC* promoter activity was reduced by approximately 35% when nucleotides -94 to -138 were deleted (compare pDJR63, pDJR57 and pDJR56). However, Ep/FeCl₂-dependent induction of *lacZ* expression still occurred in each of these constructs. Ep/FeCl₂-dependent induction of *lacZ* was significantly reduced only after deletion (pDJR58) or site specific mutation (pDJR86) of the QseB binding site (Figure 3B). This indicates that the interaction of QseB with its binding site is essential for Ep/FeCl₂-dependent induction of the operon and is consistent with a model where catecholamines and iron represent signals that are recognized by and activate QseC, which in turn activates the QseB response regulator.

The periplasmic region of *A. actinomycetemcomitans* QseC contains a sequence (EYRDD, residues 154-157) that resembles the DYRED motif previously shown to be important for the sensing of iron by the QseC paralogs of *H. influenzae* [62]. To determine if this motif in *A. actinomycetemcomitans* is important for Ep/FeCl₂-dependent activation of QseC, EYRDD was altered to EAADD by site-directed mutagenesis and the mutant (encoding QseC_{Y155A, R156A}) or wild type *qseC* alleles together with *qseB* were integrated by homologous recombination into the chromosome of *A. actinomycetemcomitans* $\Delta qseBC$ to generate strains $\Delta qseBC::61$ and $\Delta qseBC::46$, respectively. As shown in Figure 4, *lacZ* expression from pDJR29 in $\Delta qseBC::61$ was not significantly induced when cells were cultured in CDM supplemented with Ep and FeCl₂. In contrast, $\Delta qseBC::46$ exhibited a ~5-fold increase in *lacZ* activity, similar to the wild type (Figure 4). However, *lacZ* expression in $\Delta qseBC::61$ was approximately 90-fold higher than in the wild type strain even when cultured in CDM alone (Figure 4). These results suggest that QseC_{Y155A,}

R156A cannot sense Ep/FeCl₂ but may be locked in an activated conformation that results in constitutive activation of QseB and high expression of the *ygiW-qseBC* operon.

Adrenergic Receptor Antagonists Fail to Block CAT-Fe Activation of QseC

QseC has been shown to play an essential role in both virulence and biofilm formation. Therefore, it can be considered a target for any potential therapeutics as a way to modulate the course of infection. Based on the ability of QseC to sense catecholamines in *E. coli*, it was suggested that the sensor acts as a bacterial adrenergic receptor, the eukaryotic receptors that recognize and respond to catecholamines [55, 102]. Adrenergic receptor antagonists function to block the recognition of catecholamines by adrenergic receptors in eukaryotes. In *E. coli*, these same drugs have been shown to block catecholamine mediated stimulation of growth [80]. Therefore, both the alpha adrenergic receptor antagonist, phentolamine, and the beta adrenergic receptor antagonist, propranolol, were tested to determine if they could block CAT-Fe activation of QseC.

Both the alpha-blocker phentolamine and the beta blocker propranolol were tested from 0 μ M to 400 μ M to determine if they were able to block *ygiW-qseBC* activation and also induction of the operon in response to CAT-Fe. At concentrations below 400 μ M, both adrenergic receptor antagonists were unable to block CAT-Fe mediated activation of QseC (Figure 5A & B). Interestingly, both receptor antagonists alone were able to activate *qseBC* at 400 μ M (Figure 5 C) suggesting that at higher concentrations both drugs might act as QseC agonists. Activation by propranolol or phentolamine was dependent on the QseC periplasmic domain since a mutant lacking the periplasmic domain had no significant induction of the operon in response to either propranolol or phentolamine (Figure 5D).

Discussion:

The QseBC TCS has been shown previously to play a vital role in pathogenesis of periodontitis by regulating both biofilm formation and virulence , but little was known about how it controls these two complex phenotypes or the genes that are regulated by this TCS. In *E. coli* and *S. enterica*, catecholamines and a quorum sensing molecule designated AI-3 have been shown to activate Qse [61]. Previous work has shown no evidence for the production of AI-3 in *A. actinomycetemcomitans*, nor is QseC activated by reduced temperatures or zinc. Instead, our results show that a combination of iron, either ferrous or ferric, and catecholamines, e.g. epinephrine or norepinephrine, results in significant induction of the operon and the response to CAT-Fe is dependent on having a functional periplasmic sensory domain. Thus, the response of the *A. actinomycetemcomitans* QseC differs from *H. influenzae* in that it occurs with either ferrous or ferric iron and from its *E. coli* counterpart since activation of *A. actinomycetemcomitans* QseBC requires both catecholamines and iron. Ferric iron does cause an activation of *qseBC* in *E. coli*, but not directly [60]. The iron activates the PmrB sensor which in turn activates the PmrA response regulator which in turn binds to the *qseBC* promoter and induces *qseBC* expression [60]. Interestingly, the QseB binding site of the *ygiW-qseBC* promoter region in *A. actinomycetemcomitans* is identical to the consensus PmrA binding sequence of *E. coli* suggesting that in *A. actinomycetemcomitans* these two TCS might have integrated into one that responds to both catecholamines and iron.

It remains unclear as to how CAT-Fe is binding QseC: whether both the catecholamine and iron bind as a complex or if there are separate binding sites for both catecholamine and iron and activation of QseC only occurs when both sites are occupied. When comparing the amino acid sequence between eukaryotic adrenergic receptors and QseC there is no striking structural similarity that would allow for identification of the catecholamine binding pocket. The differences between eukaryotic adrenergic receptors and QseC is also evident from the data

that in *A. actinomycetemcomitans*, drugs that are used as adrenergic receptor antagonists in eukaryotes do not antagonize Cat-Fe binding and may even function as QseC agonists at higher concentrations. In addition the inhibition of growth in the presence of high concentrations of adrenergic receptor antagonists has not been previously observed in *E.coli* or *Salmonella*. This result suggests that these drugs might be toxic to *A. actinomycetemcomitans* at high concentration. Although it has been previously reported that some beta adrenergic receptor antagonists can act simultaneously as agonists and antagonists at high concentration, this has never been observed for propranolol or any of the alpha blockers [127].

Based on the results from the β -galactosidase assay, YgiW may play a role in QseC activation by CAT-Fe since the $\Delta ygiW$ mutant did not show significant induction of the operon in the presence of Ne/FeCl₂. It is possible that YgiW may play a role in delivering catecholamines, iron, or both to QseC since it is a putative periplasmic solute binding protein. One other possible explanation for the failure of Ne/FeCl₂ to induce *qseBC* expression is that the overall level of transcription of the operon may be blocked in the $\Delta ygiW$ strain. This might occur since a transcriptional attenuator exists between *ygiW* and *qseB* and transcription of *qseBC* could be significantly reduced due to the proximity of the transcriptional attenuator to the *qseB* start codon in the $\Delta ygiW$ strain. Therefore, further experiments are needed to determine if YgiW can interact with CAT-Fe or QseC.

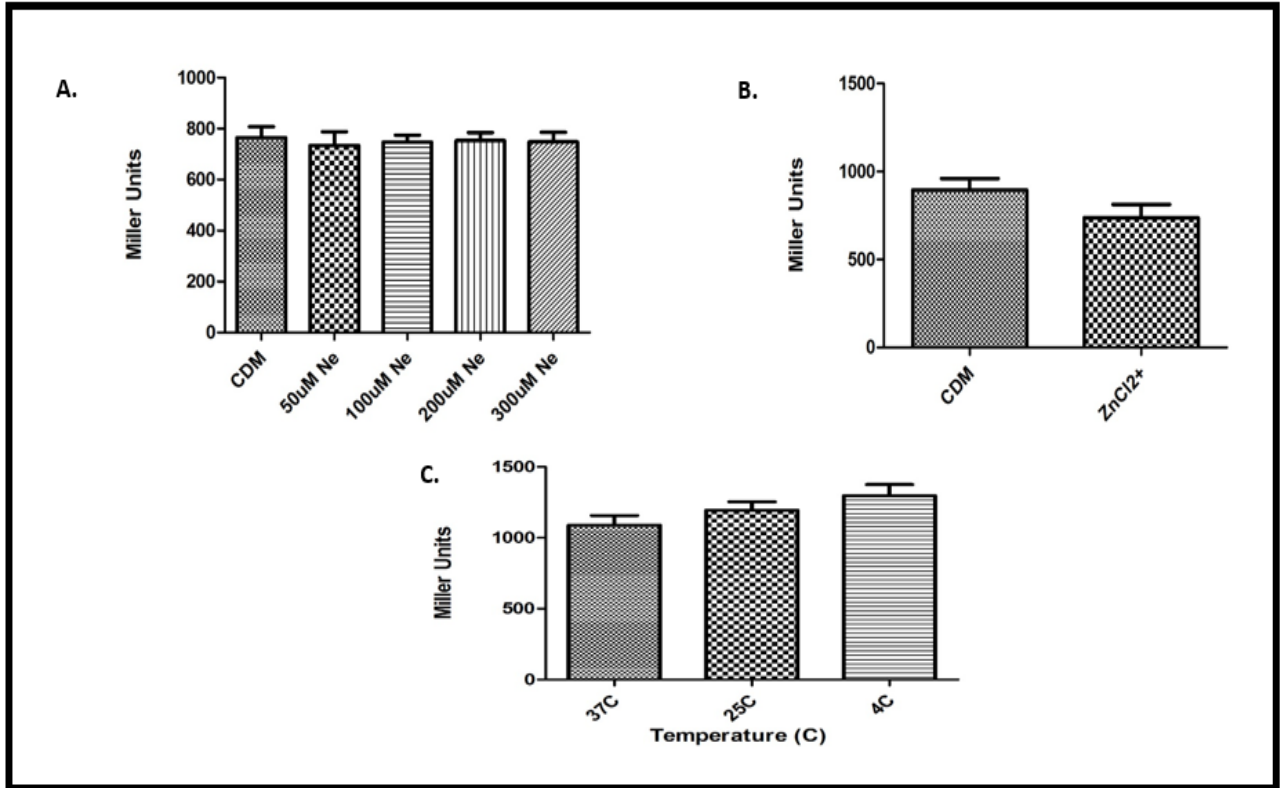


Figure 1: Expression of the *ygiW-qseBC* operon in *A. actinomycetemcomitans* cultures exposed to increasing various stimuli. β -galactosidase activity was determined after 24 hours of growth. Significant differences ($p < 0.05$) are indicated by asterisks and calculated from two independent triplicate experiments by ANOVA. **A.** *A. actinomycetemcomitans* 652 harboring the *ygiW-qseBC* promoter-*lacZ* reporter plasmid pDJR29 was grown in CDM broth and compared to those grown in CDM supplemented with increasing concentrations of catecholamine (norepinephrine Ne). **B.** *A. actinomycetemcomitans* harboring pDJ29 grown in CDM broth and compared to a culture grown in CDM supplemented with 15µM ZnCl₂. **C.** *A. actinomycetemcomitans* harboring pDJ29 grown in CDM broth at 37°C then shocked for 15 minutes at 37°C, 25°C, or 4°C.

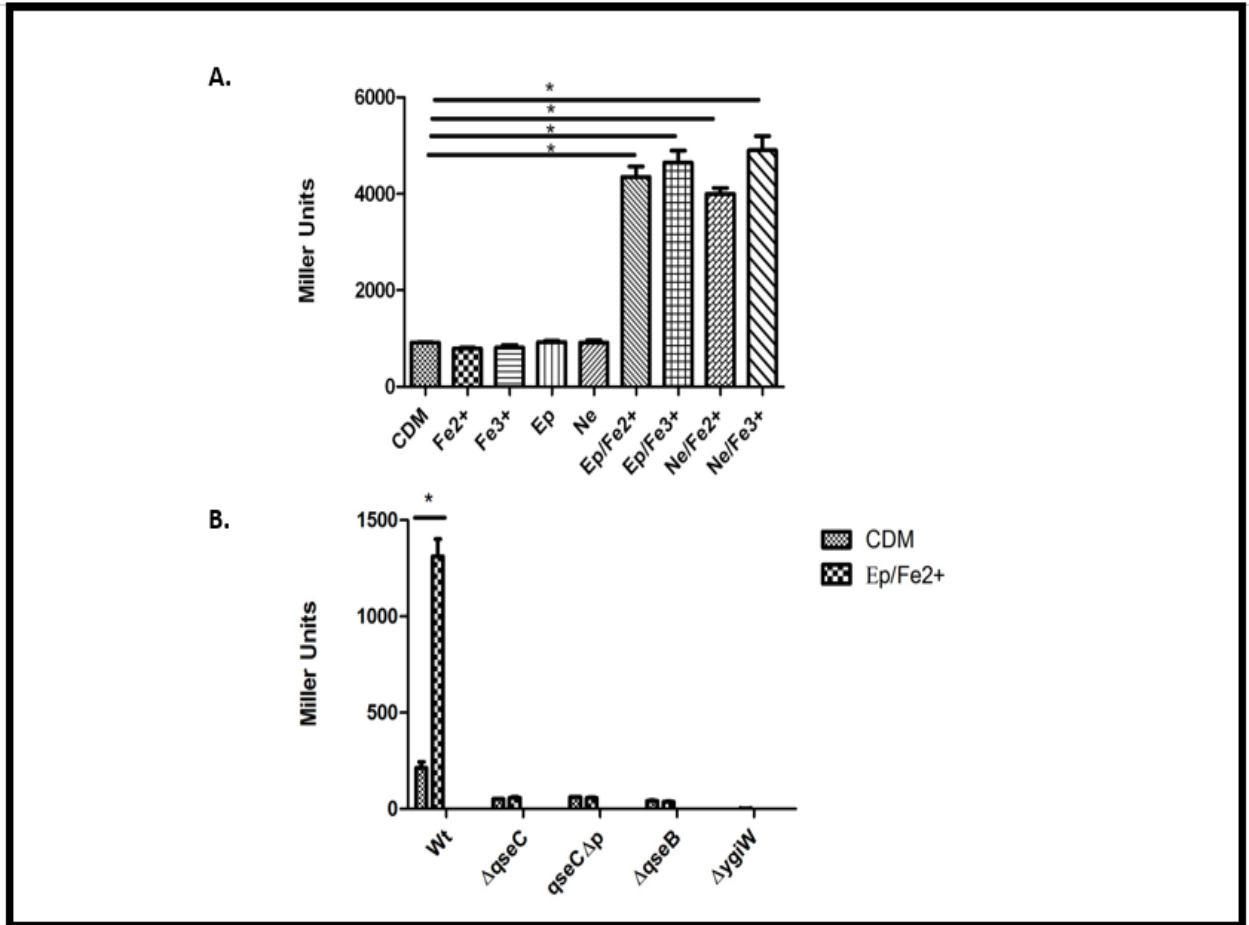


Figure 2: Expression of the *ygiW-qseBC* operon in *A. actinomycetemcomitans* cultures exposed to increasing various stimuli. β -galactosidase activity was determined after 24 hours of growth. Significant differences ($p < 0.05$) are indicated by asterisks and calculated from two independent triplicate experiments by ANOVA. **A.** Expression of the *ygiW-qseBC* operon in *A. actinomycetemcomitans* cultures exposed to catecholamines and iron. *A. actinomycetemcomitans* 652 harboring the *ygiW-qseBC* promoter-*lacZ* reporter plasmid pDJR29 was grown in CDM broth and compared to those grown in CDM supplemented with either ferrous or ferric chloride (Fe2+ or Fe3+; 100uM), epinephrine (Ep; 50uM), norepinephrine (Ne; 50uM), or a combination of both catecholamine (50uM) and iron (100uM). **B.**¹ Expression of *ygiW-qseBC* in either the Wt strain, $\Delta qseC$, a strain lacking the periplasmic domain of QseC (*qseCΔp*), $\Delta ygiW$, or $\Delta qseB$ grown in CDM broth or CDM supplemented with Ep/FeCl₂

¹ Experiments performed in Figure 2B for the $\Delta qseC$, $\Delta qseB$, and *qseCΔp* mutant were performed by Drs. Ascension Torres-Escobar and Maria Delores Juarez-Rodriguez.

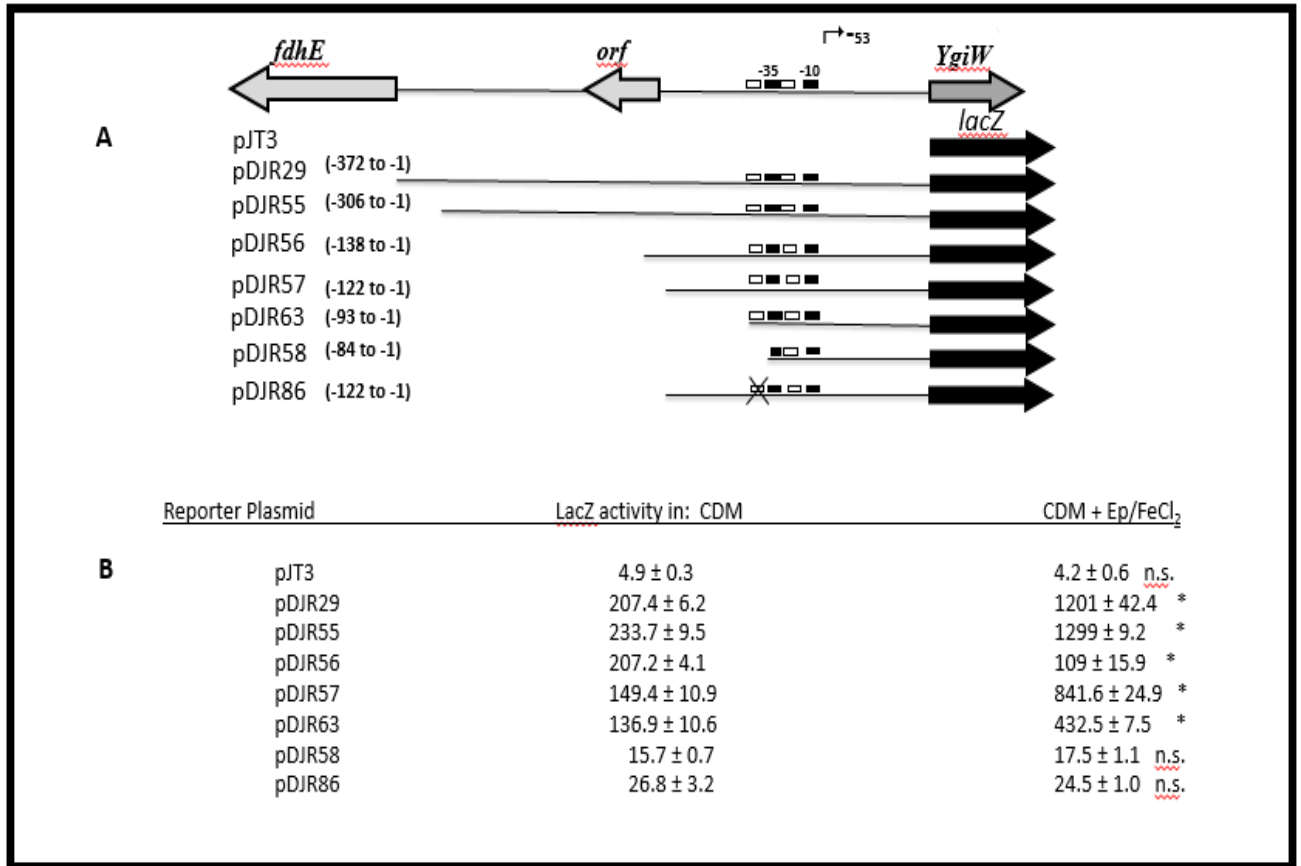


Figure 3²: CAT-Fe-dependent induction of *ygiW-qseBC* requires a functional QseB binding site. **(A)** Schematic diagram of the *ygiW-qseBC* promoter region and transcriptional fusion constructs pDJR29, pDJR55, pDJR56, pDJR57, pDJR63, pDJR58, pDJR85 and pDJR86 [53, 101] showing the binding regions for QseB (white boxes), the -10 and -35 promoter elements (black boxes) and the primary transcriptional start site (bent arrow). Site specific mutations in the QseB binding site are indicated with the x symbol. The numbering of the nucleotides is relative to the *ygiW* translational start codon. **(B)** β -galactosidase activity in *A. actinomycetemcomitans* 652 transformed individually with each reporter plasmid. Cultures were grown in CDM or CDM supplemented with Ep (50 μ M) and FeCl₂ (100 μ M) and β -galactosidase activity was determined after 24 h of growth. Values are means of results from three independent experiments \pm standard deviations. Statistical analysis was performed by using one-way analysis of variance (ANOVA) followed by Tukey's multiple-comparison test. Significant differences ($p < 0.05$) are indicated by asterisks; n.s., not significant.

² Experiments shown in Figure 3 were performed by Drs. Ascension Torres-Escobar and Maria Delores Juarez-Rodriguez.

The EYRDD motif regulates the QseC response to Ep/FeCl₂

Strain	LacZ activity in:		fold induction
	CDM	CDM + Ep/FeCl ₂	
WT	280.6 ± 44.0	1240.0 ± 207.6	4.4 (p<0.05)
<u>ΔqseBC::46</u>	273.2 ± 26.7	1422.0 ± 234.2	5.2 (p<0.05)
<u>ΔqseBC::61</u>	25,066 ± 11,041	17,246 ± 10,247	n.s. ¹

1 - not significant

Figure 4³: The CAT-Fe induction of *ygiW-qseBC* is dependent on a putative conserved iron responsive motif, EYRDD. Point mutations were constructed in the EYRDD motif resulting in QseC Y155A, R156A, which was designated as ΔqseBC::46. The complemented strain with a fully functional EYRDD motif was designated ΔqseBC::61. Each strain was tested for QseC activation through the use of the pDJR29 reporter plasmid in a β-galactosidase assay and compared to that same strain grown in CDM without any supplementation.(n.s. not significant)

³ Experiments shown in Figure 4 were performed by Drs. Ascension Torres-Escobar and Maria Delores Juarez-Rodriguez.

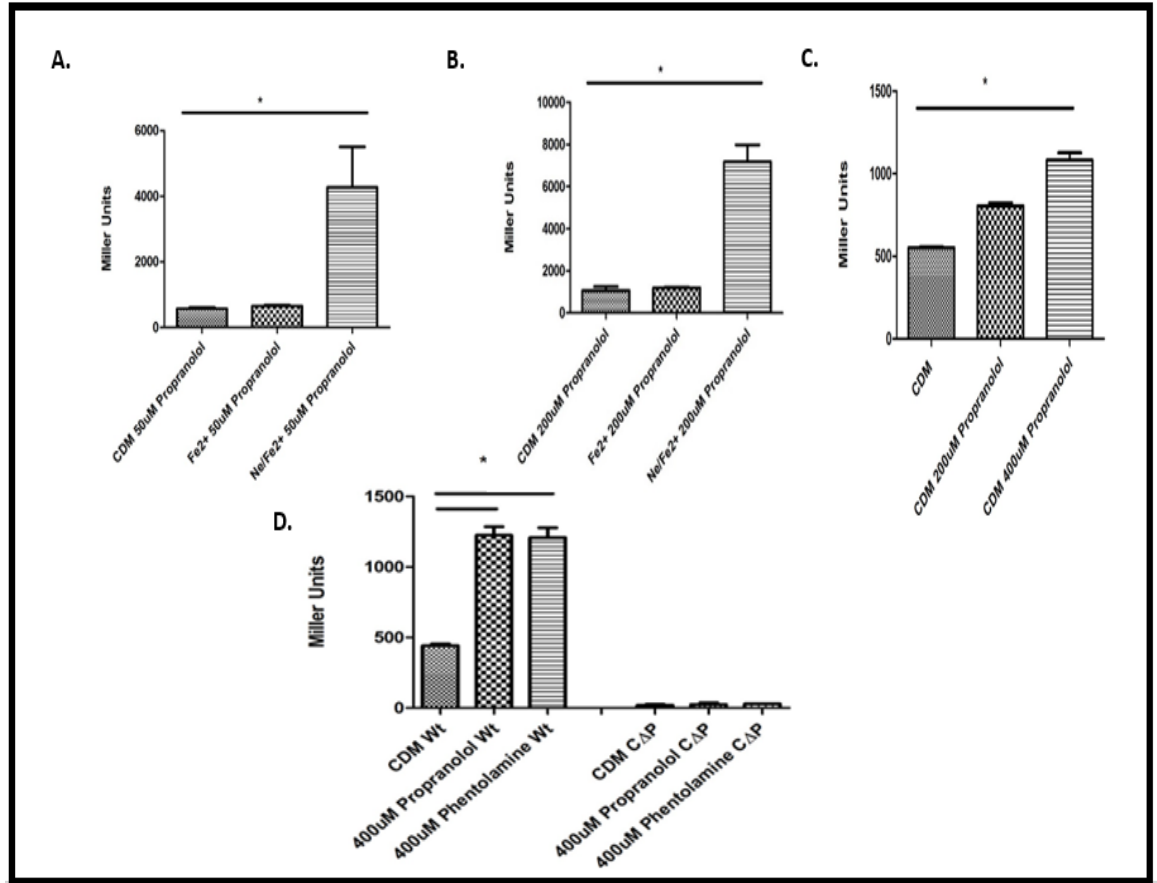


Figure 5: QseC is activated by adrenergic receptor antagonists. A & B. *lacZ* activity of a strain of *A.*

actinomycetemcomitans harboring the pDJR29 reporter plasmid cultured in CDM supplemented with ferrous iron or Ne/Fe2+ with 50µM of propranolol (A) or 200µM (B). C. Increasing concentrations of the beta adrenergic receptor antagonist propranolol (0-400µM) was added to *A. actinomycetemcomitans* harboring the reporter plasmid pDJR29 and grown in CDM. D. Wt *A. actinomycetemcomitans* or a strain lacking the periplasmic domain of QseC (*qseCΔp*) cultured in CDM with 400µM of phentolamine or propranolol. All experiments were done in triplicate with two independent trials. P < 0.05.

CHAPTER FOUR: QSEBC IS A GLOBAL REGULATOR OF *A. ACTINOMYCETEMCOMITANS*
METABOLISM, OXIDATIVE STRESS RESPONSE, AND IRON ACQUISITION

Introduction:

QseC has been previously shown to be essential for biofilm formation since a mutant lacking a functional QseC had significant reduction of biofilm formation in *A. actinomycetemcomitans* [44, 53]. This same strain was also significantly attenuated in a mouse model of periodontitis [44]. In addition, QseC has also been suggested to act as a global regulator of metabolism in *E. coli* [50]. Together this suggests that QseC plays a vital role in several essential pathogenesis mechanisms.

In the previous chapter, we showed that the QseC responds to the combination of catecholamines and iron, suggesting that it acts as a bacterial adrenergic receptor. The field of microbial endocrinology has evolved in order to characterize the functional outcomes of catecholamine and other hormone exposure on microbes [57]. The downstream outcomes of CAT-Fe exposure on *A. actinomycetemcomitans* was unknown. Although the regulon that is under the control of QseBC that is differentially regulated in the presence of catecholamines in *E. coli* is known, many of these genes do not exist in *A. actinomycetemcomitans*. For example, catecholamines have been shown to result in an up-regulation of motility associated genes, but *A. actinomycetemcomitans* is non-motile [119]. This suggests that the regulons for *E. coli* and *A. actinomycetemcomitans* evolved in a species specific manner.

Catecholamines are also thought to be used as a vector for the acquisition of an essential nutrient, iron [57]. Free iron is normally limited in the body, therefore bacteria have

evolved a wide range of mechanism to acquire it. The use of siderophores, such as enterobactin, vibriobactin, and yersiniabactin, is often a common tactic employed by bacteria to acquire iron. Siderophores work by sequestering iron at a higher affinity than host iron-binding proteins. The siderophores are then recognized by the bacteria and taken up via specific receptors and transport machinery. The ligands siderophores use to capture iron can vary, such as hydroxamate in ferrichrome or catecholates in enterobactin, which uses the same mechanism by which catecholamines can scavenge iron [57]. A variety of iron acquisition and regulatory mechanisms have been associated with virulence as well as biofilm and growth stimulation [128].

A. actinomycetemcomitans employs a wide-variety of mechanism by which to acquire iron. It can directly bind heme, and hemoglobin and lactoferrin [97-100], but so far no evidence has been found to suggest that it can synthesize any kind of siderophore. However, *A. actinomycetemcomitans* encodes a putative enterobactin transporter and receptor (D11S_1352-1357). One possible function of this operon in *A. actinomycetemcomitans* is that it imports enterobactin made by other oral pathogens, but it is also possible that it might function in catecholamine mediated iron acquisition. The catecholamine mediated growth induction seen in *E. coli* was dependent on a functional enterobactin biosynthesis and transport system, suggesting that it plays a vital role in the acquisition of catecholamines [58]. Taken together this evidence could explain the role of stress in the development of periodontitis since stress is associated with the development and exacerbation of periodontitis.

In this chapter, we characterize the QseBC regulon and show that exposure to CAT-Fe results in an up-regulation of genes encoding proteins involved in anaerobic respiration and metabolism. In addition, exposure to CAT-Fe up-regulates genes involved in the oxidative stress while down-regulating genes involved in iron acquisition, fatty acid, lipid and LPS biosynthesis.

Finally, we also show that QseBC stimulates biofilm formation and planktonic growth, which is contingent on having a functional QseC periplasmic domain and a functional TonB dependent receptor.

Results:

CAT-Fe exposure Induces Genes Involved in Anaerobic Respiration and Metabolism and Increases the Flux through the TCA Cycle

To characterize the QseBC regulon, a custom microarray was designed using oligonucleotide probes from the OligoArray Database for *A. actinomycetemcomitans* D11S at the University of Michigan. cDNA from Wt cultures grown in either CDM or CDM supplemented with Ne/FeCl₂ was hybridized to the array. There were 235 genes (roughly 11.5% of the *A. actinomycetemcomitans* genome) that were differentially regulated by 2-fold or greater when exposed to Ne/FeCl₂ compared to cells grown in just CDM (Appendix Table 1). Of these 235 genes, 135 genes were down-regulated and 99 genes were up-regulated and for many of these genes, the array results were confirmed by qRT-PCR (Appendix Table 1). In confirmation with the previous β -galactosidase assays, one of the most highly up-regulated operons with norepinephrine and iron treatment was *ygiW-qseBC*, and this was also confirmed with qRT-PCR. Interestingly, there was no significant change in expression of many of the well-characterized virulence factors: *tad* fimbriae and the collagen adhesin, EmaA. Other virulence determinants such as the cytolethal distending toxin was down-regulated around 1.5 fold and the biofilm lipoprotein *pgaB* and the leukotoxin (*ltxA* and *ltxC*) were down-regulated around 2.1 fold. Leukotoxin expression was also confirmed on a SDS-PAGE gel where the band correlating to the leukotoxin (116kDa) was reduced in CAT-Fe exposed cells (Figure 6).

Of the 99 genes up-regulated with Ne/FeCl₂ treatment, 56 of those genes encoded

proteins associated with anaerobic respiration and metabolism (Table 4). The differentially regulated genes included genes encoding proteins for a hydrogenase complex, metabolism of aspartate, fumarate, malate, oxaloacetate, pyruvate and formate, and reduction of nitrate, DMSO, trimethylamine-N-oxide, fumarate and formate. Six differentially expressed operons encoded components associated with anaerobic electron transport, e.g., the *nap* operon (D11S_0205–0210), an operon involved in the biogenesis of c-type cytochromes (D11S_2000–1990), the hydrogenase-4 complex and *hydN* (D11S_1735–1747 and D11S_1092-1093) involved in electron transport from formate to hydrogen and the oxidation of hydrogen, D11S_1412-1413 involved in trimethylamine N-oxide anaerobic respiration, and D11S_0493-0494 encoding a dimethylsulfoxide terminal reductase.

At least four additional induced operons and several other singlet genes encode proteins that may also be associated with anaerobic metabolism. D11S_0303 and D11S_1771 each encode a C4 dicarboxylate transporter involved in the utilization of aspartate and fumarate. Consistent with this, D11S_0597 encodes aspartate ammonia lyase which converts aspartate to fumarate, D11S_0810–0812 encodes a fumarate reductase, and D11S_1061 encodes fumarate hydratase. Other up-regulated operons code for oxaloacetate decarboxylase (D11S_1379-1381) which converts oxaloacetate to pyruvate. Other genes associated with anaerobic metabolism included D11S_1748-1749 and D11S_1986-1989 which encode formate dehydrogenase and catalyze the formate dependent reduction of nitrite to ammonia, respectively.

Since several of the genes that were differentially regulated were involved in formate metabolism, an extracellular formate assay was performed using supernatants from cultures grown in CDM with or without Ne/FeCl₂. Formate levels were significantly increased in supernatants from cultures supplemented with Ne/FeCl₂ compared to CDM (Figure 7) confirming

predictions based on observations from the microarray.

Since the microarray results and the formate assay suggested that significant changes to the metabolic profile of *A. actinomycetemcomitans* occur upon activation of QseBC, a metabolomics approach was used to confirm changes in metabolites suggested by the changes in gene expression and to further examine the overall global metabolic changes that occur in response to CAT-Fe. Water soluble and lipid soluble fractions were isolated from *A.*

actinomycetemcomitans cultured in CDM with or without supplementation Ne/FeCl₂ and were analyzed by mass spectroscopy as described in Materials and Methods (Chapter 2). The first group of metabolites that were significantly changed were metabolites involved in carbon metabolism. Data from the water soluble fraction (Table 5) were consistent with changes suggested by the microarray as there were significant increases in fumarate, malate, aspartate, and mannose. Combining the data from both the microarray and the metabolomics approaches suggest that there may be an increase in flux through glycolysis from the import of mannose and increase in Glucose-6-phosphate, as well as an increase in activity of the TCA cycle since many of the enzymes and intermediates of the TCA cycle are induced or increased (Figure 8). However, succinate levels were decreased most likely due to efficient conversion to fumarate. These pathways converge into the formation of pyruvate which can then be channeled to energy forming pathways such as fermentation or anaerobic respiration via the electron transport chain (Figure 8).

Treatment with Ne/FeCl₂ also resulted in an increase of gluconic acid, 6-phosphogluconate, and glucose-6-phosphate compared to cells grown in CDM alone (Table 5). These metabolites are associated with the Entner–Doudoroff pathway that catabolizes glucose to pyruvate and suggest that Ne/FeCl₂ treatment results in stimulation of part of this pathway. *A.*

actinomycescomitans does not have a complete Entner-Duodoroff pathway but does possess the genes of the pathway that result in the production of pyruvate and glyceraldehyde 3-phosphate, which is eventually converted to pyruvate. This represents one of many pathways, including oxaloacetate decarboxylase that is up-regulated in *A. actinomycescomitans* and leads increased pyruvate levels.

The metabolism of several amino acids was also significantly altered. The most striking is the increase in the levels of aspartate. This amino acid can feed into the TCA cycle through its conversion to fumarate and the gene encoding the enzyme that carries out this reaction, aspartate ammonia lyase was also significantly induced. In contrast, treatment with Ne/FeCl₂ resulted in a significant decrease of cysteine and tyrosine and consistent with this, the microarray data showed down-regulation of the tyrosine-specific transport protein (D11S_1053) and the cysteine synthase subunit alpha (D11S_1533).

CAT-Fe Results in an Up-Regulation of the Oxidative Stress Response

In addition to inducing genes involved in anaerobic metabolism, Ne/FeCl₂ treatment also up-regulates genes involved in the oxidative stress response. The up-regulated genes associated with oxidative stress included quinol peroxidase (5-fold; D11S_1676), alkylhydroperoxidase *ahpD* (4-fold; D11S_0383), catalase (1.4-fold; D11S_2121), and the oxidative stress response regulator *arcA* (1.8-fold; D11S_1888). In order to confirm changes in catalase activity, a catalase activity assay was performed with cell lysates from cultures grown in CDM alone or CDM supplemented with either Ne, FeCl₂, or Ne/FeCl₂. As shown in Figure 9B, catalase activity was significantly increased in cells grown with Ne/FeCl₂ supplementation compared to cells grown in CDM alone.

In order to determine if the changes in gene expression and catalase activity correlated with changes in the ability of the bacteria to respond to oxidative stress, an assay was performed

to measure growth of *A. actinomycetemcomitans* after exposure to H₂O₂ stress. Cells were cultured in CDM with or without supplementation with Ne, FeCl₂, or Ne/FeCl₂. At mid-log, the cultures were split into two aliquots. One aliquot was then exposed to the H₂O₂ stress for 15 minutes and the other served as a control. Growth was then assessed 5 hours and 12 hours later (only 5 hours shown). Cells exposed to Ne/FeCl₂ had a significant increase in survival after exposure to H₂O₂ compared to cells grown in CDM, norepinephrine or ferrous iron suggesting that CAT-Fe exposure results in a greater resistance to oxidative stress (Figure 9A).

It has been reported previously that high iron levels can lead to the formation of hydroxyl radicals [115, 116] which may explain the up-regulation of genes involved in oxidative stress. In addition, the up-regulation of ferritin also suggests high intracellular iron levels. Therefore, we determined if the up-regulation in oxidative stress genes and catalase activity in Ne/FeCl₂ treated cells could be explained by a significant increase in intracellular iron. An intracellular iron assay was performed with cell lysate from cells grown in CDM supplemented with either FeCl₂ or Ne/FeCl₂. Surprisingly, there was no significant differences in intracellular iron content for cells grown in CDM or cells grown in Ne/FeCl₂ (Figure 9C), although only cells grown in CDM with Ne/FeCl₂ showed significant up-regulation of oxidative stress genes, catalase activity, and had a significant reduction of inhibition of growth in the presence of H₂O₂ stress.

CAT-Fe Results in a Down-Regulation of High Affinity Iron Acquisition Genes and Up-Regulation of Ferritin

The genes that were down-regulated with Ne/FeCl₂ exposure were more diverse in their putative functions. However, twenty of the 135 down-regulated genes (~15%) encode proteins associated with high affinity iron transport (Table 6). Within this group, four operons encode putative ABC-type iron transporters (e.g., D11S_0621-0622, D11S_815-818, D11S_1128-

1131 and D11S_1557-1558). Other down-regulated genes encode putative outer membrane iron receptors (D11S_1630 and D11S_1864) and consistent with this, the expression of *tonB* components (D11S_487-489) are also reduced by approximately 5-fold. This suggests that CDM supplemented with Ne/FeCl₂ may represent an iron replete environment and consistent with this, the iron storage protein ferritin was induced by over 10-fold in the array experiment. Together these results suggest that Ne/FeCl₂ exposure increases intracellular iron storage capacity and decreases high affinity iron acquisition transporters.

CAT-Fe Exposure Down-Regulates Fatty Acid, Lipid and LPS Biosynthesis and Dramatically Changes the Lipid Profile in *A. actinomycetemcomitans*.

The most notable group of metabolites that were decreased in the water soluble group after treatment with Ne/FeCl₂ were fatty acids including myristic acid, palmitelaidic acid, palmitic acid, nonanoic acid, and hydroxymyristic acid. Using a 2-fold cutoff in the microarray experiment, there was not a notable change in the transcription of genes encoding enzymes involved in fatty acid biosynthesis. However, using a 1.5-fold cutoff showed a consistent down-regulation of genes involved in fatty acid, lipid and LPS biosynthesis (see Table 7). Some notable examples include acyl coA thioesterase (D11S_0833) which converts palmityl-coA to palmitic acid, an operon involved in forming long chain fatty acids from acetyl coA (D11S_0525-0526), *rfaL* (D11S_0359), and a gene encoding a lipopolysaccharide heptosyltransferase *rfaF* (D11S_0203). In addition, several genes encoding various lipoproteins were down-regulated such as D11S_1952, the lipoprotein *vacJ* (D11S_0144), D11S_0631, and D11S_0745. There was also a significant up-regulation of 2.2-fold of D11S_2125, the gene encoding a putative long-chain-fatty-acid--CoA ligase-like, which is involved in fatty acid degradation.

Together these data suggest that there may be a substantial alteration of the plasma

membrane in response to CAT-Fe. Consistent with this, the lipid soluble data from the metabolomics approach identified numerous lipid species that were increased or decreased in response to CAT-Fe exposure (see Table 8). While many of these metabolites could not be specifically identified by mass spectroscopy, the results suggest that for cells exposed to CAT-Fe, there may be a decrease of long-chained fatty acids (Table 8). Treatment with Ne/FeCl₂ also resulted in a significant up-regulation of an isoprenoid, which is a class of molecules that include the quinones and hydroquinones. These molecules can function in electron transport which is consistent with the induction of electron transport systems observed in the microarray results.

Discussion:

Although the QseBC regulon and downstream functional outcomes of catecholamine exposure have begun to be characterized for *E.coli* and *Salmonella* spp., little was known about the response of *A. actinomycetemcomitans*. However, given that many of the QseBC-regulated genes of *E. coli* are not present in the *A. actinomycetemcomitans* genome, it is likely that the QseBC regulon differs significantly. Indeed in *E.coli*, catecholamines induce a variety of virulence factors, but using a custom genomic microarray, we showed that under conditions in which QseBC is activated (i.e., CAT-Fe exposure) the expression of many of the well-characterized *A. actinomycetemcomitans* virulence factors, e.g., tad fimbriae, autotransporter epithelial cell adhesins, and EmaA were unchanged or decreased slightly (e.g., the leukotoxin, *pgaB*, and the cytolethal distending toxin). Approximately 11% of the *A. actinomycetemcomitans* genome was differentially expressed upon exposure to CAT-Fe and 63% of these genes were organized into operons where at least one other gene in the operon was also differentially regulated.

The most striking result was the induction of associated with anaerobic respiration and metabolism, which suggests that a primary function of QseBC is to prime the cell for growth in

an anaerobic environment. These results were further confirmed using a metabolomics approach and together, our results suggest that the activation of QseBC increases metabolism and energy production through glycolysis and the TCA cycle to generate pyruvate, which can subsequently feed into various fermentation pathways and/or anaerobic electron transport mechanisms.

Interestingly, many of the QseBC-regulated genes identified in this study were also shown to be induced using RNA-seq in an *in vivo* abscess model of *A. actinomycetemcomitans* virulence but not when *A. actinomycetemcomitans* was grown as an *in vitro* biofilm [52]. In that study, Jorth *et al* reported that 14% of the genome was differentially regulated by 2-fold or greater when *A. actinomycetemcomitans* grown *in vivo*, and many of the differentially regulated genes encoded proteins and enzymes that were involved in anaerobic respiration and metabolism [52]. Thus, we can speculate that in Jorth *et al.* [52], QseBC may sense catecholamines released by neutrophils responding to the infection [25, 74] and may be essential for priming cellular metabolism for the host environment, e.g., the anaerobic environment of the subgingival pocket. Furthermore, *A. actinomycetemcomitans* may be exploiting this aspect of the host response via QseBC to detect catecholamines and iron in order to acquire this essential nutrient. Finally, since QseBC does not significantly regulate the expression of *A. actinomycetemcomitans* virulence factors, the shift in metabolism that occurs upon activation of the TCS may represent the primary role of QseC in virulence.

Surprisingly, there was also an up-regulation of genes associated with the oxidative stress response along with an increase in catalase activity. The induction of oxidative stress genes was unexpected given the apparent metabolic shift towards anaerobic metabolism and respiration. One possibility is that *A. actinomycetemcomitans* is often exposed to H₂O₂ in the oral cavity,

produced either from the neutrophil respiratory burst or by other oral organisms such as *Streptococcus gordonii*. Therefore, an increase in expression of oxidative stress genes and resistance to H₂O₂ may be required to both persist in a complex microbial community and evade the host response. Alternatively, it has been reported that high iron levels can induce oxidative stress via hydroxyl radical formation via the Fenton reaction [115, 116]. If hydroxyl radicals from iron were the cause of the oxidative stress, then a significant increase in intracellular iron in CAT-Fe treated cells would be expected relative to ferrous iron treated cells. However, there was no significant differences in intracellular iron content for cells grown in CDM or cells grown in CAT-Fe (Figure 4E), although only cells grown in CDM with CAT-Fe showed significant up-regulation of oxidative stress genes, catalase activity, and had a significant increase in survival in the presence of H₂O₂ stress. Therefore, the increase in genes associated with oxidative stress does not appear to be caused by iron toxicity. Consistent with this, the up-regulation of ferritin suggests that iron is being safely sequestered by iron storage proteins where it is less likely to cause damage to the cell via radical formation. Catecholamines have been shown to induce oxidative stress in eukaryotic cells via their breakdown by monoamine oxidase. A search of the *A. actinomycetemcomitans* genome did not identify a gene with homology to this enzyme but the metabolomics results did identify putative breakdown products of norepinephrine in *A. actinomycetemcomitans*. The mechanism of catecholamine degradation in *A. actinomycetemcomitans* is not currently known, but this may represent another possible mechanism for inducing oxidative stress and genes involved in the oxidative stress response. It has also been previously reported that catecholamines can induce oxidative stress genes in *P. gingivalis* and *Burkholderia pseudomallei*, although the mechanisms behind the induction are not clear.

An additional group of genes that were differentially expressed upon exposure to CAT-

Fe encoded iron acquisition transporters. In general, these operons were significantly down-regulated, suggesting that CDM supplemented with CAT-Fe represented an iron replete medium and that under these conditions, *A. actinomycetemcomitans* does not require high affinity iron uptake systems. Interestingly, expression of the putative enterobactin transport/receptor operon was unchanged when cells were exposed to CAT-Fe, suggesting that it may be the main iron uptake system that is present in cells grown in CAT-Fe supplemented medium. In contrast to iron transport operons, ferritin was significantly up-regulated by 10-fold, suggesting that the bacteria required an increase in iron storage. This is consistent with cellular growth in an iron replete environment and the need to safely sequester high levels of intracellular iron.

Lastly, CAT-Fe exposure dramatically changed the lipid profile of *A. actinomycetemcomitans* and resulted in down-regulation of genes involved in fatty acid, and lipid and LPS biosynthesis. Since LPS is an endotoxin and one of the pathogen associated molecular patterns (PAMP), the down-regulation of LPS synthesis may aid in the persistence of the pathogen and evasion of killing by immune cells. In addition, the significant decrease in several fatty acids, most notably stearic and myristic acid is interesting since these fatty acids are often used to modify leukotoxin, and important virulence factor. Interestingly, leukotoxin expression was also significantly down-regulated. The functional outcomes of the changes in the lipid profile of the cell are still unknown. In cells exposed to CAT-Fe, there appeared to be a decrease in long-chained fatty acids (Table 8). This may result in greater fluidity in the plasma membrane. Interestingly, a change in membrane fluidity has been shown to act a mechanism of regulation of TCS and specifically, temperature dependent membrane fluidity regulates the activation status of the DesK sensor kinase of *Bacillus subtilis*. We can speculate that QseBC-mediated signaling may be influenced by changes in membrane fluidity.

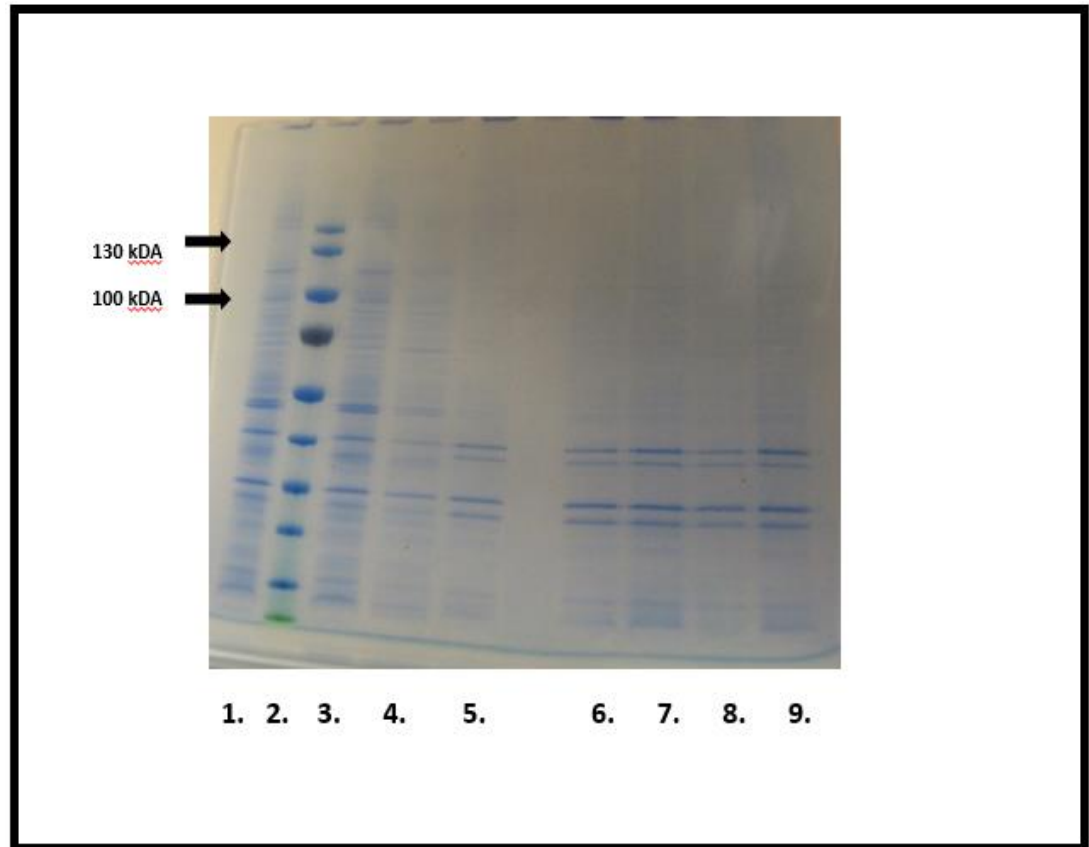


Figure 6: Leukotoxin expression in response to Ne/FeCl₂. Whole cell extract from cells grown in triplicate from two independent experiments was run on a PAGE gel and stained to visualize proteins. A representative gel is shown in Figure 6. The lanes on the representative gel were as follows: 1) the soluble fraction of *A. actinomycetemcomitans* grown in CDM, 2) ladder, 3) the soluble fraction of cells grown with ferrous iron supplementation, 4) the soluble fraction of cells grown with Ne supplementation, 5) the soluble fraction of cells grown with Ne/FeCl₂ supplementation, 6) the insoluble fraction of cells grown in CDM 7) the insoluble fraction of cells grown with ferrous iron supplementation, 8) the insoluble fraction of cells grown with Ne supplementation, 9) the soluble fraction of cells grown with Ne/FeCl₂ supplementation. The band for the leukotoxin appears at 116 kilodaltons.

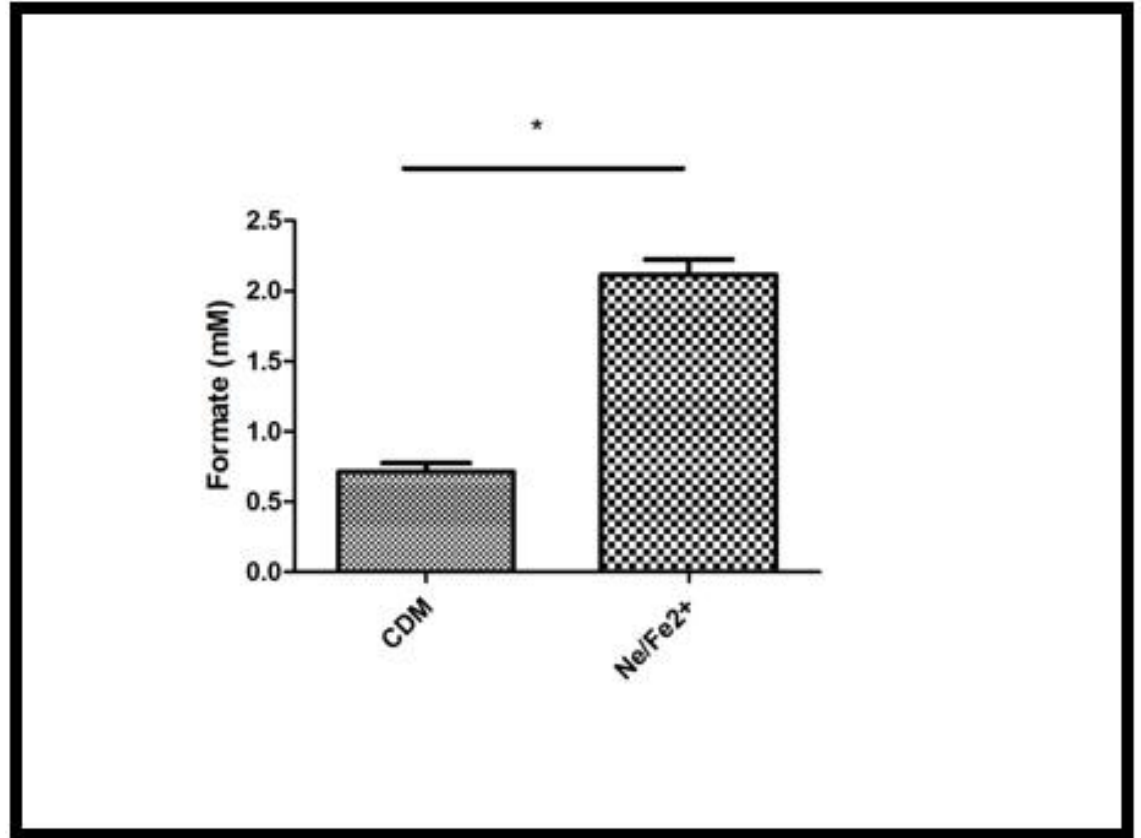


Figure 7: Extracellular concentration of formate. Supernatant from *A. actinomycetemcomitans* was collected from cultures grown in CDM or with Ne/Fe²⁺ supplementation and analyzed for extracellular formate. Formate concentrations were determined from two independent experiments performed in triplicate. Statistical significance is determined from a $p < 0.05$.

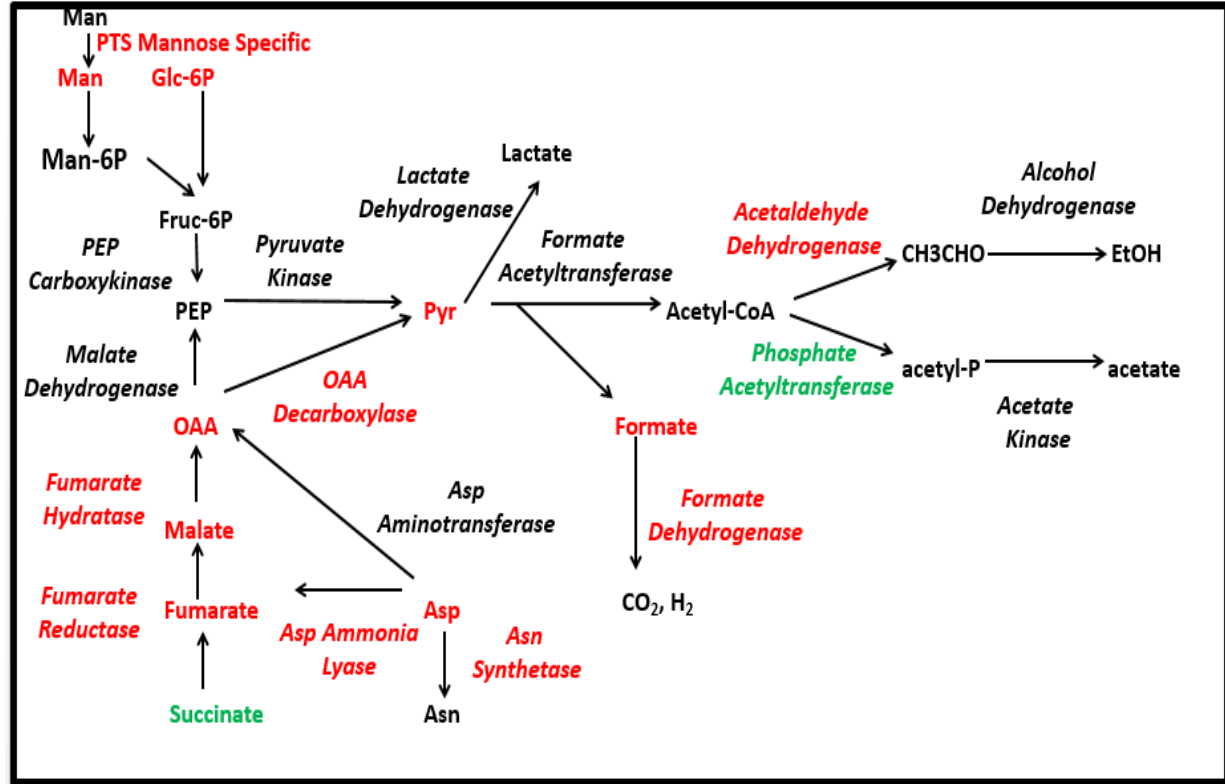


Figure 8: Changes in metabolic flux in *A. actinomycetemcomitans* in response to CAT-Fe exposure as suggested by metabolomics and microarray data. Metabolites and enzymes in red are increased or up-regulated, ones in green are decreased or down-regulated, and ones in black experienced no change.

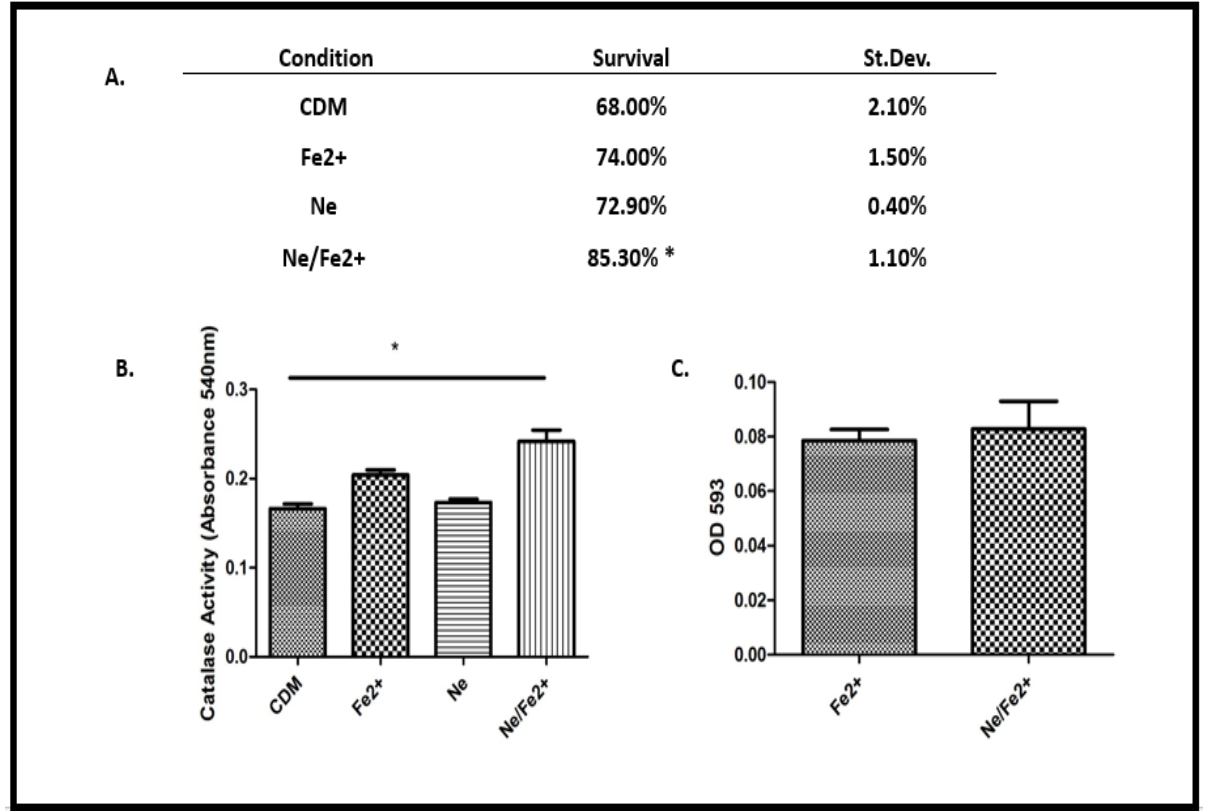


Figure 9: Oxidative stress response resulting from exposure to Ne/FeCl₂. A) *A. actinomycetemcomitans* was grown for 16 hours in CDM with or without Fe²⁺, Ne, or both and then stressed for 15 minutes with H₂O₂ or rested. Growth was measured by O.D._{600nm} 5 hours afterwards and inhibition of growth in response to H₂O₂ was calculated and subtracted from 100 to get percent survival. B) *A. actinomycetemcomitans* grown in CDM with or without Fe²⁺, Ne, or both was lysed after 24 hours and analyzed for catalase activity. C) The intracellular iron content for cells cultured in CDM with Fe²⁺ or Ne/Fe²⁺ as measured by O.D._{540nm} by the reaction of free iron from cell lysate with Ferene S. All experiments were done in triplicate with two independent trials. P < 0.05.

Table 4 Genes Associated with Anaerobic Metabolism

ID Tag	Product	Fold Change	P-Value
D11S_0205	cytochrome c-type protein TorC	3.05	3.52E-06
D11S_0206	periplasmic nitrate reductase, diheme cytochrome	2.94	2.25E-06
D11S_0207	ferredoxin-type protein NapH	3.36	1.20E-05
D11S_0208	quinol dehydrogenase periplasmic component	2.74	1.28E-05
D11S_0209	periplasmic nitrate reductase, large subunit	4.92	7.68E-06
D11S_0210	NapD protein	6.69	7.91E-07
D11S_0303	anaerobic C4-dicarboxylate membrane transporter	2.41	5.75E-05
D11S_0493	anaerobic dimethyl sulfoxide reductase chain A	2.26	1.52E-04
D11S_0494	anaerobic dimethyl sulfoxide reductase chain B	2.23	9.61E-06
D11S_0495	anaerobic dimethyl sulfoxide reductase chain C	1.85	2.10E-03
D11S_0809	fumarate reductase subunit D	1.95	6.12E-04
D11S_0810	fumarate reductase subunit C (Fumarate reductase	2.39	1.51E-05
D11S_0811	fumarate reductase iron-sulfur subunit	2.39	2.15E-05
D11S_0982	glycerate dehydrogenase	1.66	1.76E-03
D11S_1092	hydrogenase accessory protein HypB	1.80	3.50E-05
D11S_1093	hydrogenase expression/formation protein HypD	1.57	1.16E-03
D11S_1094	hydrogenase expression/formation protein HypE	1.40	2.01E-03
D11S_1256	cytochrome c-type biogenesis protein CcdA	1.56	2.29E-03
D11S_1257	peptide methionine sulfoxide reductase	1.72	6.12E-04
D11S_1264	glycerol-3-phosphate dehydrogenase, (gpd-m)	1.95	1.75E-02
D11S_1376	hydrogenase assembly chaperone HypC/HupF	1.88	6.28E-05
D11S_1379	oxaloacetate decarboxylase gamma chain 3	4.74	3.30E-07
D11S_1380	oxaloacetate decarboxylase alpha subunit	4.44	3.21E-07
D11S_1381	oxaloacetate decarboxylase beta chain	4.31	2.69E-06
D11S_1412	cytochrome c-type protein TorY	7.68	3.50E-05

D11S_1413	trimethylamine-n-oxide reductase 2	4.67	1.16E-03
D11S_1735	[NiFe] hydrogenase maturation protein HypF	2.58	8.83E-04
D11S_1736	electron transport protein HydN	18.44	5.00E-09
D11S_1737	hydrogenase-4 component B	14.93	1.54E-08
D11S_1738	hydrogenase-4 component B	15.02	1.42E-09
D11S_1739	hydrogenase-4 component C	10.68	1.60E-07
D11S_1740	hydrogenase-4 component D	10.59	3.57E-08
D11S_1741	hydrogenase-4 component E	7.95	5.22E-07
D11S_1742	hydrogenase-4 component F	7.76	4.85E-08
D11S_1743	hydrogenase-4 component G	5.89	1.38E-07

69

D11S_1744	hydrogenase-4 component H	5.87	3.07E-07
D11S_1745	hydrogenase-4 component I	5.40	5.18E-07
D11S_1746	hydrogenase-4 component J	4.62	8.70E-08
D11S_1747	hydrogenase maturation peptidase Hycl	4.79	1.03E-06
D11S_1748	formate dehydrogenase H	10.42	5.29E-09
D11S_1749	formate dehydrogenase, alpha subunit	10.01	5.95E-08
D11S_1771	C4-dicarboxylate membrane transporter	1.73	1.02E-05
D11S_1811	bifunctional acetaldehyde-CoA/alcohol dehydrogenase	2.72	1.04E-06
D11S_1888	TorCAD operon transcriptional regulatory protein	1.86	1.62E-04
D11S_1982	cytochrome C-type biogenesis protein	1.95	5.63E-04
D11S_1984	cytochrome c-type biogenesis protein CcmF	3.87	1.84E-05
D11S_1986	NrfD protein	11.60	1.14E-07
D11S_1987	cytochrome c nitrite reductase, Fe-S protein	13.63	4.20E-07
D11S_1988	cytochrome c nitrite reductase, pentaheme	17.09	2.38E-09
D11S_1989	nitrite reductase (cytochrome; ammonia-forming)	18.44	5.00E-09

D11S_1993	cytochrome c-type biogenesis protein CcmH	1.57	1.41E-03
D11S_1995	cytochrome c-type biogenesis protein CcmF	2.39	5.05E-05
D11S_1996	cytochrome c-type biogenesis protein CcmE	2.45	3.65E-06
D11S_1997	Heme exporter protein D (CcmD)	2.66	5.69E-07
D11S_1998	CcmC	3.16	7.34E-06
D11S_1999	heme exporter protein CcmB	2.69	1.88E-06
D11S_2000	heme ABC exporter, ATP-binding protein CcmA	3.30	1.80E-05
D11S_2131	anaerobic ribonucleotide reductase-activating	1.84	8.83E-04

Table 5: Water Soluble Metabolites

Metabolite	Fold Change	P-value	Confirmed with Standard
Malic acid(S);(C) (Y)	3.22	7.25E-06	Yes
Fumaric Acid(Y)	3.15	4.35E-05	Yes
D-glucose 6-phosphate (Y)	2.30	2.03E-04	No
Succinic acid (C) (Y)	0.42	8.13E-04	Yes
Oxalic acid (Y)	1.89	8.22E-04	Yes
Gluconic acid, γ -lactone (Y)	1.52	6.42E-03	No
d-Mannose; d(+)-Mannose (Y)	1.56	1.68E-02	Yes
Lactic acid (C) (Y)	0.80	3.28E-02	Yes
L-Aspartic acid (C) (Y)	3.18	3.35E-03	Yes
4-Ketoglucose (Y)	1.17	3.21E-02	No
D-Galactofuranose 6-phosphate (Y)	2.50	9.73E-04	No
Hypoxanthine (Y)	1.78	3.28E-02	No
Uracil (Y)	1.99	3.26E-05	No
Cytosine (Y)	1.97	1.34E-04	No

2-amino-6-hydroxypurine (Y)	1.75	1.25E-03	No
Thymine (Y)	1.50	3.08E-03	No
Adenine (Y)	1.49	3.14E-03	No
2,6-Dihydroxypurine (Y)	1.65	1.76E-02	No
4-Hydroxypyridine; 4-Pyridinol (Y)	1.22	3.06E-02	No
5-oxo-L-Proline; L-Pyroglutamic acid; Pidolic acid (C) (Y)	1.29	3.06E-02	Yes
Tyrosine (Y)	0.78	4.01E-03	Yes
L-Cysteine	0.36	3.12E-03	Yes
L-Isoleucine(Y)	1.56	2.04E-02	No
Hydroxyproline (Y)	1.37	2.84E-02	No
Glycine (Y)	0.90	2.84E-02	No
Palmitelaidic acid (C) (Y)	0.34	1.23E-03	Yes
Myristic acid; Tetradecanoic acid (Y)	0.47	1.25E-03	Yes
Palmitic acid (Y)	0.67	3.12E-03	Yes
Myristoleic acid (Y)	0.51	5.79E-03	Yes
3-Hydroxymyristic acid,3-hydroxytetradecanoic acid (Y)	0.52	7.21E-03	No

Nonanoic acid; Pelargonic acid (Y)	0.73	3.27E-02	No
Pyroglutamic acid; PCA (Y)	1.83	1.89E-04	No
Putrescine; 1,4-Diaminobutane (Y)	0.44	1.81E-03	No
Ethanimidic acid (Y)	2.23	7.21E-03	No
Lanthionine (Y)	2.75	7.67E-03	No

Table 6: Genes Involved in Iron Acquisition

ID Tag	Product	Fold Change	P-value
D11S_0236	heme utilization protein	0.55	3.28E-02
D11S_0237	heme-utilization protein Hup	0.62	4.07E-03
D11S_0620	ferric cations import ATP-binding protein FbpC	0.57	3.49E-02
D11S_0621	iron(III)-transport system permease protein FbpB	0.18	1.94E-05
D11S_0622	ferric iron binding protein	0.19	1.30E-07
D11S_0815	iron(III) dicitrate transport ATP-binding	0.12	2.42E-05
D11S_0816	ABC transporter, iron chelate uptake transporter	0.11	1.72E-04
D11S_0817	iron(III) dicitrate transport system permease	0.17	6.78E-06
D11S_0818	iron(III) dicitrate-binding periplasmic protein	0.16	1.05E-06
D11S_0842	hemoglobin binding protein A	0.58	2.67E-02
D11S_1128	iron(III) dicitrate transport ATP-binding	0.22	3.94E-05
D11S_1129	iron(III) transport system permease protein	0.33	1.98E-03
D11S_1130	putative iron/heme permease	0.23	4.24E-04
D11S_1131	putative periplasmic siderophore binding protein	0.14	5.47E-05
D11S_1557	high-affinity Fe ²⁺ /Pb ²⁺ permease	0.25	3.03E-04
D11S_1558	high affinity Fe ²⁺ transporter	0.12	1.28E-05
D11S_1559	putative Fe ²⁺ permease	0.14	4.81E-05
D11S_1560	FtsX-like permease	0.16	3.33E-04
D11S_1809	heme acquisition system receptor	0.46	1.04E-04

**Genes Involved in Fatty Acid, Lipid and LPS
Synthesis**

Table 7

ID Tag	Product	Fold Change	P-value
D11S_0011	phosphatidylserine decarboxylase	0.71	2.80E-03
D11S_0033	phospholipase/carboxylesterase	0.63	3.49E-03
D11S_0077	acetyl-CoA:acetoacetyl-CoA transferase subunit	0.51	1.76E-02
D11S_0079	short chain fatty acids transporter	0.51	1.53E-02
D11S_0144	lipoprotein VacJ	0.50	5.55E-03
D11S_0166	PgaA	0.53	6.91E-03
D11S_0167	biofilm PGA synthesis lipoprotein PgaB	0.47	3.95E-06
D11S_0168	biofilm PGA synthesis N-glycosyltransferase	0.56	7.22E-03
D11S_0203	lipopolysaccharide heptosyltransferase II	0.70	1.03E-02
D11S_0250	UDP-3-O-[3-hydroxymyristoyl] glucosamine	0.67	1.71E-03
D11S_0253	lipid-A-disaccharide synthase	0.77	1.95E-02
D11S_0257	CDP-alcohol phosphatidyltransferase	0.72	5.28E-03
D11S_0259	phosphatidate cytidyltransferase	0.67	1.59E-03
D11S_0284	N-acetylmuramic acid 6-phosphate etherase	0.41	4.20E-05
D11S_0352	CDP-diacylglycerol--serine	0.52	1.74E-03
D11S_0359	RfaL protein	0.42	1.20E-03
D11S_0381	3-deoxy-D-manno-octulosonic acid kinase (KDO	0.78	1.95E-02
D11S_0394	glycerophosphoryl diester phosphodiesterase	0.59	1.12E-02
D11S_0525	beta-ketoacyl-ACP synthase IV	0.61	6.46E-04
D11S_0526	3-oxoacyl-(acyl-carrier-protein) reductase,	0.79	1.11E-02
D11S_0533	glycosyl transferase, family 2	0.54	3.33E-03
D11s_0534	glycosyl transferase, group 2 family protein	0.57	2.86E-02
D11S_0631	lipoprotein	0.65	1.83E-03
D11S_0745	lipoprotein, putative	0.65	6.93E-03

D11S_0829	monofunctional biosynthetic peptidoglycan	0.51	2.75E-04
D11S_0833	hypothetical protein; acyl-CoA thioesterase YciA	0.58	8.78E-04
D11S_0916	CDP-diacylglycerol--glycerol-3-phosphate	0.50	5.96E-04
D11S_0994	phosphatidylglycerophosphatase A	0.45	6.65E-03
D11S_1076	enoyl-[acyl-carrier-protein] reductase	0.75	4.95E-03
D11S_1181	acetyl-CoA carboxylase, carboxyl transferase,	0.80	9.47E-03
D11S_1219	3-deoxy-D-manno-octulosonate	0.49	2.82E-03
D11S_1221	tetraacyldisaccharide 4'-kinase	0.54	6.65E-03
D11S_1260	phosphoheptose isomerase (Sedoheptulose	0.79	1.94E-02
D11S_1320	2-acyl-glycerophospho-ethanolamine	0.82	3.25E-02
D11S_1369	3-deoxy-D-manno-octulosonate 8-phosphate	0.78	7.95E-03
D11S_1578	N-acetylglucosamine-6-phosphate deacetylase	0.66	3.58E-03
D11S_1610	lipid A biosynthesis (KDO)2-(lauroyl)-lipid IVA	0.62	4.48E-03
D11S_1612	peptidoglycan amidase MepA	0.78	3.13E-02
D11S_1667	HldE	0.59	4.36E-03
D11S_1668	lipid A biosynthesis lauroyl acyltransferase	0.36	3.73E-03
D11S_1704	lipopolysaccharide biosynthesis protein	0.63	1.59E-03
D11S_1944	UDP-2,3-diacylglucosamine hydrolase	0.72	8.05E-03
D11S_1945	1-acyl-sn-glycerol-3-phosphate acyltransferase	0.73	4.92E-03
D11S_1952	lipoprotein, putative	0.63	6.99E-03
D11S_2089	acetyl-CoA carboxylase, biotin carboxylase	0.80	4.04E-02
D11S_2104	prolipoprotein diacylglyceryl transferase	0.57	3.04E-03
D11S_2137	lipoic acid synthetase	0.52	3.00E-03
D11S_2154	fatty acid/phospholipid synthesis protein PlsX	0.43	2.01E-04

Table 8: Lipid Soluble Metabolites in Ne/FeCl₂

MetSign_ID	m/z	Fold_change (C/NF)	Class of molecule
C37H72O5	579.53	41.31	Diacylglycerol
C52H100N1O8P1	897.72	2.18	Diacylglycerolphosphocholine
C22H30O6	432.24	0.61	Isoprenoid
C20H26O6	404.21	0.60	Flavanoid
C37H70N1O8P1	686.48	0.61	Glycerophospholipid
C68H112O6	1024.85	16.65	Triacylglycerol
C42H78N1O10P1	786.53	0.45	Diacylglycerolphosphoserine
C39H76O5	642.60	11.71	Diacylglycerol
C37H72N1O8P1	688.49	0.59	Diacylglycerolphosphocholine
C18H34N1O10P1	438.19	1.77	Diacylglycerolphosphoserine
C39H76O5	647.56	2.81	Diacylglycerol
C64H112O6	977.85	3.73	Triacylglycerol
C18H28O11	438.20	1.24	Isoprenoid
C19H22O6	410.16	1.50	Isoprenoid
C30H42O6	516.33	3.46	Sterol
C30H56N1O8P1	588.37	0.25	Glucuronide
C16H30O2	253.22	0.50	Branched Fatty Acid
C42H70O5	689.49	0.69	Diacylglycerol
C35H68O5	591.50	2.26	Diacylglycerol
C21H36O5	391.24	0.41	Prostaglandin
C37H72O5	631.51	11.51	Diacylglycerol
C21H42N1O7P1	450.26	0.44	Glycerophosphocholine
C39H47N1O14	795.34	0.65	Polyketide
C57H108O6	906.85	14.04	Triacylglycerol

C40H76N1O10P1	760.51	0.25	Glycerophosphoserine
C24H24O6; C24H26O7	409.16	2.01	Polyketide
C35H67N1O8S1	660.45	0.59	Sphingolipid
C39H74N1O8P1	714.51	0.57	Glycerophosphoethanolamine
C59H112O6	934.88	5.28	Triacylglycerol
C37H74N1O8P1	714.50	0.29	Diacylglycerophosphocholine
C37H71O8P1; C39H74N1O8P1	738.50	0.12	Glycerophosphoethanolamine
C53H98N2O16	1017.68	5.17	Sphingolipid

CHAPTER FIVE: CAT-FE EXPOSURE STIMULATES BIOFILM FORMATION AND PLANKTONIC GROWTH OF *A. ACTINOMYCETEMCOMITANS*

Introduction:

Work done on *E. coli* and other bacteria has shown that catecholamines can stimulate planktonic growth and biofilm formation [119, 103, 58, 94]. This stimulation of planktonic growth is independent of a functional QseC [92], but biofilm formation is attenuated for a QseC mutant in the presence of catecholamines [119]. In addition, the stimulation of planktonic growth in *E. coli* can be blocked by the addition of adrenergic receptor antagonists [80, 55].

For *A. actinomycetemcomitans*, QseC is essential for biofilm formation [44,53]. A strain lacking *qseC* has a significant decrease in biofilm depth and mass compared to Wt, but no defect in planktonic growth is observed [44, 53]. It is unknown as to whether activation of QseC by CAT-Fe would result in any changes in planktonic growth or biofilm formation.

The microarray data in Chapter 4 showed a significant up-regulation 2.7 fold of the anaerobic ribonucleoside triphosphate reductase (D11S_2128) of fold. In addition, the metabolomics showed significant increases in every ribonucleoside (Table 5). The increase of flux to pyruvate and energy producing pathways (Figure 9) as well as the significant up-regulation of the ribonucleoside triphosphate and increase in the pool of available ribonucleosides suggested that CAT-Fe was priming the cell for rapid growth. Therefore, the effect of CAT-Fe exposure on planktonic growth and biofilm formation was explored.

Results:

A. actinomycetemcomitans QseC has been shown to be essential for biofilm formation

since a strain lacking *qseC* exhibited a significant reduction in biofilm depth and biomass [44, 53]. To determine if CAT-Fe influenced biofilm growth in a QseBC-mediated manner, the ability of the bacteria to form biofilms in the presence of CAT-Fe, ferrous iron or Ne was examined. *A. actinomycetemcomitans* was grown for 62 hours in CDM (Figure 10) and analyzed by confocal microscopy. As shown in Figure 9, the Wt strain grown in CDM supplemented with Ne/FeCl₂ resulted in a significant increase in biomass compared to CDM alone. In contrast, the *qseCΔp* mutant did not exhibit a significant increase in biofilm formation in the presence of CAT-Fe (Figure 11A) relative to ferrous iron (Figure 11B) supplementation, suggesting that stimulation of biofilm growth required a functional QseC sensor.

In *E. coli*, catecholamine mediated stimulation of growth was dependent on having a functional enterobactin biosynthesis and uptake system. As previously discussed, *A. actinomycetemcomitans* does not have the capability to synthesize enterobactin or other siderophores, but does code for a putative enterobactin receptor and transport system (D11S_1357-1352; Figure 12). The potential role of this putative enterobactin transport system was explored by making an in-frame deletion of the beta-barrel region of the TonB dependent receptor (D11S_1352) and comparing biofilm formation of this mutant strain and wt cells. As shown in Figure 13A & B, biofilm growth of the mutant strain was similar when cultured in CDM supplemented either with FeCl₂ or CAT-Fe, respectively, and was significantly less than the Wt strain cultured in CDM supplemented with CAT-Fe (see Figure 10D). The wt biofilm phenotype was restored in the TonB dependent receptor mutant by complementing the strain with a full length copy of the gene (Figure 13D).

Freestone *et al* previously showed that catecholamines act as pseudosiderophores by scavenging iron from holo-transferrin and the concentration of catecholamine (50uM) used in

these experiments also resulted in increased planktonic growth of *E.coli* [57, 80]. This suggests that catecholamines may function as siderophores. To determine if exposure to CAT-Fe also induces *A. actinomycetemcomitans* growth, cells were cultured in CDM supplemented with either 100 μ M of ferrous iron, 50 μ M of Ep or Ne, or a combination of the both (CAT-Fe). There were no significant changes in growth when *A. actinomycetemcomitans* was cultured in CDM or in CDM/Ne, but growth was significantly increased with the supplementation of ferrous iron (Figure 14A). Growth of the bacteria was further increased significantly upon supplementation with Ne/FeCl₂ (Figure 14A). Ep/FeCl₂ also resulted in significant induction of growth over bacteria grown in just CDM (Figure 14B). However, in contrast to biofilm growth (see above), the increase in planktonic growth was not contingent on a functional QseC since the mutant strain lacking the periplasmic domain of QseC (*qseC Δ p*) still showed a significant increase of growth with Ne/FeCl₂ supplementation over ferrous iron supplementation (Figure 14C).

CAT-Fe stimulation of planktonic growth was also tested for the TonB dependent mutant and the complemented strain. This mutant strain still exhibited significant activation of QseC in the presence of Ne/FeCl₂ compared to the control CDM (Figure 15A), indicating the QseC function is unaffected by inactivating the siderophore receptor. The TonB dependent receptor mutant strain exhibited no significant changes in planktonic growth under these conditions, suggesting that a functional TonB receptor is required for growth stimulation by CAT-Fe (Figure 15B). When the mutant strain was complemented with an intact copy of the TonB receptor gene, the Wt growth phenotype was restored (Figure 15C).

Adrenergic Receptor Antagonists Fail to Block CAT-Fe Growth Stimulation and Inhibit Overall Growth of *A. actinomycetemcomitans*

In Chapter 3, it was shown that the alpha and beta adrenergic receptor antagonists failed

to block QseC activation by CAT-Fe and at a concentration of 400 μ M appeared to stimulate QseBC. Therefore, the effect of these drugs on CAT-Fe stimulation of planktonic growth of *A. actinomycetemcomitans* was tested to confirm that the growth phenotype is independent of QseC. At a concentration of 200 μ M, both adrenergic receptor antagonists failed to block CAT-Fe stimulation of growth (Figure 16A), consistent with the previous β -galactosidase results obtained with these drugs. At 400 μ M of propranolol or phentolamine, there was an overall inhibition of growth compared to Wt when grown in CDM (Figure 16B) or BHI. The growth inhibition was independent from QseC signaling since the mutant lacking the periplasmic domain of QseC still showed significant growth inhibition in response to 400 μ M of propranolol or phentolamine (Figure 16C).

Discussion:

Catecholamines have been shown to lead to a stimulation of planktonic growth and biofilm formation in a wide variety of species such as *E.coli*, *Salmonella*, *P. burkholderia*, *A. pleuropneumoniae*, and a variety of dental pathogens [58, 57, 66, 103, 93]. In addition, catecholamines also lead to an increase in biofilm formation in *E. coli* [119]. For *A. actinomycetemcomitans*, exposure to CAT-Fe and the resulting QseBC activation resulted in an increase in the nucleoside pool and up-regulation of the anaerobic ribonucleoside triphosphate reductase (D11S_2128) which converts nucleosides to deoxyribonucleosides (Chapter 4). Together with the metabolomics and microarray data suggested that energy production was increased (Chapter 4), this data suggested that CAT-Fe primed the cell for increase growth, which was confirmed when analyzing planktonic growth and biofilm formation.

Exposure to ferrous iron resulted in a significant increase of planktonic growth, but growth was further significantly stimulated with the addition of CAT-Fe. For the biofilms,

although one of the lipoproteins associated with biofilm formation, *pgaB*, was down-regulated in response to CAT-Fe exposure, biofilm formation was significantly increased during exposure to CAT-Fe.

For *E.coli*, *Salmonella*, and *A. pleuropneumoniae*, it was found that the stimulation of planktonic growth was independent of QseC since a mutant strain still underwent catecholamine mediated planktonic growth stimulation [57, 80, 92]. This is consistent with the results of the CAT-Fe mediated planktonic growth stimulation in *A. actinomycetemcomitans*, which was also independent of a functional QseC. However, for both *E.coli* and *A. actinomycetemcomitans*, a functional QseC was required for the biofilm phenotype in response to catecholamines [119] or CAT-Fe, respectively.

One possible explanation for the planktonic growth stimulation in the presence of CAT-Fe but in the absence of *qseC* is that there exists the possibility of another sensor that is responsive to CAT-Fe. Several other putative receptors (QseE, BasS and CpxA) have been reported to function as catecholamine sensors [102]. The other explanation is that QseC has not been shown to be essential for planktonic growth, but has been for biofilm formation. It has already been shown that the loss of *qseC* resulted in significant biofilm reduction [44, 53]. The significant increase in biofilm formation during QseC activation by CAT-Fe is consistent with these previous results. In addition, the role of QseC as a regulator of anaerobic metabolism fits within this narrative (Chapter 4). Since QseC activation results in an up-regulation of anaerobic respiration and metabolism, this response might assist *A. actinomycetemcomitans* during growth in the biofilm where oxygen levels may be decreased.

The planktonic growth stimulation and biofilm stimulation in response to CAT-Fe was found to be dependent on the TonB dependent receptor. This is consistent with the reports that

E. coli requires a functional enterobactin transport and synthesis operon [58]. *A. actinomycetemcomitans* does not encode for enterobactin, nor any other siderophore. Therefore, one potential reason for *A. actinomycetemcomitans* encoding the enterobactin transporter and receptor could be for acquiring iron via catecholamine mediated scavenging. It is also possible that this operon functions to scavenge enterobactin made by other oral species, or that the operon can be used for both functions.

Interestingly, the TonB dependent receptor mutant still underwent CAT-Fe mediated activation of QseC. This suggests that the enterobactin transport and receptor operon may lay downstream of QseC activation. The enterobactin transport and receptor operon was not one of the high affinity iron acquisition genes that was down-regulated in the microarray. One possible reason for this could be that the operon is required for *A. actinomycetemcomitans* to respond to CAT-Fe.

As reported in Chapter 3, the growth stimulation in response to catecholamines could be blocked in the presence of adrenergic receptor antagonists in *E. coli* [80], but in *A. actinomycetemcomitans*, the activation of QseC was not blocked by these drugs. Instead, at high concentrations, they appeared to act as QseC agonists. Therefore, the effect of the adrenergic receptor antagonists was analyzed in *A. actinomycetemcomitans* to see if the activation of QseC at high levels of antagonist resulted in a growth phenotype. The reason for this is that QseC has been proposed as a potential target for therapeutics since it plays such a vital role in regulating virulence, metabolism, and biofilm formation [107].

At concentrations that were sufficient to block catecholamine stimulation of growth (i.e. 50 μ M), there was no significant effect on CAT-Fe stimulation of planktonic growth in *A. actinomycetemcomitans*. However, the addition of 400 μ M of adrenergic receptor antagonist,

the same concentration that resulted in QseC activation in Chapter 3, resulting in a significant inhibition of growth in either CDM or BHI. This inhibition of growth was independent of QseC, therefore it appears these drugs have an overall toxic effect on the cell at high concentrations. Interestingly, this inhibition of growth was not reported in *E.coli* or *Salmonella*. It is unlikely that these drugs can be used as a therapeutic against *A. actinomycetemcomitans*, since it was only at high concentrations this effect was observed, and this same concentration is well outside the recommended dose for humans.

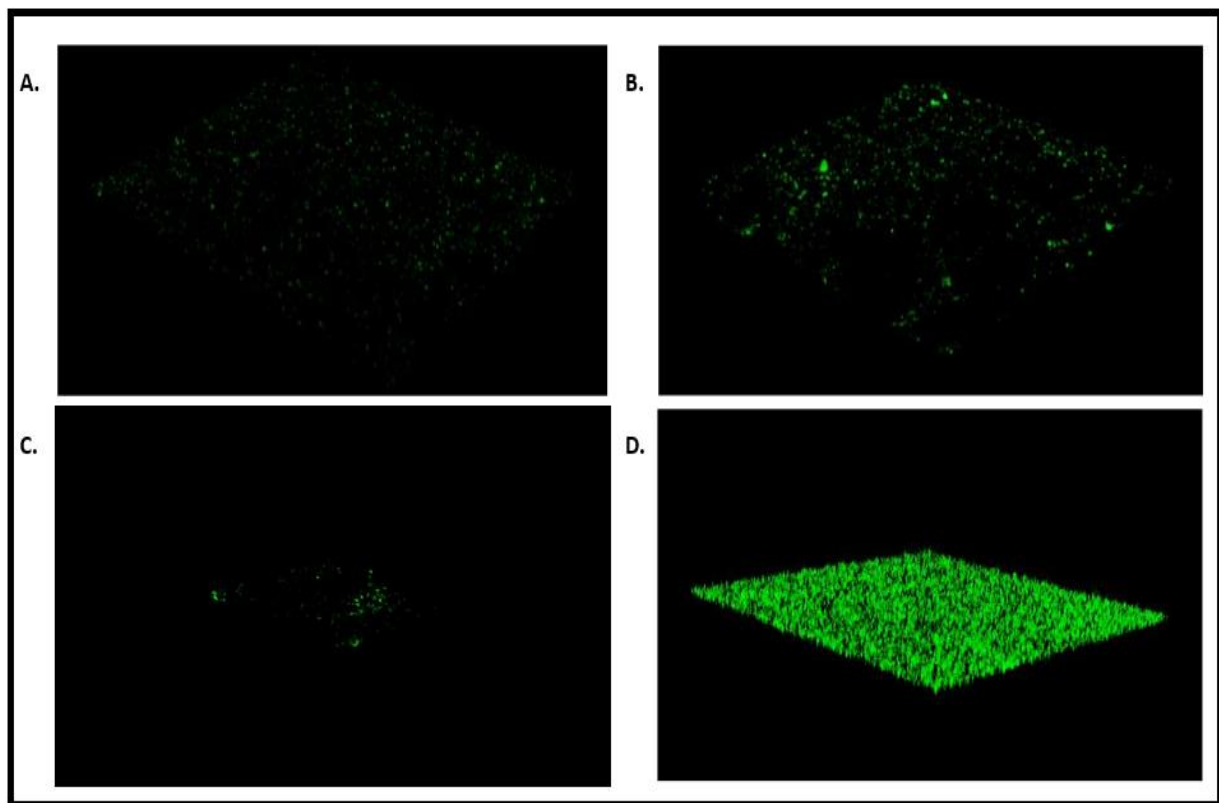


Figure 10: Biofilm formation in *A. actinomycetemcomitans* grown in CDM with iron and/or catecholamines. Representative photos of *A. actinomycetemcomitans* grown in a biofilm in CDM (A), or with supplementation of FeCl_2 (B) Ne (C), or Ne/ FeCl_2 (D). All biofilm experiments were performed independently in triplicate with 5 to 10 pictures taken per biofilm.

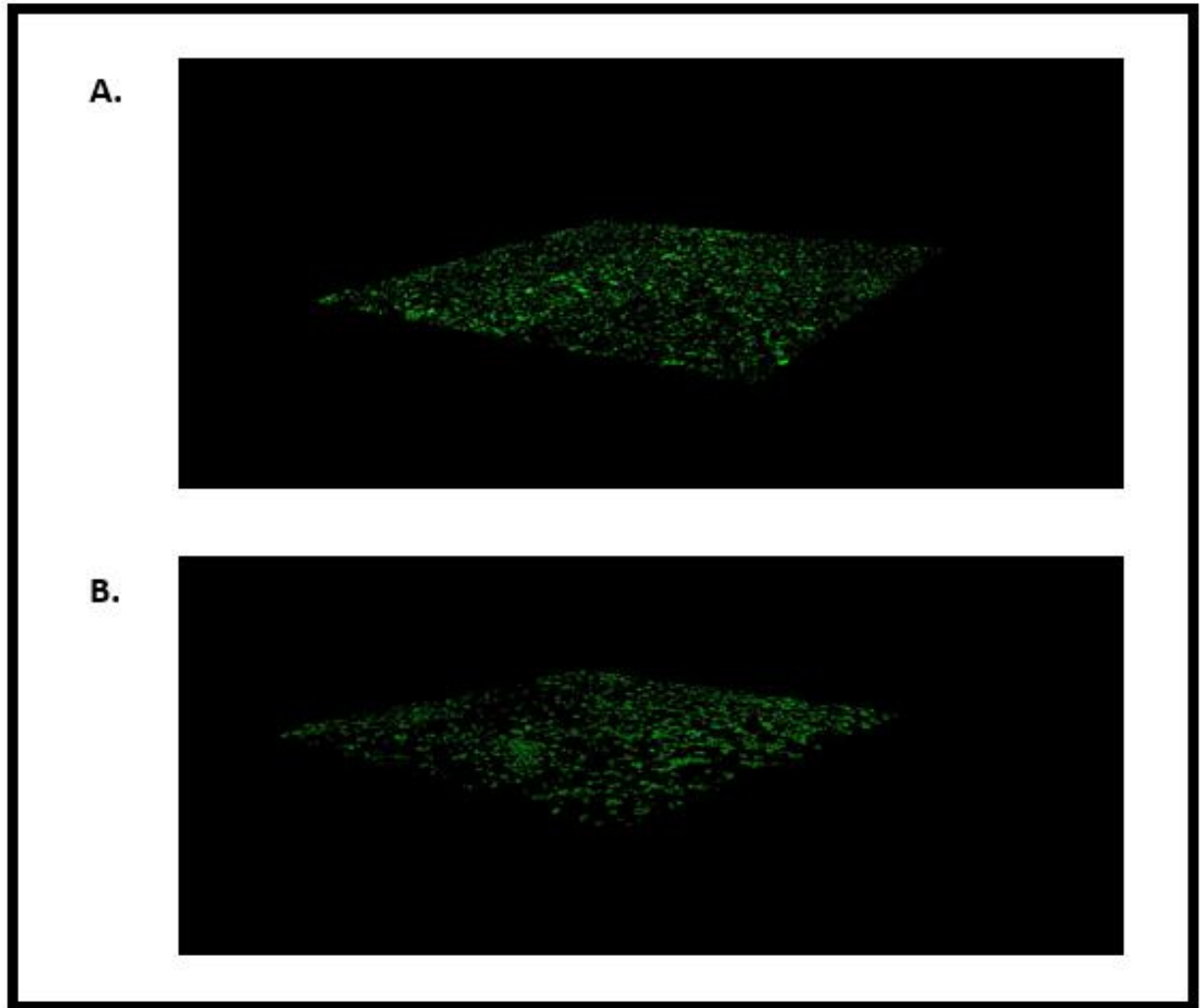


Figure 11: Biofilm formation in *qseCΔp* strain. Representative photos of the *qseCΔp* strain of *A.*

actinomycetemcomitans grown in CDM with ferrous iron (A) or Ne/FeCl₂ (B). All biofilm experiments were performed independently in triplicate with 5 to 10 pictures taken per biofilm.

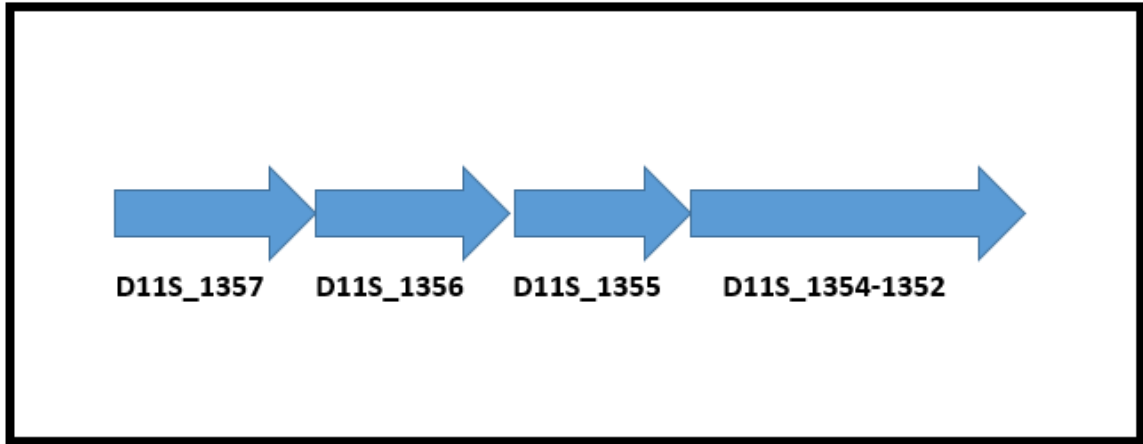


Figure 12: The enterobactin transport and receptor operon of *A. actinomycetemcomitans* serotype c D11S. The TonB receptor was originally annotated as D11S_1354 with D11S_1353 being an outer membrane receptor and D11S_1352 annotated as either *fepA* or a pseudogene. However, based on sequence similarity from *E.coli* and the D7S strain of *A. actinomycetemcomitans* and the data from this study, it is most likely that D11S_1354-1352 together encode the TonB dependent receptor.

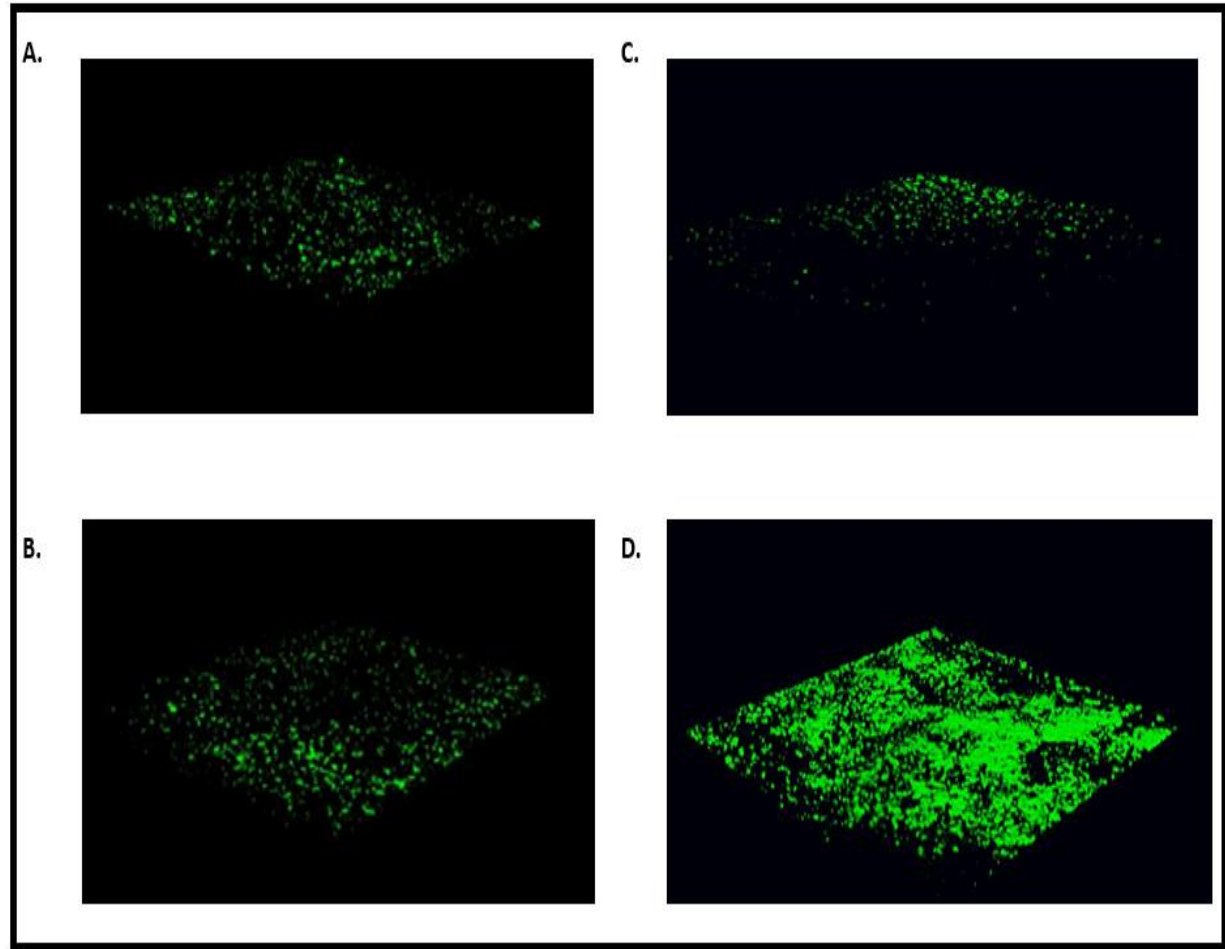


Figure 13: Biofilm formation in Δ TonB dependent receptor strain. Representative photos of the Δ TonB dependent receptor mutant strain of *A. actinomycetemcomitans* grown in CDM with ferrous iron (A) or Ne/FeCl₂ (B) or of the TonB dependent receptor complement strain grown in CDM with ferrous iron (C) or Ne/FeCl₂ (D). All biofilm experiments were performed independently in triplicate with 5 to 10 pictures taken per biofilm.

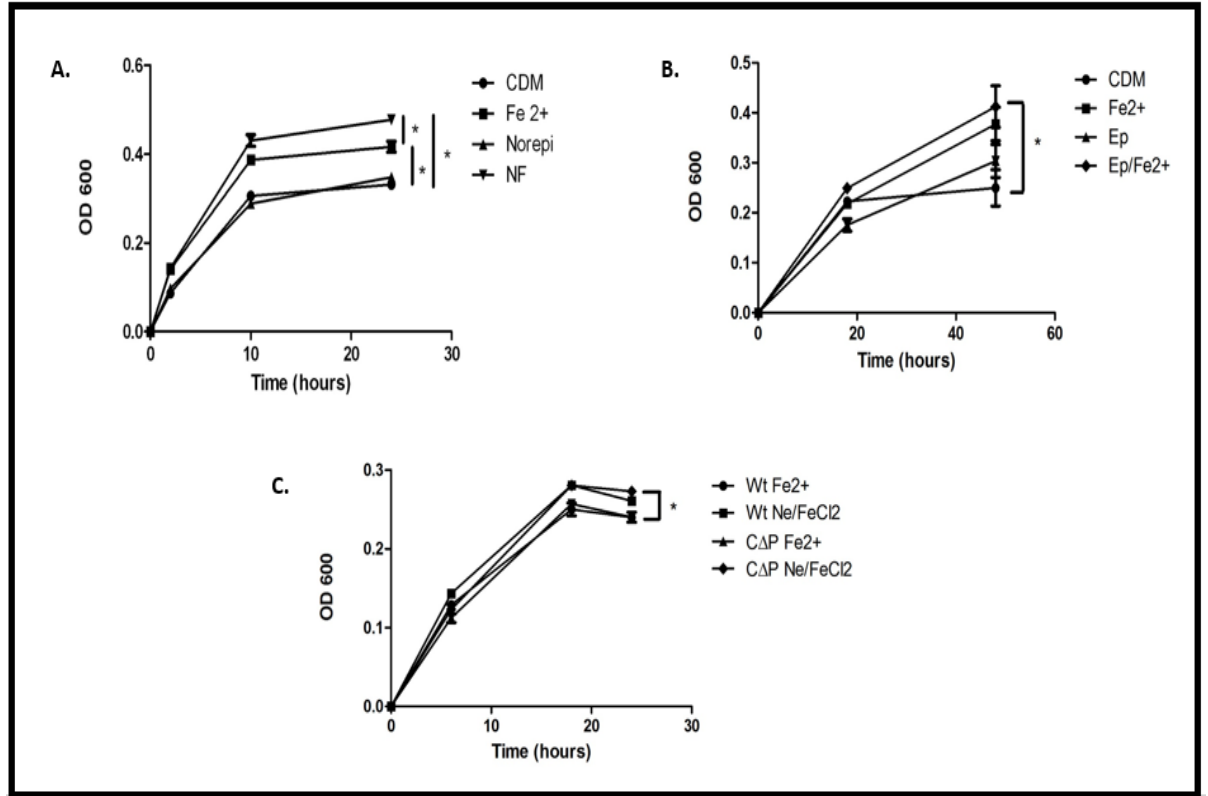


Figure 14: Planktonic growth response in the presence of CAT-Fe. A) Aliquots were taken at various time points of *A. actinomycetemcomitans* grown in triplicate for two independent experiments in CDM with or without supplementation with Ne, ferrous iron, or both and measured for the O.D. 600nm. B) Growth was followed using the same methods but for *A. actinomycetemcomitans* grown in CDM with or without supplementation with ferrous iron, Ep, or both. C) Growth of wild type bacteria or a strain lacking the periplasmic domain of Qsec (*qseCΔp*) was measured using OD600 for cultures grown in CDM with either ferrous iron or Ne/FeCl₂⁺ supplementation. All experiments were done in triplicate with two independent trials. P < 0.05.

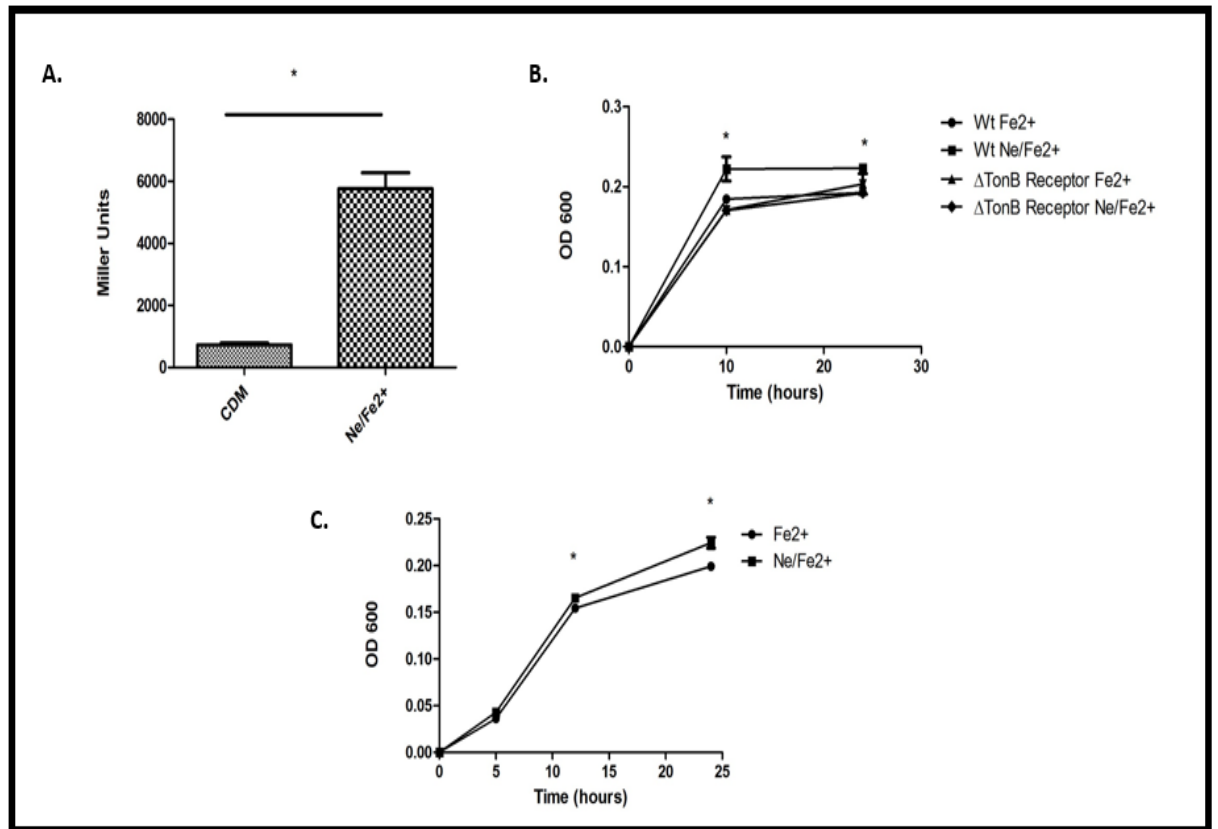


Figure 15: The response of the Δ TonB dependent receptor strain to CAT-Fe. A) Expression of *ygiW-qseBC* was measured in a β -galactosidase assay after 24 hours for the Δ TonB dependent receptor strain of *A. actinomycetemcomitans* grown in CDM or with Ne/Fe²⁺. Each condition was tested in triplicate in two independent assays. B) Growth was measured using the O.D._{600NM} of the Wt strain or the Δ TonB dependent receptor strain grown in CDM with either ferrous iron supplementation or Ne/FeCl₂. C) Growth of the Δ TonB dependent receptor complement strain in CDM with Fe²⁺ or Ne/Fe²⁺ supplementation. All growth curves were performed in triplicate with two independent experiments. P<0.05

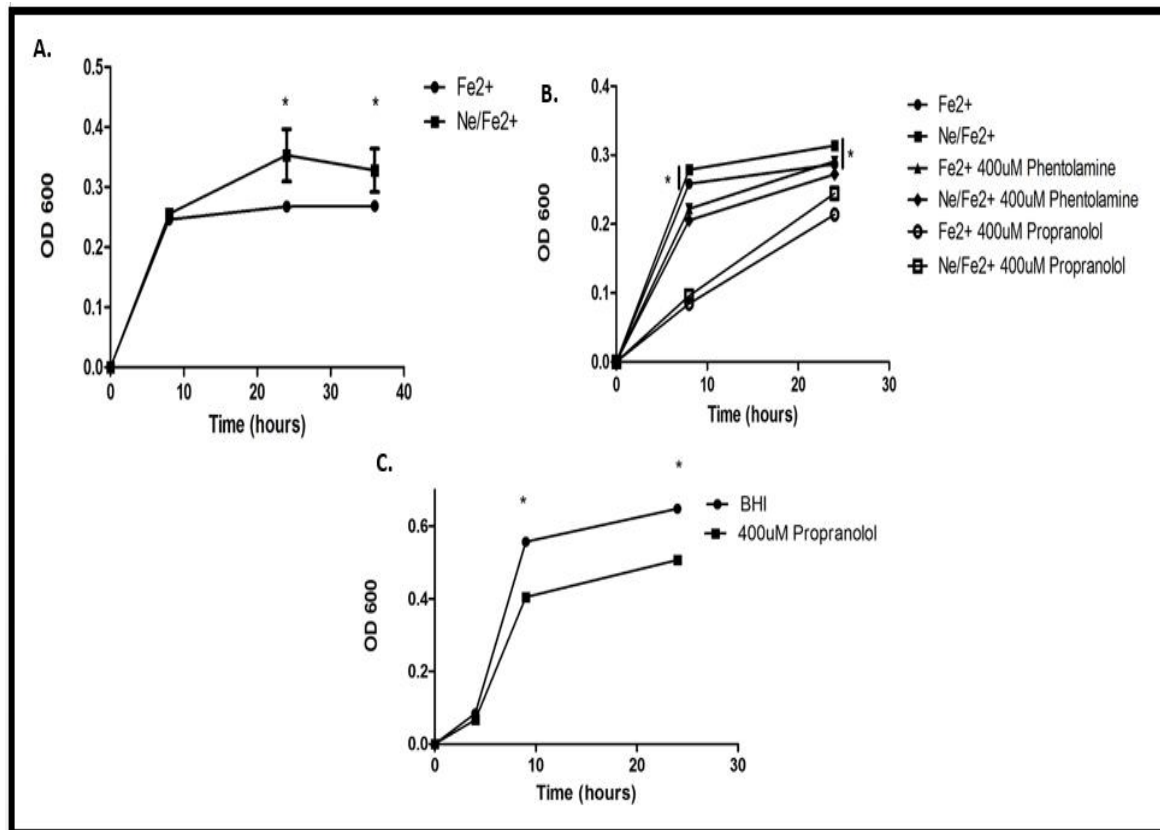


Figure 16: The growth response of *A. actinomycetemcomitans* to the alpha adrenergic receptor antagonist phentolamine or the beta adrenergic receptor antagonist propranolol. A) Growth was measured by O.D._{600nm} for *A. actinomycetemcomitans* was grown in CDM with supplementation of either Fe²⁺, Ne/Fe²⁺, and 200µM propranolol. B) Growth was measured for *A. actinomycetemcomitans* grown in CDM with of supplementation either Fe²⁺, Ne/Fe²⁺, 400µM of propranolol or 400µM of phentolamine. C) Growth was measured for the *qseCΔp* strain of *A. actinomycetemcomitans* grown in BHI with or without 400µM of propranolol. All experiments were done in triplicate with two independent trials. P < 0.05.

CHAPTER SIX: THE IRON-RESPONSIVE TOXIN/ANTI-TOXIN (TA) SYSTEM D11S_2133-2134 AND ITS
ROLE IN *YGIW-QSEBC* REGULATION

Introduction:

The oral cavity is a harsh environment due to fluctuations in pH, nutrients, temperature, exposure to antibiotics, competition from other resident microbes and the shear force arising from the flow of saliva [129]. In order to compete and thrive, bacteria need to tightly regulate gene expression and adapt quickly to changes that occur in the local environment. Inter- and intra- species communication allows bacteria to sense changes in population sizes and adapt accordingly through quorum sensing. *A. actinomycetemcomitans* is able to quorum sense via the production of AI-2 by LuxS and its subsequent detection by the receptors LsrB and RbsB [44]. The *qseBC* TCS is downstream of AI-2 detection, but its activation is not directly controlled by AI-2 detection [44]. In *E. coli*, AI-2 detection leads to the activation of MqsR, which positively regulates expression of *qseBC* [71] and it is possible that a similar mechanism occurs in *A. actinomycetemcomitans*. In *E. coli*, MqsR is the toxin in the MqsRA TA system that acts as a CGU-specific mRNA interferase [108].

TA systems are mechanisms that allow bacteria to respond to stress [84]. They comprise an anti-toxin that is co-transcribed with its cognate toxin [81]. In type II TA systems, both the toxin and the anti-toxin are proteins with the anti-toxin being more labile and therefore more easily degraded by proteases such as Clp [83] and Lon [82]. Normally, the anti-toxin protein binds to the toxin protein to neutralize its effects. Many anti-toxins also bind to their own promoter to auto-regulate expression of the operon. Toxin activity can vary but most toxins function as either ribosome dependent or independent mRNA endoribonucleases that cleave mRNA at certain specific sequences [81, 109, 110]. Some cleave mRNA promiscuously such as

the RelE of *E.coli* which cleaves between the second and third position of an upstream purine [111]. TA systems are also thought to play a vital role in the development of the persister phenotype that allows the cell to survive environmental stress [81].

In bacterial populations there exists phenotypic heterogeneity meaning that there can be distinct populations within a community of the same species. This often happens during persister cell formation where a small percentage of the population represents the slow-growing persister phenotype [86]. This phenotype is thought to be the result of activation of TA systems. In these cells, there may be a stochastic switch to the persister phenotype that activates the Lon protease, which then degrades the anti-toxin to activate the toxin [85]. This mechanism of TA activation is dependent on the accumulation of (p)ppGpp [85] which is produced by RelA/SpoT and accumulates in cells and inhibits exopolyphosphatase (PPX) [85]. PPX degrades polyphosphate (polyP), which is synthesized by polyphosphate kinase (PPK) [85]. At high levels, polyP activates the Lon protease, which will in turn degrade the anti-toxins and release the toxin [85]. *A. actinomycetemcomitans* contains 10 putative type II TA systems and previous work identified various environmental stressors that induced expression of these TA systems and showed that one TA system (D11S_2133-2134) was highly up-regulated under iron limited growth conditions (i.e., the presence of the iron chelator 2,2'-bipyridyl [DIP]).

In this Chapter, we show that QseB plays a role in the stress response of *A. actinomycetemcomitans* and influences expression of the Lon protease and the iron-responsive TA system D11S_2133-2134. We also show that over-expression of D11S_2133 inhibits growth in *E. coli* while D11S_2134 over-expression had no significant effect on growth, suggesting that D11S_2133 is the toxin and D11S_2134 is the anti-toxin. In addition, over-expression of D11S_2134 results in a significant up-regulation of expression of the *ygiW-qseBC* operon in *A. actinomycetemcomitans*.

Results:

Deletion of *qseB* Results in an Up-regulation of Stress Response Genes

QseB is the DNA binding response regulator of the QseBC TCS that is activated by QseC in response to CAT-Fe. In Chapter 3, we identified changes in the transcriptome of Wt *A. actinomycetemcomitans* when QseC was activated by CAT-Fe. To further define the QseBC regulon, a genomic microarray was used to identify differentially expressed genes in a $\Delta qseB$ strain of *A. actinomycetemcomitans*. A total of 250 genes were differentially regulated 2 fold or greater in $\Delta qseB$ compared to Wt (Appendix Table 2). Of the 250 genes, 89 were up-regulated and 161 were down-regulated.

Of the 89 genes that were up-regulated, 16 were genes involved in the stress response (Table 9). These genes were highly up-regulated with 6 of the top 10 results being genes associated with the stress response, e.g., the ATP-dependent ClpB protease (D11S_0551), the chaperonin *groS-groEL* (D11S_599-600), the universal stress protein A (D11S_0656), molecular chaperone *dnaK* (D11S_D11S_0922), and *lon* (D11S_1522). In order to confirm the role of QseBC in the stress response, qRT-PCR was performed to measure the expression of *lon* in $\Delta ygiW$, $\Delta qseB$, $\Delta qseC$, and a $\Delta qseC$ complemented strain (Figure 17). While the $\Delta ygiW$ did not show a significant change in *lon* expression, $\Delta qseC$ and $\Delta qseB$ exhibited up-regulation of *lon* and the QseC complemented strain was able to restore *lon* expression back to Wt levels (Figure 17). Interestingly, the activation of QseC by CAT-Fe also resulted in an up-regulation of several genes involved in the stress response: the universal stress protein A (D11S_0656), *clpB* (D11S_0551), *groS-groEL* (D11S_0599-0600), two putative *relEB* TA systems (D11S_1194-1195 & D11S_1798-1799), and the molecular chaperone *dnaK* (D11S_0922).

Ectopic Expression of *lon* Induces *ygiW-qseBC* and Results in Significant Decrease in Growth

The Lon protease (D11S_1522) degrades the labile anti-toxins of TA systems thereby releasing the toxin during the stress response [82]. Since deletion of *qseB* and *qseC* resulted in an up-regulation of *lon*, we next determined the effect of ectopic expression of *lon* on expression of *qseBC*. The *lon* gene was ectopically expressed using the Trc inducible promoter of plasmid pWAW17. *A. actinomycetemcomitans* harboring pWAW17 was confirmed to exhibit up-regulation of *lon* (Figure 18A). The *A. actinomycetemcomitans* strain carrying pWAW17 also showed significant up-regulation of *ygiW* suggesting that Lon may play a role in regulating *ygiW-qseBC* (Figure 18B).

Activation of Lon results in the activation of TA systems by degrading the anti-toxin and release of the toxin. The toxins are hypothesized to inhibit cellular processes like translation and inhibit growth. In part, this mechanism may allow the cell to transition to a slow-growing persister cell. In *E. coli* transformed with pWAW17, no significant growth difference was observed with or without 1mM IPTG until late log phase (Figure 19A). At late exponential and stationary phase, induction of the Lon protease resulted in significant reduction of cell density in *E. coli* (Figure 19A). A similar result occurred with *A. actinomycetemcomitans* transformed with pWAW17 (Figure 19B).

D11S_2133-2134 is Up-regulated during Iron Starvation and in $\Delta qseC$ and $\Delta qseBC$

Different stress conditions, including iron stress, were used to determine under which condition each of the 10 putative TA systems were activated. D11S_2133-2134, a putative RelE- like type II TA system, was highly up-regulated during iron starvation

(Figure 21A). Consistent with this, the D11S_2133-2134 TA system was significantly up-regulated when cells were cultured in CDM without any iron supplementation relative to iron replete cultures grown in BHI. In addition, there was no significant change in expression of the TA system in the Wt strain when cultured in CDM supplemented with CAT-Fe (Figure 20B). Finally, D11S_2133-2134 was up-regulated in the Δ TonB receptor strain, a strain that did not have a growth response to CAT-Fe and therefore may have a defect in acquiring iron (Figure 20C).

Real-time PCR was also used to determine expression of D11S_2133-2134 in both Δ *qseC* and Δ *qseBC* strains relative to Wt. Consistent with the previous microarray results using the Δ *qseB* mutant, the TA system was significantly upregulated in both Δ *qseBC* and Δ *qseC* (Figure 20D). Together with the data showing that this TA system is activated during iron starvation, it is possible that this system may be involved in regulating *qseBC* and fine-tuning the response of *A. actinomycetemcomitans* to changes in environmental iron content.

D11S_2133 and D11S_2134 are Co-transcribed and Ectopic Expression of D11S_2133 but Not D11S_2134 Results in Inhibition of Growth in *E. coli*

We next confirmed the identities of the putative toxin and anti-toxin. In Type II TA systems, the toxin and the anti-toxin are co-transcribed [81, 118]. To confirm that D11S_2133 and D11S_2134 were co-transcribed, primers were designed to amplify the intergenic region between D11S_2133 and D11S_2134. The positive control genomic DNA and the cDNA resulted in a fragment for the intergenic region (Figure 21A). In contrast, primers amplifying an intergenic region between D11S_2134 and the unrelated D11S_2135 gene gave a product only for the genomic DNA, but not the cDNA confirming that D11S_2133 and D11S_2134 are co-transcribed. In addition, the promoter which

transcribes D11S_2133-2134 was identified by 5' cDNA RACE as being within the intergenic region between D11S_2134 and D11S_2135. The transcriptional start site was mapped to nucleotide -36 as shown in Figure 21B.

Conventionally, the anti-toxin is transcribed first followed by the toxin [118], but there have also been reports of this operon structure order being reversed. In order to confirm their functional identities, both D11S_2133 and D11S_2134 were ectopically expressed using the Trc inducible promoter to generate pWAW20 (Trc-D11S_2133) and pWAW19 (Trc-D11S_2134). Confirmation of ectopic expression in both strains was performed by qRT-PCR. The growth of *E.coli* and *A. actinomycetemcomitans* strains transformed with these plasmids was then determined. When the *E.coli* strain carrying pWAW19 (D11S_2134) was grown in LB or LB with 1mM IPTG, there was no significant difference in cell density (Figure 22A). In contrast, the *E.coli* strain carrying pWAW20 (D11S_2133) showed significant reduction of cell density when IPTG was added to induce expression of D11S_2133 (Figure 22C). The reduction in cell density of the strain carrying D11S_2133, but not D11S_2134 suggests that the organization of the operon is similar to the normal convention for type II TA systems in that the anti-toxin (D11S_2134) is transcribed first followed by the toxin (D11S_2133).

In *A. actinomycetemcomitans*, the strains carrying pWAW20 or pWAW19 showed no difference in cell density in the presence or absence of IPTG. In addition, there were no changes in cell density of the Wt strain in the presence or absence of IPTG (Figure 23A). However, there was a significant reduction of cell density for both the pWAW19 and pWAW20 strains versus the Wt strain (Figure 23A &B). The reduction of growth due to the ectopic expression of D11S_2134 could also be seen in *E.coli* when high levels (2mM) of IPTG was added to the media to induce higher levels of expression

from the pTRC promoter (Figure 22B).

Ectopic Expression of D11S_2134 Induces the Expression of the *ygiW-qseBC* Operon

In order to test the hypothesis that D11S_2133-2134 regulates expression of the *ygiW-qseBC* operon, qRT-PCR was performed with Wt *A. actinomycetemcomitans* and each of the ectopic expression strains. Since ectopic expression of *lon* resulted in an up-regulation of *ygiW-qseBC* mRNA, we hypothesized that ectopic expression of the putative toxin, D11S_2133, would result in the up-regulation of *ygiW-qseBC* mRNA.

Both strains for the ectopic expression of either D11S_2133 (pWAW20) or D11S_2134 (pWAW19) were confirmed by qRT-PCR to exhibit increased mRNA expression (Figure 24A & B). Using qRT-PCR, induction of pWAW19 resulted in a 5000 fold increased expression of the *ygiW-qseBC* operon, whereas induction of pWAW20 resulted in only a 4 fold increase (Figure 24C). These results were also confirmed using the inducible *lrsA* promoter to generate plasmids pWAW14 (D11S_2133) and pWAW16 (D11S_2134). The *lrsA* promoter contains a *crp* binding site and in the absence of glucose, expression is induced. Again, ectopic expression was confirmed by qRT-PCR (Figure 25A & B). In agreement with the results seen with pWAW19 and pWAW20, ectopic expression of D11S_2134 (pWAW16) still resulted in a significant increase in mRNA expression of *ygiW-qseBC* while expression of D11S_2133 (pWAW14) did not (Figure 26B). There was no significant difference in *ygiW-qseBC* expression in Wt cells grown in LB or LB with glucose (Figure 26A).

Discussion:

QseBC appears to be involved in sensing iron via CAT-Fe which activates the TCS and results in regulation of iron acquisition genes. However, as shown in Chapter 3, this TCS is not highly activated during times of iron-limitation (i.e. CDM), and there is a basal

level of activity under iron limiting conditions. In addition, our previous results and studies of QseBC in other species suggest that QseB may be activated by non-cognate sensor kinases [60, 101]. This suggests that a minimal level of QseB activity is essential for *A. actinomycetemcomitans* and the absence of functional QseB triggers a stress response. As seen in the microarray data and confirmed with qRT-PCR data performed with $\Delta qseC$, the absence of this TCS elicits the up-regulation of several stress response genes, including *lon*.

Lon is involved in activating TA systems by degrading the labile anti-toxin and releasing the toxin. Most of these toxins act as endoribonucleases allowing them to post-transcriptionally regulate a variety of mRNA's in the cell. The ectopic expression of *lon* in *A. actinomycetemcomitans* was shown to result in an up-regulation of *ygiW-qseBC* mRNA, suggesting that it may regulate the expression of this TCS and our hypothesis is that the activation of an iron responsive TA system by Lon regulates the expression of *qseBC* under iron limitation. Only one TA system in *A. actinomycetemcomitans*, D11S_2133-2134, was found to be highly up-regulated during iron starvation, suggesting that it may be the TA system involved in *qseBC* regulation. The proposed regulatory circuit involving QseBC, Lon and the TA system is illustrated in Figure 27. We propose that these component function in concert to fine tune the response of *A. actinomycetemcomitans* to changes in environmental iron content.

D11S_2133-2134 was significantly up-regulated in the $\Delta qseC$ and $\Delta qseBC$ strains, yet the consensus binding sequence for QseB, CTAA-N6-CTAA, does not exist the putative promoter of D11S_2133-2134 [49]. This suggests that QseBC might regulate expression of the TA system through indirect means, possibly through the stimulation of *lon* expression.

Based on the growth kinetics in *E. coli* from the ectopic expression strains, D11S_2133 encodes for the toxin and D11S_2134 for the anti-toxin. Based on the qRT-PCR results to confirm expression of D11S_2133/2134, the Trc promoter appears to be “leaky” in *A. actinomycetemcomitans* and this could explain the less robust growth phenotypes seen in *A. actinomycetemcomitans*. In addition, high level induction of D11S_2134 led to significant growth inhibition even in *E. coli* suggesting that at high levels, the product encoded by this gene may be toxic to the cell.

Since ectopic expression of *lon* resulted in a significant increase in expression of *ygiW-qseBC* mRNA, we hypothesized that ectopic expression of the putative toxin (D11S_2133), would result in a significant increase in expression of *ygiW-qseBC*. Therefore, it was unexpected that ectopic expression of the putative anti-toxin (D11S_2134) resulted in significant up-regulation of *ygiW-qseBC*. There are several explanations for this result. First, the functional assignment of the toxin and anti-toxin based on the growth phenotypes may be misleading and clearly there are examples where the toxin gene precedes the anti-toxin [120, 121]. Second, since D11S_2133-2134 is a RelE-like TA system and presumably functions as an endoribonuclease, the use of qRT-PCR to measure changes in *qseBC* expression using only one housekeeping gene as reference may be misleading. These results could be confirmed by using additional internal controls or alternatively by determining the levels of QseBC proteins.

The data from this chapter suggests then that Lon and the D11S_2133-2134 TA system are involved in regulating expression of the *ygiW-qseBC* operon (Figure 27) and co-ordinating the response of the bacteria to iron-limiting conditions. In addition, appropriate expression and activation of QseB appears to be essential for the cell since the absence of *qseB* results in a significant up-regulation of the stress response.

Therefore, QseBC may play a vital role in adapting to the host environment by regulating metabolism, iron uptake, virulence and biofilm formation in response to activation by CAT-Fe (Figure 27) and loss of that function results in an attenuation of virulence [44]. Since QseBC appears to play such a vital role, it may represent a target for potential therapeutics. In order to develop these potential treatments, more information is needed about the regulation of QseBC by D11S_2133-2134 and other mechanisms as well as about the structure of QseC and the potential role of YgiW.

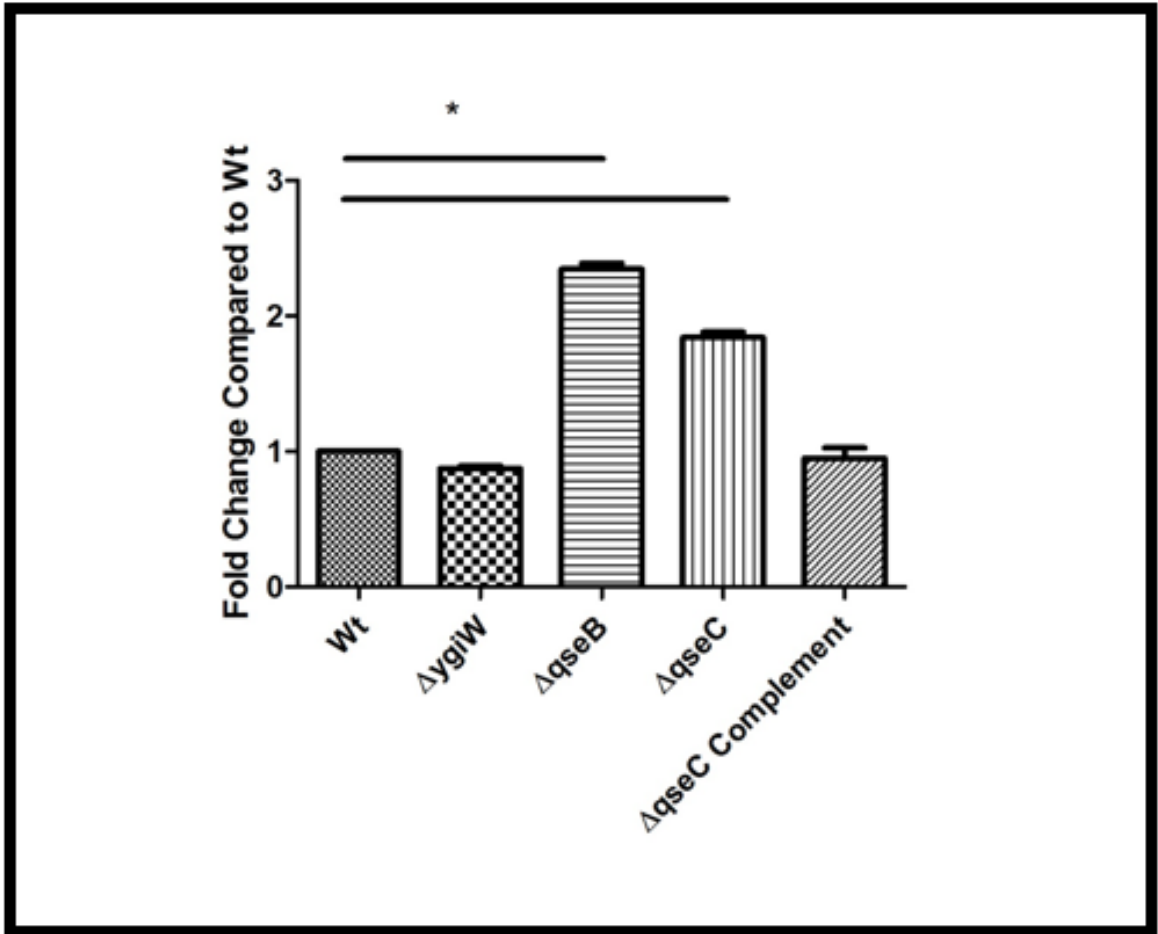


Figure 17: Expression of *lon*. Real-time expression of the Lon protease compared to the Wt strain of *A. actinomycetemcomitans* grown in BHI compared to $\Delta ygiW$, $\Delta qseB$, $\Delta qseC$, and $\Delta qseC$ complement. RT-PCR was done in triplicate with two independent trials. $P < 0.05$.

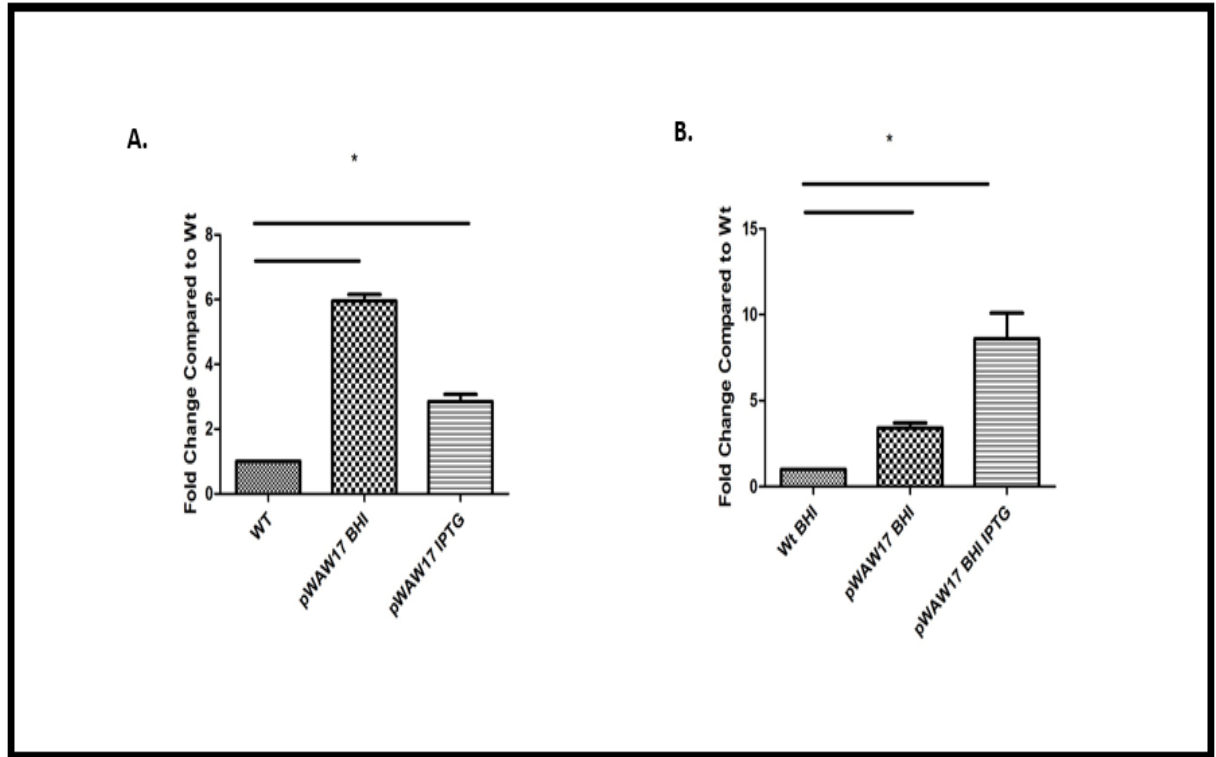


Figure 18: Regulation of *ygiW* expression by Lon. A) Real-time expression of *lon* in Wt *A. actinomycetemcomitans* compared to strains harboring pWAW17 grown in BHI or BHI with IPTG. B) Real-time expression of *ygiW* in Wt *A. actinomycetemcomitans* grown in BHI compared to a strain carrying a plasmid for the ectopic expression of Lon (pWAW17) grown in BHI with or without 1mM IPTG. All experiments were done in triplicate with two independent trials. $P < 0.05$.

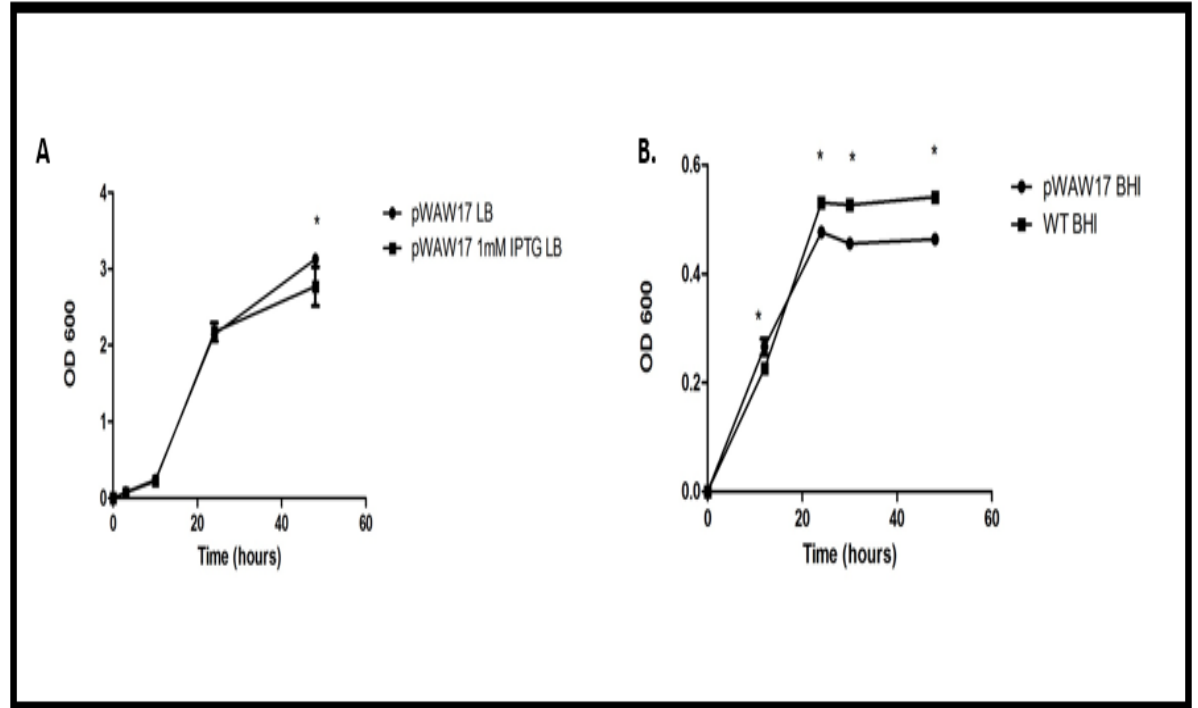


Figure 19: Growth response of *E. coli* and *A. actinomycetemcomitans* to ectopic expression of Lon. A) Growth of *E. coli* carrying the plasmid for ectopic expression of Lon (pWAW17) grown in LB or with 1mM IPTG. B) Growth of Wt *A. actinomycetemcomitans* with the empty vector pJT3 or strain carrying pWAW17 in BHI. All experiments were done in triplicate with two independent trials. $P < 0.05$.

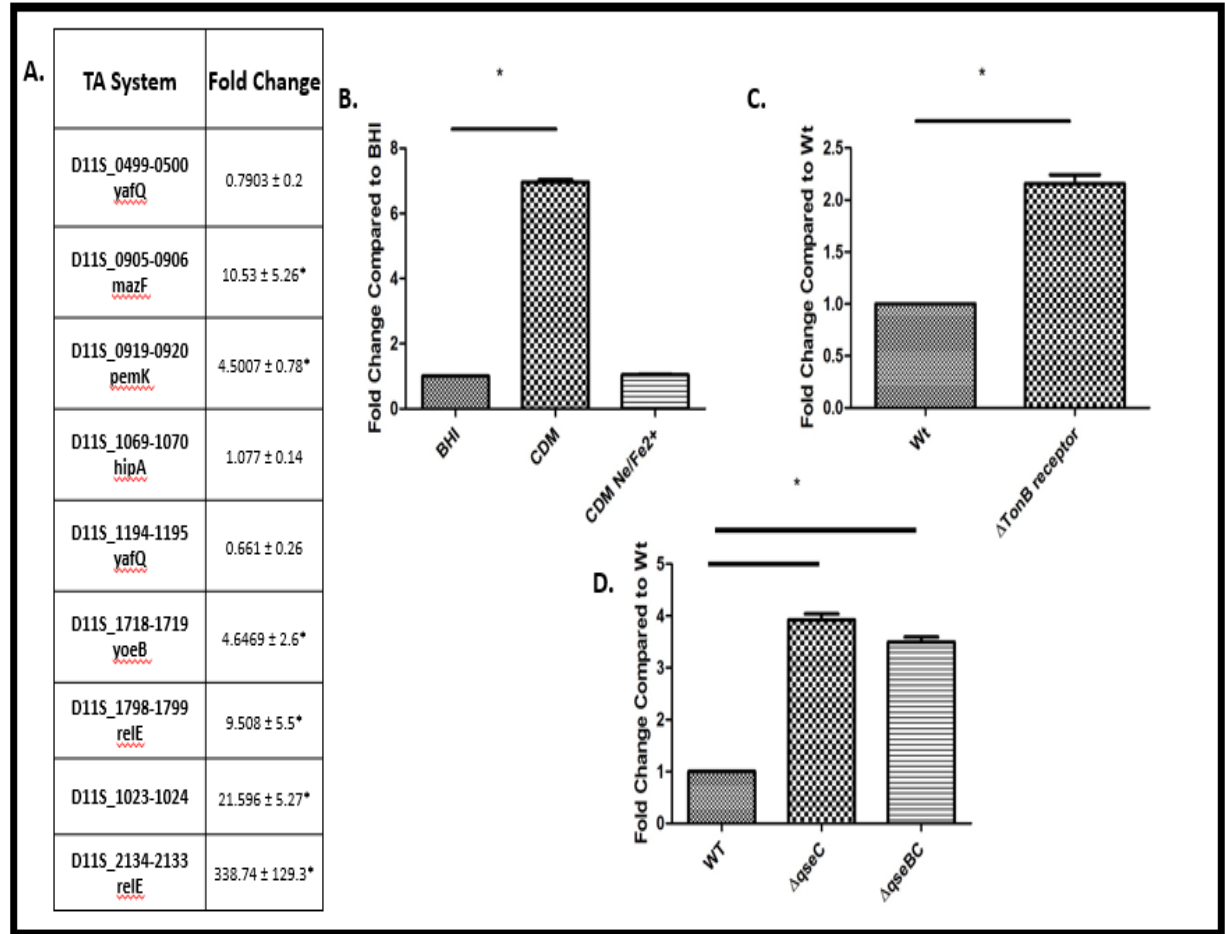


Figure 20: Response of TA systems to iron starvation. A) Real-time expression of putative TA systems in *A. actinomycetemcomitans* grown in CDM with 2,2'-dipyridyl (DIP)⁴. B) Real-time expression of D11S_2133-2134 grown in BHI, CDM and CDM with Ne/Fe²⁺. C) Real-time expression of D11S_2133-2134 in Wt *A. actinomycetemcomitans* or ΔTonB dependent receptor mutant grown in BHI. D) Real-time expression of D11S_2133-2134 in Wt *A. actinomycetemcomitans*, ΔqseC, or ΔqseBC grown in BHI. . All experiments were done in triplicate with two independent trials. P < 0.05.

⁴ Experiments shown in Figure A were completed by Blair Schneider

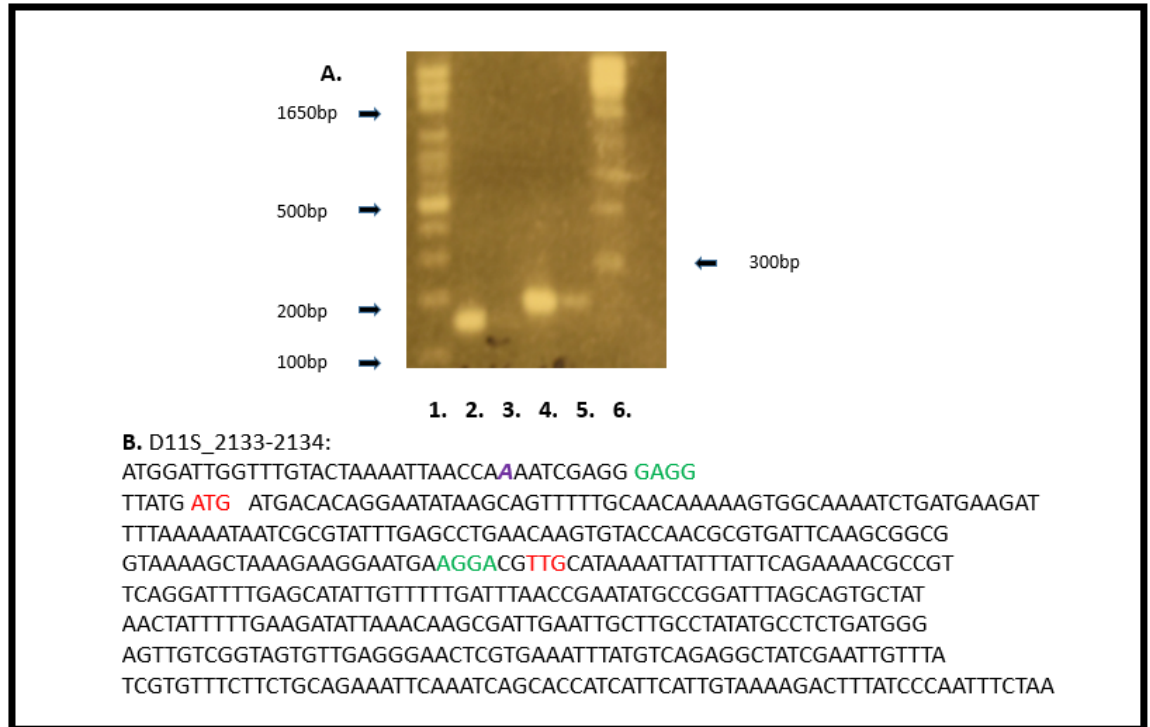


Figure 21: The D11S_2133-2134 Operon. A) DNA gel showing 1) 5000kb ladder, 2) PCR product from chromosomal DNA amplified with primers specific for the intergenic region between D11S_2134-2135, 3) PCR product from cDNA amplified with primers specific for the intergenic region between D11S_2134-2135, 4) PCR product from chromosomal DNA amplified with primers specific for the intergenic region between D11S_2134-2133, 5) PCR product from cDNA amplified with primers specific for the intergenic region between D11S_2134-2133, 6) 1kb ladder. B) The sequence for the upstream and coding region for D11S_2133-2134, including the transcriptional start site (purple and italic), ribosome binding site (green) and start codon (red). The transcriptional start site was determined by cDNA RACE using 10 transformed colonies that were sequenced for the inserted 5' untranslated region.

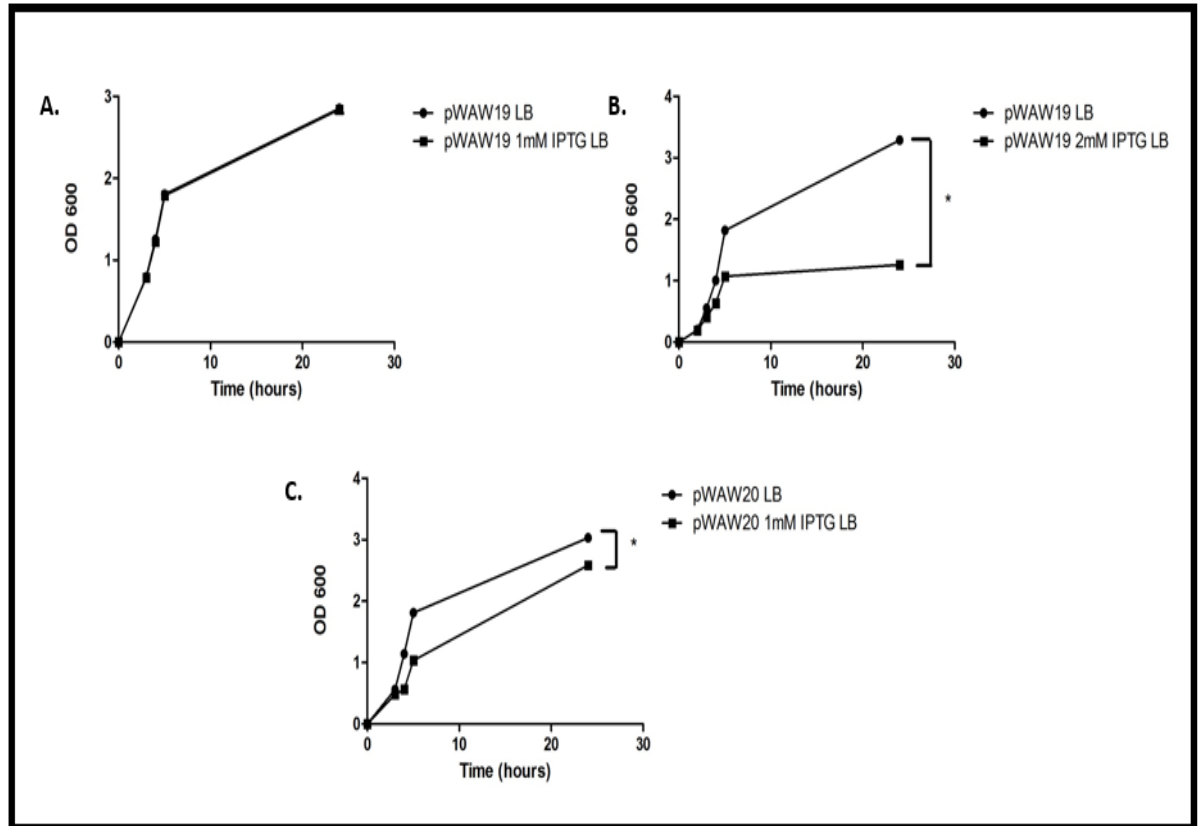


Figure 22: Growth response of *E. coli* to ectopic expression of D11S_2133 and D11S_2134. A) Growth of *E. coli* strain carrying plasmid for ectopic expression of D11S_2134 (pWAW19) grown in LB or with 1mM IPTG supplementation. B) Growth of *E. coli* strain carrying pWAW19 grown in LB or with 2mM IPTG supplementation. C) Growth of *E. coli* strain carrying plasmid for ectopic expression of D11S_2133 (pWAW20) grown in LB or with 1mM IPTG supplementation. All experiments were done in triplicate with two independent trials. $P < 0.05$.

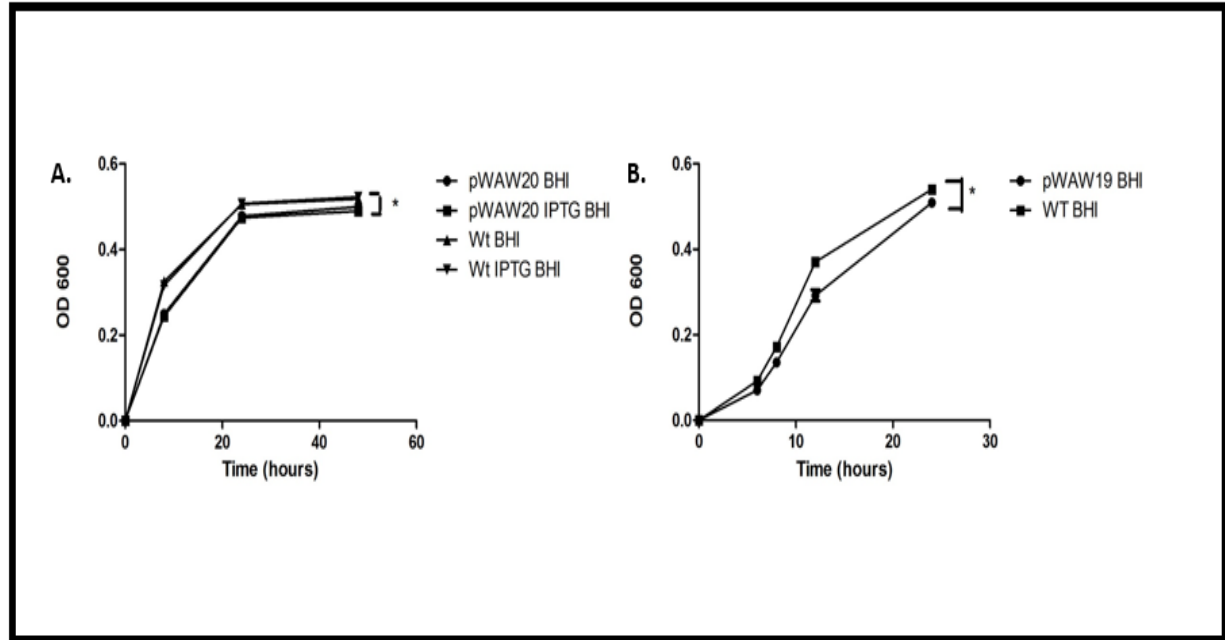


Figure 23: Growth of *A. actinomycetemcomitans* in response to ectopic expression of D11S_2133 or D11S_2134. A) Growth of Wt strain of *A. actinomycetemcomitans* with the empty vector pJT3 or a strain carrying pWAW20 grown in BHI or BHI with 1mM IPTG. B) Growth of Wt of a strain carrying pWAW19 grown in BHI. All experiments were done in triplicate with two independent trials. $P < 0.05$.

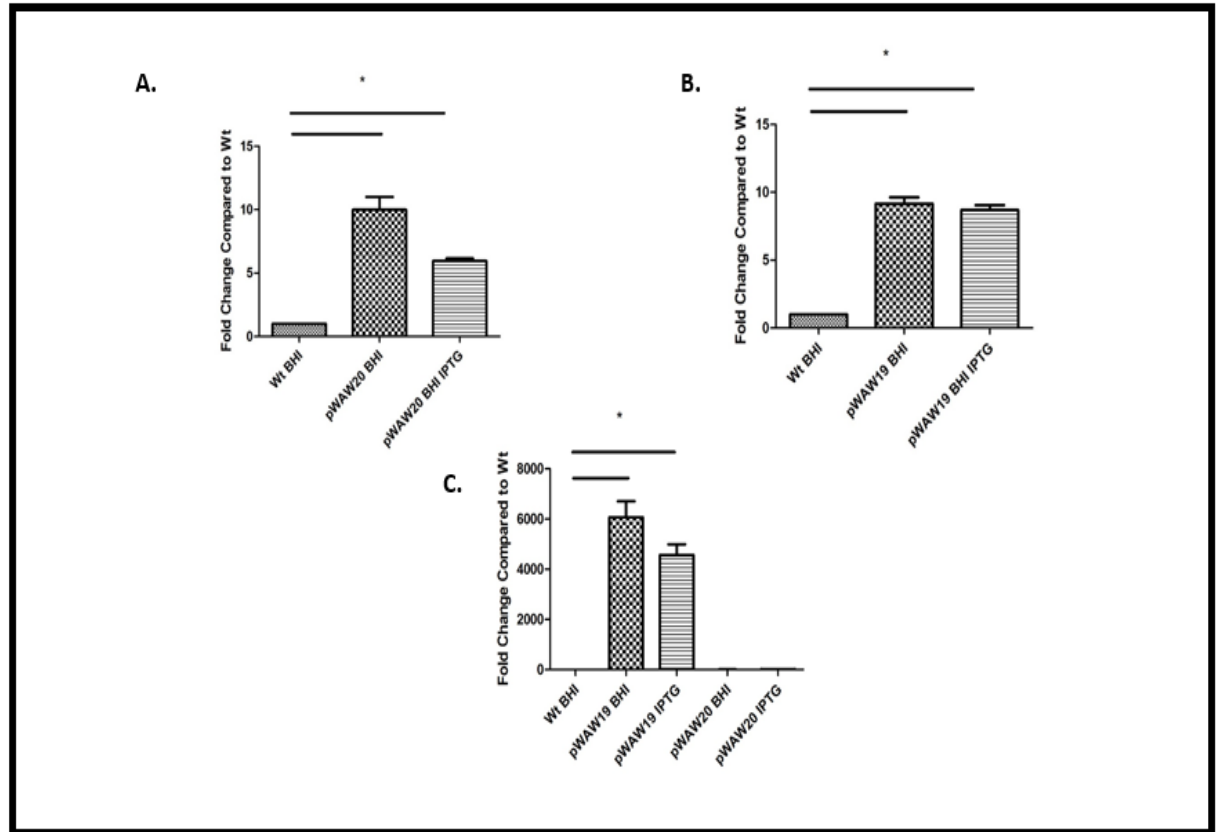


Figure 24: Real-time expression of D11S_2133, D11S_2134, and *ygiW*. A) Real-time expression of D11S_2133 in Wt *A. actinomycetemcomitans* compared to a strain carrying a plasmid for ectopic expression of D11S_2133 (pWAW20) grown in BHI with or without 1mM IPTG. B) Real-time expression of D11S_2133 in Wt *A. actinomycetemcomitans* compared to a strain carrying a plasmid for ectopic expression of D11S_2134 (pWAW19) grown in BHI with or without 1mM IPTG. C) Real-time expression of *ygiW* in Wt *A. actinomycetemcomitans* compared to a strain carrying the plasmid for ectopic expression of D11S_2134 (pWAW19) or D11S_2133 (pWAW20) grown in BHI with or without 1mM IPTG. All experiments were done in triplicate with two independent trials. $P < 0.05$.

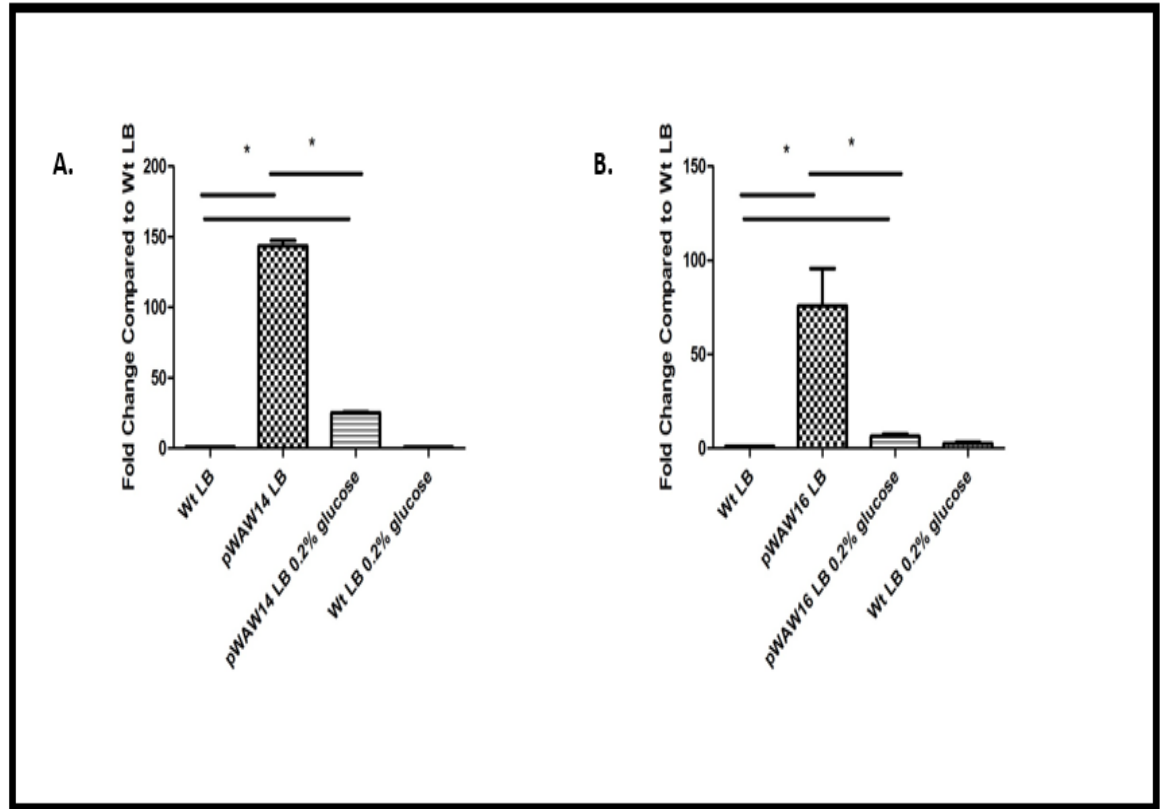


Figure 25: Real-time Expression of D11S_2133 or D11S_2134. A) Real-time expression of D11S_2133 in Wt *A. actinomycetemcomitans* grown in LB compared to Wt grown in LB with 0.2% glucose or a strain carrying plasmid for ectopic expression of D11S_2133 (pWAW14) grown in LB or LB with 0.2% glucose. B) Real-time expression of D11S_2134 in Wt *A. actinomycetemcomitans* grown in LB compared to Wt grown in LB with 0.2% glucose or a strain carrying plasmid for ectopic expression of D11S_2134 (pWAW16) grown in LB or LB with 0.2% glucose. All experiments were done in triplicate with two independent trials. $P < 0.05$.

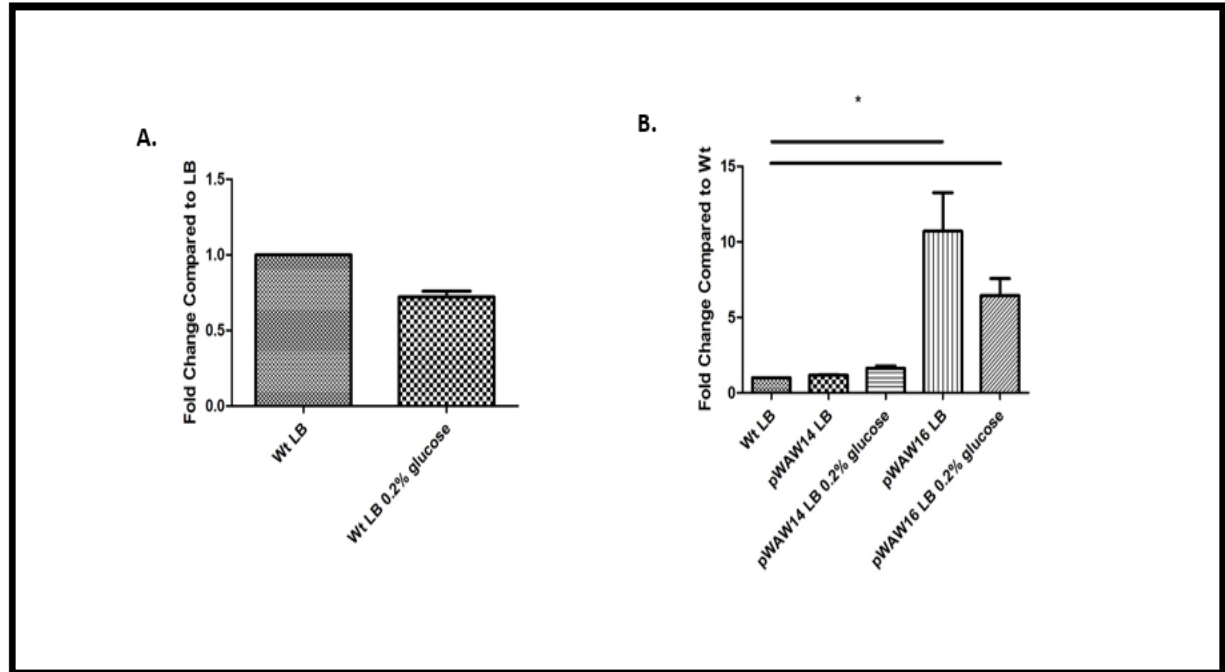


Figure 26: Regulation of *ygiW* expression by D11S_2133-2134. A) Real-time expression of *ygiW* in Wt *A. actinomycetemcomitans* grown in LB compared to grown in LB with 0.2% glucose. B) Real-time expression of *ygiW* in Wt *A. actinomycetemcomitans* grown in LB compared to *A. actinomycetemcomitans* carrying pWAW16 (D11S_2134) or pWAW14 (D11S_2133) grown in LB or LB with 0.2% glucose. All experiments were done in triplicate with two independent trials. P < 0.05.

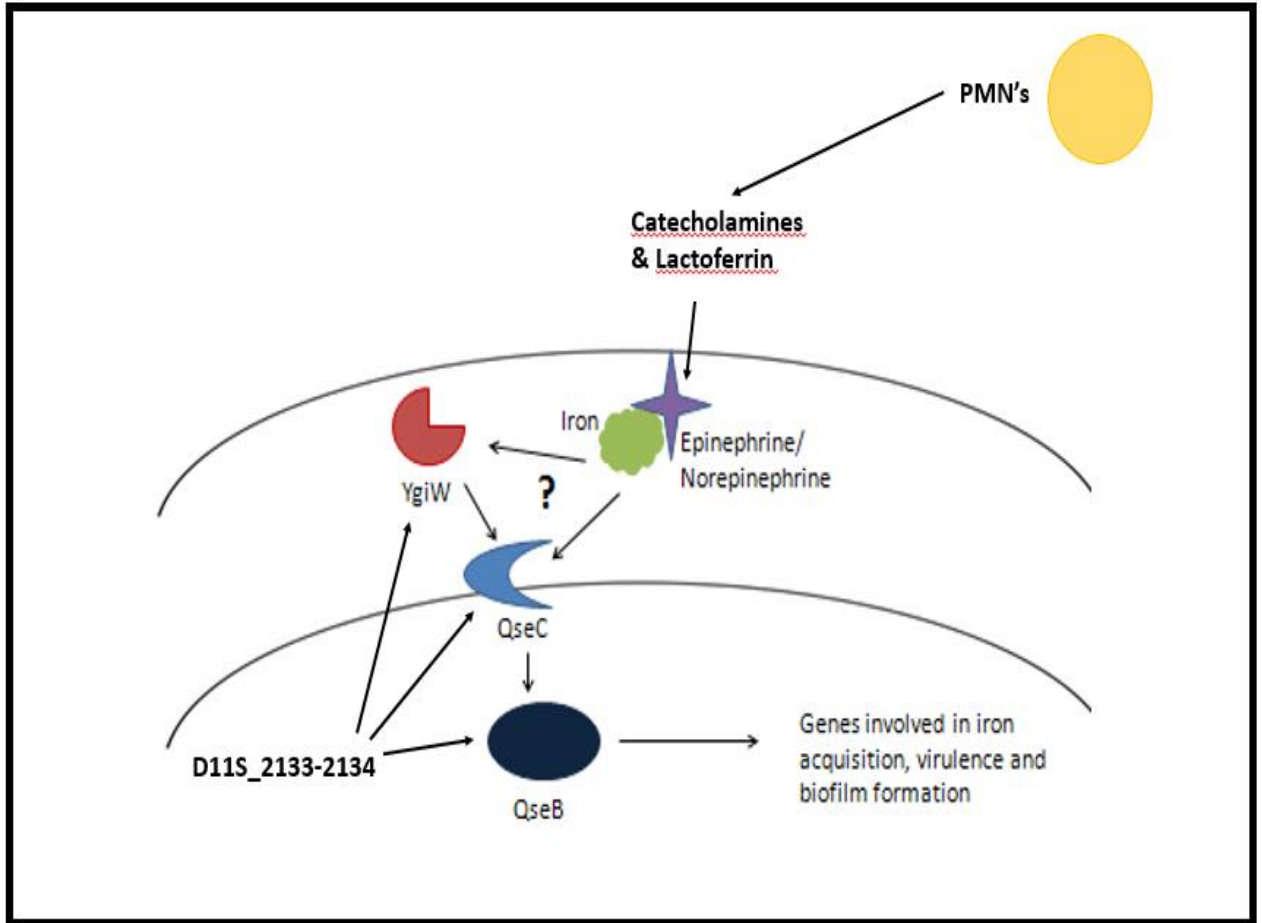


Figure 27: Schematic of QseBC activation by CAT-Fe and regulation by D11S_2133-2134. Activated polymorphonuclear cells release catecholamines and lactoferrin. The holo-lactoferrin is bound by catecholamines that scavenge the iron from them. The CAT-Fe complex is recognized by QseC (with or without the help of YgiW) and activates QseC, in turn activating QseB. QseB regulates genes involved in iron uptake, virulence and biofilm formation. Increased levels of the anti-toxin encoded for by D11S_2134 results in increased expression of *qseBC*.

Table 9: Expression of Genes Involved in Stress Response

ID Tag	Product	Fold Change	P-value
D11S_0146	heat shock protein HslVU, ATPase subunit HslU	8.24	8.79E-03
D11S_0147	ATP-dependent protease peptidase subunit	8.15	7.00E-03
D11S_0551	ATP-dependent chaperone ClpB	14.5	9.08E-03
D11S_0599	chaperonin GroS	5.36	7.96E-03
D11S_0656	universal stress protein A	2.17	3.35E-04
D11S_0739	RNA polymerase sigma factor RpoE	4.3	4.10E-02
D11S_0795	heat shock protein 90	11.32	1.97E-02
D11S_0838	RecN protein	1.77	1.09E-02
D11S_0841	heat shock protein GrpE	6.96	3.77E-02
D11S_0922	molecular chaperone DnaK	8.91	7.63E-03
D11S_1074	DNA protection during starvation protein	1.74	1.72E-02
D11S_1431	cold shock domain protein CspD	1.8	2.05E-02
D11S_1480	DNA mismatch repair protein	2.16	1.28E-02
D11S_1522	ATP-dependent protease La	4.51	6.74E-03
D11S_1798	Stability protein StbD	2.41	3.07E-02
D11S_1799	putative relE protein	2.13	2.94E-02

CHAPTER SEVEN: SUMMARY

QseBC is a conserved TCS in the *Enterobacteriaceae* and *Pasteurellaceae* that has been shown previously to play a role in regulating several complex phenotypes including virulence [44, 112], biofilm formation [44, 53, 71, 113], and metabolism [50, 69]. Interestingly, the activating signal varies from species to species. In *E. coli* and *Salmonella*, QseC was shown to be activated by AI-3 and by catecholamines [54-56]. In *H. influenzae*, QseBC (FirRS) did not respond to catecholamines but was activated by ferrous iron, cold temperatures and zinc [62]. The activating signal for the QseC in *A. actinomycetemcomitans* was found to be the combination of both catecholamines and iron (either ferrous or ferric), and the activation was dependent on having a functional YgiW, QseB and QseC. The exact role of YgiW is still unclear as to whether it binds to catecholamine and/or iron in the periplasm and perhaps shuttles the complex to the QseC sensor or if perhaps YgiW interacts with QseC. In addition, questions still remain as to the nature of the binding pocket(s) of CAT-Fe: whether there are two different pockets for each component, or if CAT-Fe binds one pocket as a complex.

Although it was previously shown that QseC is vital for virulence and biofilm formation, the complete regulon and downstream functional outcomes of QseC activation via CAT-Fe was unknown. Interestingly, the largest group of genes that were differentially transcribed in *A. actinomycetemcomitans* were genes involved in anaerobic respiration and metabolism. There was a significant up-regulation of genes involved in formate, fumarate, mannose, succinate, and aspartate metabolism as well as an up-regulation of components of the electron transport chain. Metabolomics performed with samples treated with Ne/FeCl₂ confirmed the outcomes suggested by changes in

gene transcription. The up-regulation of genes and increase in metabolites associated with anaerobic respiration and metabolism is consistent with the findings of Jorth *et al* that showed that the same genes and pathways were highly up-regulated *in vivo* and therefore might be essential for the ability of *A. actinomycetemcomitans* to colonize the host [52].

In contrast, genes involved in the metabolism of fatty acids, lipid and LPS biosynthesis were consistently down-regulated. The down-regulation of these genes translated into significant decreases in the amount of several fatty acids such as palmitic acid, myristic acid, and palmitelaidic acid and significant changes in the lipid profile of the plasma membrane. Most notable was that several long-chained fatty acids were decreased in cells treated with Ne/FeCl₂ compared to CDM. The decrease in length of fatty acid chains suggests that there is a change in membrane fluidity, specifically an increase in fluidity with Ne/FeCl₂ treatment.

Ne/FeCl₂ represents an iron-rich environment, which is confirmed by the fact that ferritin was highly up-regulated while iron acquisition genes were down-regulated. The genes involved in iron acquisition were most likely down-regulated as a mechanism to maintain iron homeostasis. In addition, there was an up-regulation of genes involved in oxidative stress with exposure to Ne/FeCl₂, but this up-regulation was most likely not due to iron toxicity. The up-regulation of oxidative stress genes was confirmed by a significant increase in catalase activity and a protective effect against H₂O₂ stress. This suggests that the ability to detect Ne/FeCl₂ might prepare *A. actinomycetemcomitans* for growth in the oral cavity, an environment where H₂O₂ exposure is common either from host cells like the respiratory burst from neutrophils or other oral bacteria.

Other functional outcomes due to Ne/FeCl₂ exposure included increase in

planktonic growth and biofilm formation. The increase in planktonic growth was not dependent on a functional QseC as a strain lacking the periplasmic domain of QseC still saw a significant increase in growth with Ne/FeCl₂ supplementation. However, the increase in biofilm formation in response to Ne/FeCl₂ was dependent on QseC. The presence of a planktonic growth phenotype despite the absence of a functional QseC suggests that there might be other receptors that might respond to catecholamines or CAT-Fe, as has been suggested for other bacteria [102], or that QseC isn't as vital to planktonic growth as biofilm formation. The dependence on QseC for biofilm formation has been previously shown [44], so the lack of a biofilm phenotype in response to CAT-Fe may be due to the overall importance of QseC on the ability of *A. actinomycetemcomitans* to form biofilms.

In contrast, the TonB dependent receptor was found to be essential for both the planktonic growth and biofilm phenotype, but not for the ability of QseC to respond to catecholamines. The TonB dependent receptor is part of the putative enterobactin receptor of *A. actinomycetemcomitans*. Enterobactin biosynthesis and uptake was shown to be essential for catecholamine mediated growth enhancements in *E. coli* [58]. Since it was shown to also be essential for catecholamine mediated growth phenotypes, but not for QseC activation, the TonB dependent receptor likely lies downstream of QseC activation and plays a role in allowing *A. actinomycetemcomitans* to take advantage of catecholamine mediated iron acquisition. This also suggests there is some other uptake system that is responsible for bringing catecholamines or CAT-Fe into the periplasm to be sensed by QseC.

The impact of both alpha and beta adrenergic receptor antagonists to block CAT-Fe activation of QseC and the downstream effect on planktonic growth was also

explored. Surprisingly, both adrenergic receptor antagonists resulted in a significant activation of QseC at 400 μ M. At this same concentration the activation of QseC in the presence of just the receptor antagonists was not significantly different than the activation of QseC in the presence of the antagonists and Ne/FeCl₂. The adrenergic receptor antagonists could still be potential therapeutics since the addition of them to the media resulted in significant inhibition of growth suggesting that it has some overall toxic effect to the cell that is not dependent on QseC.

The role that QseBC plays on a variety of complex and essential processes in *A. actinomycetemcomitans* means that its presence is essential for the cell to sense the environment and adapt to any changes. Therefore, the lack of QseB results in an up-regulation of the stress response, either due to a direct role of QseB on regulating the stress response or an indirect role of the lack of regulating genes via QseB causing stress to the bacteria. Several of the genes that were up-regulated in the $\Delta qseB$ strain include the TA response system: the Lon protease and two putative RelE TA systems (D11S_1194-1195 & D11S_1798-1799). Lon was also up-regulated in the $\Delta qseC$ strain showing that both components of this two-component system play a role in the stress response.

One of the putative RelE TA systems was shown to be highly up-regulated during iron starvation suggesting that it might play a role in regulating the response of *A. actinomycetemcomitans* to variations in environmental iron, particularly in regulating expression of *ygiW-qseBC*. Ectopic expression of the anti-toxin encoded for by D11S_2134 resulted in a significant up-regulation of expression of the *ygiW-qseBC* operon as did the Lon protease suggesting that these systems function together to regulate *ygiW-qseBC* expression to fine tune it depending on the concentration of iron in

the local environment.

CHAPTER EIGHT: FUTURE DIRECTIONS

Determining the Structure and the Binding Pocket(s) for CAT-Fe:

The QseC of *E. coli* and *Salmonella* can be activated by catecholamines in iron-limiting conditions, but the QseC of *A. actinomycetemcomitans* is only activated in the presence of both catecholamines and iron. In addition, unlike the QseC of *E. coli*, the QseC of *A. actinomycetemcomitans* was activated by adrenergic receptor antagonists. There is a 70% sequence similarity between the QseC of *E. coli* and *A. actinomycetemcomitans* and no strong similarity has been shown between QseC and the eukaryotic adrenergic receptors.

Since the QseC of *A. actinomycetemcomitans* functions uniquely, it suggests that the structure and binding pocket of QseC might also be unique. In order to understand more about how QseC recognizes the activating signal or why adrenergic receptor antagonists activate QseC, the structure of the binding pocket still needs to be elucidated.

Particularly, it is unknown as to whether CAT-Fe binds in the same pocket or if there are separate binding pockets for catecholamine and iron. Since QseC plays an essential role in virulence, it offers a good target for therapeutics. Understanding more about the binding pocket may be essential for the development of therapeutics for targeting *A. actinomycetemcomitans* mediated periodontitis.

In order to answer this question, equilibrium dialysis using purified QseC and either catecholamine, iron or both will be used to determine if QseC binds to the CAT-Fe complex or to each individual component. Furthermore, if catecholamine and iron bind separately, the question remains as to whether there are two binding independent binding pockets or one. Each component could bind separately, but based on the β -galactosidase assay, both are needed for QseC to become activated. In order to answer

this, further structural and functional analysis of QseC would need to be done, particularly of the periplasmic domain. One possible approach is to crystallize this domain for 3-dimensional structural determination.

Determining the Potential Role of YgiW in Binding CAT-Fe

YgiW is a putative solute binding protein of the OB-fold family. It is also co-transcribed with *qseBC* in *A. actinomycetemcomitans* and closely associated with the TCS in *E. coli* on the chromosome. Since the $\Delta ygiW$ strain showed no activation of QseC in the presence of CAT-Fe, this suggests that it is essential for QseC mediated CAT-Fe binding. However, whether it directly binds either component is unknown. This question could also be addressed by equilibrium dialysis. Further structural analysis of YgiW can be done by introducing mutations in the putative solute binding loops.

CAT-Fe Mediated Changes to Virulence:

Stress is one of the risk factors for the development and worsening of periodontitis [130]. One possible explanation for this link is that stress causes an increase in catecholamine stress hormones which can be exploited by the bacteria in order to acquire iron. The link between stress and worsening of infection has been demonstrated previously and the exposure of *E. coli*, *P. gingivalis*, and *Salmonella* to catecholamines has been shown to increase virulence and expression of various virulence factors. It remains unknown if exposure to CAT-Fe results in increased virulence. CAT-Fe did result in the down-regulation of several well-characterized virulence factors in the microarray, e.g. leukotoxin, cytolethal distending toxin, and *pgaB*. Interestingly, *pgaB* was down-regulated, but CAT-Fe exposure resulted in a significant increase in biofilm formation. The ability of bacteria to form biofilms has been linked to disease and persistence of infection, so it is possible that although many well-

characterized virulence factors were down-regulated, there could be an increase in virulence in a mouse model of periodontitis. Further, there was a large overlap between the genes that were up-regulated in the microarray to those that were up-regulated when *A. actinomycetemcomitans* was grown *in vivo* in an abscess model. This suggests that the ability of the bacteria to detect catecholamines is essential for its ability to respond and adapt to the host environment.

In addition, the inflamed gingiva is most likely an environment high in catecholamines and lactoferrin due to their release by activated neutrophils. The exposure to CAT-Fe would lead to an activation of QseC, which has been shown to be an important regulator of virulence in *A. actinomycetemcomitans*. The previous work showing that QseC is vital for virulence in *A. actinomycetemcomitans* was performed using a mouse model of periodontitis [44]. Any changes to bone loss levels is correlated to changes in virulence. Mice could be given exogenous catecholamines in their water prior to infection with *A. actinomycetemcomitans* or alternatively, the C.129-Chgatm1Gnh/J strain of mice (<https://www.jax.org/strain/023514>) with high systemic levels of catecholamines can be used for these studies.

Determine if QseC can be Activated by Catecholamines and Holo-Transferrin

Catecholamines have been shown to act as pseudosiderophores by being able to scavenge iron from holo-transferrin or holo-lactoferrin [57]. QseC is activated by the combination of catecholamines and ferrous iron, but there is little free iron in the host. Most iron is bound by a host iron binding protein like lactoferrin or transferrin. In order to confirm that *A. actinomycetemcomitans* is responding to CAT-Fe in the host by recognizing catecholamines that have scavenged iron from lactoferrin, catecholamines and holo-lactoferrin, instead of ferrous iron, can be added to the media to determine if it

results in the same phenotype of QseC activation in response to CAT-Fe. Similarly, the addition of apo-lactoferrin and catecholamines should not result in any QseC activation since there would be no iron for the catecholamine to scavenge.

Determining the effect of *A. actinomycetemcomitans* on Neutrophils in Terms of Catecholamine Release

Activated neutrophils have been reported to release catecholamines up to millimolar amounts in response to inflammatory signals [25]. Based on this information, we hypothesized that the CAT-Fe activating signal for QseC is from activated neutrophils that are releasing catecholamines in response to being activated by *A. actinomycetemcomitans*. However, the degree to which *A. actinomycetemcomitans* can stimulate neutrophils to release catecholamines has not been extensively examined. Therefore, it is important to demonstrate that *A. actinomycetemcomitans* induces catecholamine release and at what multiplicity of infection (MOI) the release occurs at. For this experiment, different MOI's for *A. actinomycetemcomitans* will be tested against isolated neutrophil. The mechanisms of catecholamine release by neutrophils can also be studied.

Determining the Mechanism of Action for the D11S_2133-2134 TA system

The toxins from most type II TA systems work as endoribonucleases, either ribosome dependent or ribosome independent [84]. D11S_2133-2134 is a putative RelE-like type II TA system. Based on the growth results in *E. coli* with the ectopic expression of D11S_2133 and D11S_2134, D11S_2133 is correctly annotated as a putative toxin and D11S_2134 is the anti-toxin, but in order to confirm these labels, functional assays will need to be performed. RelE toxins have been shown to act as endoribonucleases that cleave between the second and third position of an upstream purine [111]. In order to

confirm that D11S_2133 acts as endoribonuclease, then different mRNA's with known sequences will be incubated together with the purified toxin and then ran on a gel to look for RNA degradation. Since some of the toxins act as ribosome dependent nucleases then the experiment would also need to be repeated using isolated ribosomes from *A. actinomycetemcomitans*.

REFERENCES

1. Li, X., et al., *Systemic diseases caused by oral infection*. Clin Microbiol Rev, 2000. **13**(4): p. 547-58.
2. Newman, H.N., *Focal infection*. J Dent Res, 1996. **75**(12): p. 1912-9.
3. Gendron, R., D. Grenier, and L. Maheu-Robert, *The oral cavity as a reservoir of bacterial pathogens for focal infections*. Microbes Infect, 2000. **2**(8): p. 897-906.
4. Vaizey, J.M. and A.E. Clark-Kennedy, *Dental Sepsis: Anaemia, Dyspepsia, and Rheumatism*. Br Med J, 1939. **1**(4094): p. 1269-73.
5. Kinane, D.F., *Periodontal diseases' contributions to cardiovascular disease: an overview of potential mechanisms*. Ann Periodontol, 1998. **3**(1): p. 142-50.
6. Wegner, N., et al., *Peptidylarginine deiminase from Porphyromonas gingivalis citrullinates human fibrinogen and alpha-enolase: implications for autoimmunity in rheumatoid arthritis*. Arthritis Rheum, 2010. **62**(9): p. 2662-72.
7. Townsend, T.R. and J.Y. Gillenwater, *Urinary tract infection due to Actinobacillus actinomycetemcomitans*. JAMA, 1969. **210**(3): p. 558.
8. Zijlstra, E.E., et al., *Pericarditis, pneumonia and brain abscess due to a combined Actinomyces--Actinobacillus actinomycetemcomitans infection*. J Infect, 1992. **25**(1): p. 83-7.
9. Whyman, R.A. and E.E. MacFadyen, *Dens in dente associated with infective endocarditis*. Oral Surg Oral Med Oral Pathol, 1994. **78**(1): p. 47-50.
10. Lass, J.H., et al., *Actinobacillus actinomycetemcomitans endophthalmitis with subacute endocarditis*. Ann Ophthalmol, 1984. **16**(1): p. 54-61.
11. Rahamat-Langendoen, J.C., et al., *Brain abscess associated with Aggregatibacter actinomycetemcomitans: case report and review of literature*. J Clin Periodontol, 2011. **38**(8): p. 702-6.
12. Armitage, G.C., *Clinical evaluation of periodontal diseases*. Periodontol 2000, 1995. **7**: p. 39-53.
13. Eke, P.I., et al., *Update on Prevalence of Periodontitis in Adults in the United States: NHANES 2009 to 2012*. J Periodontol, 2015. **86**(5): p. 611-22.
14. Brown, L.J., B.A. Johns, and T.P. Wall, *The economics of periodontal diseases*. Periodontol 2000, 2002. **29**: p. 223-34.
15. Mesa, F., et al., *Catecholamine metabolites in urine, as chronic stress biomarkers, are associated with higher risk of chronic periodontitis in adults*. J Periodontol, 2014. **85**(12): p. 1755-62.
16. Whitacre, C.C., S.C. Reingold, and P.A. O'Looney, *A gender gap in autoimmunity*. Science, 1999. **283**(5406): p. 1277-8.
17. Duan, X., et al., *Sex dimorphism in periodontitis in animal models*. J Periodontol Res, 2015.
18. Valencia, A., et al., *Racial and ethnic disparities in utilization of dental services among children in Iowa: the Latino experience*. Am J Public Health, 2012. **102**(12): p. 2352-9.
19. Zambon, J.J., et al., *Cigarette smoking increases the risk for subgingival infection with periodontal pathogens*. J Periodontol, 1996. **67**(10 Suppl): p. 1050-4.
20. Umeda, M., et al., *Risk indicators for harboring periodontal pathogens*. J Periodontol, 1998. **69**(10): p. 1111-8.

21. Bagaitkar, J., et al., *Tobacco smoke augments Porphyromonas gingivalis-Streptococcus gordonii biofilm formation*. PLoS One, 2011. **6**(11): p. e27386.
22. Lie, M.A., et al., *Oral microbiota in smokers and non-smokers in natural and experimentally-induced gingivitis*. J Clin Periodontol, 1998. **25**(8): p. 677-86.
23. Bagaitkar, J., et al., *Tobacco upregulates P. gingivalis fimbrial proteins which induce TLR2 hyposensitivity*. PLoS One, 2010. **5**(5): p. e9323.
24. Nair, S.P., et al., *Bacterially induced bone destruction: mechanisms and misconceptions*. Infect Immun, 1996. **64**(7): p. 2371-80.
25. Flierl, M.A., et al., *Upregulation of phagocyte-derived catecholamines augments the acute inflammatory response*. PLoS One, 2009. **4**(2): p. e4414.
26. Chahboun, H., et al., *Bacterial profile of aggressive periodontitis in Morocco: a cross-sectional study*. BMC Oral Health, 2015. **15**: p. 25.
27. Kolenbrander, P.E., et al., *Bacterial interactions and successions during plaque development*. Periodontol 2000, 2006. **42**: p. 47-79.
28. Socransky, S.S., et al., *Microbial complexes in subgingival plaque*. J Clin Periodontol, 1998. **25**(2): p. 134-44.
29. Kim, T.S., et al., *Serotypes of Aggregatibacter actinomycetemcomitans in patients with different ethnic backgrounds*. J Periodontol, 2009. **80**(12): p. 2020-7.
30. Brigido, J.A., et al., *Serotypes of Aggregatibacter actinomycetemcomitans in relation to periodontal status and geographic origin of individuals-a review of the literature*. Med Oral Patol Oral Cir Bucal, 2014. **19**(2): p. e184-91.
31. Kilian, M. and C.R. Schiott, *Haemophili and related bacteria in the human oral cavity*. Arch Oral Biol, 1975. **20**(12): p. 791-6.
32. Molina, F., et al., *Infectious arthritis of the knee due to Actinobacillus actinomycetemcomitans*. Eur J Clin Microbiol Infect Dis, 1994. **13**(8): p. 687-9.
33. Zhang, T., et al., *Aggregatibacter actinomycetemcomitans accelerates atherosclerosis with an increase in atherogenic factors in spontaneously hyperlipidemic mice*. FEMS Immunol Med Microbiol, 2010. **59**(2): p. 143-51.
34. Lally, E.T., et al., *Structure and function of the B and D genes of the Actinobacillus actinomycetemcomitans leukotoxin complex*. Microb Pathog, 1991. **11**(2): p. 111-21.
35. Guthmiller, J.M., D. Kolodrubetz, and E. Kraig, *Mutational analysis of the putative leukotoxin transport genes in Actinobacillus actinomycetemcomitans*. Microb Pathog, 1995. **18**(5): p. 307-21.
36. Hritz, M., E. Fisher, and D.R. Demuth, *Differential regulation of the leukotoxin operon in highly leukotoxic and minimally leukotoxic strains of Actinobacillus actinomycetemcomitans*. Infect Immun, 1996. **64**(7): p. 2724-9.
37. Haubek, D. and A. Johansson, *Pathogenicity of the highly leukotoxic JP2 clone of Aggregatibacter actinomycetemcomitans and its geographic dissemination and role in aggressive periodontitis*. J Oral Microbiol, 2014. **6**.
38. Shenker, B.J., et al., *The toxicity of the Aggregatibacter actinomycetemcomitans cytolethal distending toxin correlates with its phosphatidylinositol-3,4,5-triphosphate phosphatase activity*. Cell Microbiol, 2015.
39. Fives-Taylor, P.M., et al., *Virulence factors of Actinobacillus actinomycetemcomitans*. Periodontol 2000, 1999. **20**: p. 136-67.
40. Ohguchi, Y., et al., *Capsular polysaccharide from Actinobacillus actinomycetemcomitans inhibits IL-6 and IL-8 production in human gingival fibroblast*. J Periodontal Res, 2003. **38**(2): p. 191-7.

41. Wang, P.L., et al., *Purification and characterization of a trypsin-like protease from the culture supernatant of Actinobacillus actinomycetemcomitans Y4*. Eur J Oral Sci, 1999. **107**(2): p. 147-53.
42. Tang, G., et al., *EmaA, a potential virulence determinant of Aggregatibacter actinomycetemcomitans in infective endocarditis*. Infect Immun, 2008. **76**(6): p. 2316-24.
43. Saito, T., et al., *Fimbriae-associated genes are biofilm-forming factors in Aggregatibacter actinomycetemcomitans strains*. Bull Tokyo Dent Coll, 2010. **51**(3): p. 145-50.
44. Novak, E.A., et al., *Autoinducer-2 and QseC control biofilm formation and in vivo virulence of Aggregatibacter actinomycetemcomitans*. Infect Immun, 2010. **78**(7): p. 2919-26.
45. Lai, P.C., M.R. Schibler, and J.D. Walters, *Azithromycin enhances phagocytic killing of Aggregatibacter actinomycetemcomitans Y4 by human neutrophils*. J Periodontol, 2015. **86**(1): p. 155-61.
46. Permpanich, P., M.J. Kowolik, and D.M. Galli, *Resistance of fluorescent-labelled Actinobacillus actinomycetemcomitans strains to phagocytosis and killing by human neutrophils*. Cell Microbiol, 2006. **8**(1): p. 72-84.
47. Meyer, D.H., J.E. Lippmann, and P.M. Fives-Taylor, *Invasion of epithelial cells by Actinobacillus actinomycetemcomitans: a dynamic, multistep process*. Infect Immun, 1996. **64**(8): p. 2988-97.
48. Schenkein, H.A., et al., *Invasion of human vascular endothelial cells by Actinobacillus actinomycetemcomitans via the receptor for platelet-activating factor*. Infect Immun, 2000. **68**(9): p. 5416-9.
49. Torres-Escobar, A., et al., *Transcriptional regulation of Aggregatibacter actinomycetemcomitans *IsrACDBFG* and *IsrRK* operons and their role in biofilm formation*. J Bacteriol, 2013. **195**(1): p. 56-65.
50. Hadjifrangiskou, M., et al., *A central metabolic circuit controlled by QseC in pathogenic Escherichia coli*. Mol Microbiol, 2011. **80**(6): p. 1516-29.
51. Heroven, A.K. and P. Dersch, *Coregulation of host-adapted metabolism and virulence by pathogenic yersiniae*. Front Cell Infect Microbiol, 2014. **4**: p. 146.
52. Jorth, P., et al., *Probing bacterial metabolism during infection using high-resolution transcriptomics*. J Bacteriol, 2013. **195**(22): p. 4991-8.
53. Juarez-Rodriguez, M.D., A. Torres-Escobar, and D.R. Demuth, *ygiW and qseBC are co-expressed in Aggregatibacter actinomycetemcomitans and regulate biofilm growth*. Microbiology, 2013. **159**(Pt 6): p. 989-1001.
54. Sperandio, V., et al., *Bacteria-host communication: the language of hormones*. Proc Natl Acad Sci U S A, 2003. **100**(15): p. 8951-6.
55. Clarke, M.B., et al., *The QseC sensor kinase: a bacterial adrenergic receptor*. Proc Natl Acad Sci U S A, 2006. **103**(27): p. 10420-5.
56. Williams, P.H., et al., *Catechol receptor proteins in Salmonella enterica: role in virulence and implications for vaccine development*. Vaccine, 2006. **24**(18): p. 3840-4.
57. Freestone, P.P., et al., *Microbial endocrinology: how stress influences susceptibility to infection*. Trends Microbiol, 2008. **16**(2): p. 55-64.
58. Burton, C.L., et al., *The growth response of Escherichia coli to neurotransmitters and related catecholamine drugs requires a functional enterobactin biosynthesis and uptake system*. Infect Immun, 2002. **70**(11): p. 5913-23.

59. Wosten, M.M., et al., *A signal transduction system that responds to extracellular iron*. Cell, 2000. **103**(1): p. 113-25.
60. Guckes, K.R., et al., *Strong cross-system interactions drive the activation of the QseB response regulator in the absence of its cognate sensor*. Proc Natl Acad Sci U S A, 2013. **110**(41): p. 16592-7.
61. Walters, M., M.P. Sircili, and V. Sperandio, *AI-3 synthesis is not dependent on luxS in Escherichia coli*. J Bacteriol, 2006. **188**(16): p. 5668-81.
62. Steele, K.H., et al., *Characterization of a ferrous iron-responsive two-component system in nontypeable Haemophilus influenzae*. J Bacteriol, 2012. **194**(22): p. 6162-73.
63. Reading, N.C., et al., *A novel two-component signaling system that activates transcription of an enterohemorrhagic Escherichia coli effector involved in remodeling of host actin*. J Bacteriol, 2007. **189**(6): p. 2468-76.
64. Clarke, M.B. and V. Sperandio, *Transcriptional regulation of flhDC by QseBC and sigma (FliA) in enterohaemorrhagic Escherichia coli*. Mol Microbiol, 2005. **57**(6): p. 1734-49.
65. Bansal, T., et al., *Differential effects of epinephrine, norepinephrine, and indole on Escherichia coli O157:H7 chemotaxis, colonization, and gene expression*. Infect Immun, 2007. **75**(9): p. 4597-607.
66. Pullinger, G.D., et al., *Norepinephrine augments Salmonella enterica-induced enteritis in a manner associated with increased net replication but independent of the putative adrenergic sensor kinases QseC and QseE*. Infect Immun, 2010. **78**(1): p. 372-80.
67. Li, L., et al., *Global effects of catecholamines on Actinobacillus pleuropneumoniae gene expression*. PLoS One, 2012. **7**(2): p. e31121.
68. Graziano, T.S., et al., *Catecholamines promote the expression of virulence and oxidative stress genes in Porphyromonas gingivalis*. J Periodontal Res, 2014. **49**(5): p. 660-9.
69. Weigel, W.A., et al., *Aggregatibacter actinomycetemcomitans QseBC is activated by catecholamines and iron and regulates genes encoding proteins associated with anaerobic respiration and metabolism*. Mol Oral Microbiol, 2015.
70. Shao, H., et al., *Differential interaction of Aggregatibacter (Actinobacillus) actinomycetemcomitans LsrB and RbsB proteins with autoinducer 2*. J Bacteriol, 2007. **189**(15): p. 5559-65.
71. Gonzalez Barrios, A.F., et al., *Autoinducer 2 controls biofilm formation in Escherichia coli through a novel motility quorum-sensing regulator (MqsR, B3022)*. J Bacteriol, 2006. **188**(1): p. 305-16.
72. Kvetnansky, R., X. Lu, and M.G. Ziegler, *Stress-triggered changes in peripheral catecholaminergic systems*. Adv Pharmacol, 2013. **68**: p. 359-97.
73. Tsigos, C. and G.P. Chrousos, *Hypothalamic-pituitary-adrenal axis, neuroendocrine factors and stress*. J Psychosom Res, 2002. **53**(4): p. 865-71.
74. Brown, S.W., et al., *Catecholamines in a macrophage cell line*. J Neuroimmunol, 2003. **135**(1-2): p. 47-55.
75. Broadley, K.J., *The vascular effects of trace amines and amphetamines*. Pharmacol Ther, 2010. **125**(3): p. 363-75.
76. Freestone, P. and M. Lyte, *Stress and microbial endocrinology: prospects for ruminant nutrition*. Animal, 2010. **4**(7): p. 1248-57.
77. Sandrini, S.M., et al., *Elucidation of the mechanism by which catecholamine stress*

- hormones liberate iron from the innate immune defense proteins transferrin and lactoferrin.* J Bacteriol, 2010. **192**(2): p. 587-94.
78. Flierl, M.A., et al., *Phagocyte-derived catecholamines enhance acute inflammatory injury.* Nature, 2007. **449**(7163): p. 721-5.
 79. Esaguy, N., A.P. Aguas, and M.T. Silva, *High-resolution localization of lactoferrin in human neutrophils: labeling of secondary granules and cell heterogeneity.* J Leukoc Biol, 1989. **46**(1): p. 51-62.
 80. Freestone, P.P., R.D. Haigh, and M. Lyte, *Blockade of catecholamine-induced growth by adrenergic and dopaminergic receptor antagonists in Escherichia coli O157:H7, Salmonella enterica and Yersinia enterocolitica.* BMC Microbiol, 2007. **7**: p. 8.
 81. Wen, Y., E. Behiels, and B. Devreese, *Toxin-Antitoxin systems: their role in persistence, biofilm formation, and pathogenicity.* Pathog Dis, 2014. **70**(3): p. 240-9.
 82. Hansen, S., et al., *Regulation of the Escherichia coli HipBA toxin-antitoxin system by proteolysis.* PLoS One, 2012. **7**(6): p. e39185.
 83. Donegan, N.P., et al., *Proteolytic regulation of toxin-antitoxin systems by ClpPC in Staphylococcus aureus.* J Bacteriol, 2010. **192**(5): p. 1416-22.
 84. Maisonneuve, E., et al., *Bacterial persistence by RNA endonucleases.* Proc Natl Acad Sci U S A, 2011. **108**(32): p. 13206-11.
 85. Maisonneuve, E., M. Castro-Camargo, and K. Gerdes, *(p)ppGpp controls bacterial persistence by stochastic induction of toxin-antitoxin activity.* Cell, 2013. **154**(5): p. 1140-50.
 86. Amato, S.M. and M.P. Brynildsen, *Nutrient transitions are a source of persisters in Escherichia coli biofilms.* PLoS One, 2014. **9**(3): p. e93110.
 87. Zhang, Y., et al., *MazF cleaves cellular mRNAs specifically at ACA to block protein synthesis in Escherichia coli.* Mol Cell, 2003. **12**(4): p. 913-23.
 88. Socransky, S.S., J.L. Dzink, and C.M. Smith, *Chemically defined medium for oral microorganisms.* J Clin Microbiol, 1985. **22**(2): p. 303-5.
 89. Schroeder, A., et al., *The RIN: an RNA integrity number for assigning integrity values to RNA measurements.* BMC Mol Biol, 2006. **7**: p. 3.
 90. Juarez-Rodriguez, M.D., A. Torres-Escobar, and D.R. Demuth, *Construction of new cloning, lacZ reporter and scarless-markerless suicide vectors for genetic studies in Aggregatibacter actinomycetemcomitans.* Plasmid, 2013. **69**(3): p. 211-22.
 91. Ginalski, K., et al., *BOF: a novel family of bacterial OB-fold proteins.* FEBS Lett, 2004. **567**(2-3): p. 297-301.
 92. Li, L., et al., *Catecholamines promote Actinobacillus pleuropneumoniae growth by regulating iron metabolism.* PLoS One, 2015. **10**(4): p. e0121887.
 93. Roberts, A., et al., *Stress and the periodontal diseases: effects of catecholamines on the growth of periodontal bacteria in vitro.* Oral Microbiol Immunol, 2002. **17**(5): p. 296-303.
 94. Roberts, A., et al., *Stress and the periodontal diseases: growth responses of periodontal bacteria to Escherichia coli stress-associated autoinducer and exogenous Fe.* Oral Microbiol Immunol, 2005. **20**(3): p. 147-53.
 95. Scott, D.A. and J. Krauss, *Neutrophils in periodontal inflammation.* Front Oral Biol, 2012. **15**: p. 56-83.
 96. Zaric, S., et al., *Impaired immune tolerance to Porphyromonas gingivalis lipopolysaccharide promotes neutrophil migration and decreased apoptosis.*

- Infect Immun, 2010. **78**(10): p. 4151-6.
97. Hayashida, H., K. Poulsen, and M. Kilian, *Differences in iron acquisition from human haemoglobin among strains of Actinobacillus actinomycetemcomitans*. Microbiology, 2002. **148**(Pt 12): p. 3993-4001.
 98. Rhodes, E.R., et al., *Evaluation of different iron sources and their influence in biofilm formation by the dental pathogen Actinobacillus actinomycetemcomitans*. J Med Microbiol, 2007. **56**(Pt 1): p. 119-28.
 99. Rhodes, E.R., et al., *Iron acquisition in the dental pathogen Actinobacillus actinomycetemcomitans: what does it use as a source and how does it get this essential metal?* Biometals, 2007. **20**(3-4): p. 365-77.
 100. Alugupalli, K.R., et al., *Lactoferrin interaction with Actinobacillus actinomycetemcomitans*. Oral Microbiol Immunol, 1995. **10**(1): p. 35-41.
 101. Juarez-Rodriguez, M.D., A. Torres-Escobar, and D.R. Demuth, *Transcriptional regulation of the Aggregatibacter actinomycetemcomitans ygiW-qseBC operon by QseB and IHF proteins*. Microbiology, 2014.
 102. Karavolos, M.H., et al., *Pathogen espionage: multiple bacterial adrenergic sensors eavesdrop on host communication systems*. Mol Microbiol, 2013. **87**(3): p. 455-65.
 103. Intarak, N., et al., *Growth, motility and resistance to oxidative stress of the melioidosis pathogen Burkholderia pseudomallei are enhanced by epinephrine*. Pathog Dis, 2014. **72**(1): p. 24-31.
 104. Peekhaus, N. and T. Conway, *What's for dinner?: Entner-Doudoroff metabolism in Escherichia coli*. J Bacteriol, 1998. **180**(14): p. 3495-502.
 105. Inda, M.E., et al., *A lipid-mediated conformational switch modulates the thermosensing activity of DesK*. Proc Natl Acad Sci U S A, 2014. **111**(9): p. 3579-84.
 106. Albanesi, D., M.C. Mansilla, and D. de Mendoza, *The membrane fluidity sensor DesK of Bacillus subtilis controls the signal decay of its cognate response regulator*. J Bacteriol, 2004. **186**(9): p. 2655-63.
 107. Curtis, M.M., et al., *QseC inhibitors as an antivirulence approach for Gram-negative pathogens*. MBio, 2014. **5**(6): p. e02165.
 108. Yamaguchi, Y., J.H. Park, and M. Inouye, *MqsR, a crucial regulator for quorum sensing and biofilm formation, is a GCU-specific mRNA interferase in Escherichia coli*. J Biol Chem, 2009. **284**(42): p. 28746-53.
 109. Prysak, M.H., et al., *Bacterial toxin YafQ is an endoribonuclease that associates with the ribosome and blocks translation elongation through sequence-specific and frame-dependent mRNA cleavage*. Mol Microbiol, 2009. **71**(5): p. 1071-87.
 110. Zhu, L., et al., *Staphylococcus aureus MazF specifically cleaves a pentad sequence, UACAU, which is unusually abundant in the mRNA for pathogenic adhesive factor SraP*. J Bacteriol, 2009. **191**(10): p. 3248-55.
 111. Goeders, N., P.L. Dreze, and L. Van Melderen, *Relaxed cleavage specificity within the RelE toxin family*. J Bacteriol, 2013. **195**(11): p. 2541-9.
 112. Moreira, C.G., D. Weinshenker, and V. Sperandio, *QseC mediates Salmonella enterica serovar typhimurium virulence in vitro and in vivo*. Infect Immun, 2010. **78**(3): p. 914-26.
 113. Unal, C.M., et al., *QseC controls biofilm formation of non-typeable Haemophilus influenzae in addition to an AI-2-dependent mechanism*. Int J Med Microbiol, 2012. **302**(6): p. 261-9.

114. Sperandio, V., et al., *Quorum sensing controls expression of the type III secretion gene transcription and protein secretion in enterohemorrhagic and enteropathogenic Escherichia coli*. Proc Natl Acad Sci U S A, 1999. **96**(26): p. 15196-201.
115. Nicolaou, S., et al., *Overexpression of fetA (ybbL) and fetB (ybbM), Encoding an Iron Exporter, Enhances Resistance to Oxidative Stress in Escherichia coli*. Appl Environ Microbiol, 2013. **79**(23): p. 7210-7219.
116. Andrews, S.C., et al., *Bacterial Iron Homeostasis*. FEMS Microbiol Rev, 2003. **27**(2-3): p. 215-37.
117. Greene, J.C., *Oral Hygiene and Periodontal Disease*. Am J Public Health Nations Health, 1963. **53**: p. 913-22.
118. Leplae, R., et al., *Diversity of bacterial type II toxin-antitoxin systems: a comprehensive search and functional analysis of novel families*. Nucleic Acids Res, 2011. **39**(13): p. 5513-5525.
119. Yang, K. et al., *The role of the QseC quorum-sensing kinase in epinephrine-enhanced motility and biofilm formation by Escherichia coli*. Cell Biochem Biophys, 2014. **70**(1): p. 391-8.
120. Unterholzner, S. J., et al., *Toxin-antitoxin systems: Biology, identification, and application*. Mob Genet Elements, 2013. **3**(5): p. e26219.
121. Tian, Q.B., *Specific protein-DNA and protein-protein interaction in the hig gene system, a plasmid-borne proteic killer gene system of plasmid Rts1*. Plasmid, 2001. **45**(2): p. 63-74.
122. Kostakioti, M., et al., *Bacterial Biofilms: Development, Dispersal, and Therapeutic Strategies in the Dawn of the Postantibiotic Era*. Cold Spring Harb Perspect Med, 2013. **3**(4): a010306.
123. Jakubovics, N. S., *Intermicrobial Interactions as a Driver for Community Composition and Stratification of Oral Biofilms*. J Mol Biol, 2015. **427**(23): p. 3662-3675.
124. Lewis, J. P., *Metal Uptake in host-pathogen interactions: Role of iron in Porphyromonas gingivalis interactions with host organisms*. Periodontol 2000, 2011. **52**(1): p. 94-116.
125. Prax, M., *Metabolic aspects of bacterial persisters*. Front Cell Infect Microbiol, 2014. **4**.
126. Weigel, W. A., et al., *QseBC is a two component bacterial adrenergic receptor and global regulator of virulence in Enterobacteriaceae and Pasteurellaceae*. Mol Oral Microbiol, 2015.
127. Baker, J. G., et al., *Agonist Actions of β -Blockers Provide Evidence for Two Agonist Activation Sites or Conformations of the Human β 1-Adrenoreceptor*. Molecular Pharmacology, 2003. **63**(6): p. 1312-1321.
128. Garcia, C. A., *Iron is a signal for Stenotrophomonas maltophilia biofilm formation, oxidative stress response, OMPs expression, and virulence*. Front Microbiol, 2015. **4**.
129. Bowden, G. H., *Survival of oral bacteria*. Crit Rev Oral Biol Med, 1998. **9**(1): p. 54-85.
130. Goyal, S, et al., *Stress and periodontal disease: The link and logic*. Ind Psychiatry J, 2013. **22**(1): p. 4-1

Appendix

Table 1

Genes Differentially Regulated by Ne/FeCl₂

ID Tag	Product	Fold Change	Direction	P-value	rtPCR
D11S_0087	asparagine synthetase AsnA	2.9	up	5.61E-07	
D11S_0159	pts system mannose-specific eiiab component	2.99	up	7.69E-06	
D11S_0160	fructose permease iic component	2.39	up	4.84E-06	
D11S_0161	mannose permease iid component	2.1	up	5.71E-06	
D11S_0205	cytochrome c-type protein TorC	3.05	up	3.52E-06	
D11S_0206	periplasmic nitrate reductase, diheme cytochrome	2.94	up	2.25E-06	1.9 ± 0.06
D11S_0207	ferredoxin-type protein NapH	3.36	up	1.20E-05	
D11S_0208	quinol dehydrogenase periplasmic component	2.74	up	1.28E-05	
D11S_0209	periplasmic nitrate reductase, large subunit	4.92	up	7.68E-06	
D11S_0210	NapD protein	6.69	up	7.91E-07	
D11S_0270	regulatory protein RecX	2.32	up	9.40E-06	
D11S_0271	protein RecA	2.35	up	5.87E-05	
D11S_0281	transporter	2.41	up	1.11E-06	
D11S_0303	anaerobic C4-dicarboxylate membrane transporter	2.41	up	5.75E-05	
D11S_0310	fructose-1,6-bisphosphatase, class II	2.65	up	2.19E-06	
D11S_0383	alkylhydroperoxidase AhpD core	4.03	up	4.31E-06	5.9 ± 0.13
D11S_0493	anaerobic dimethyl sulfoxide reductase chain A	2.26	up	1.52E-04	
D11S_0494	anaerobic dimethyl sulfoxide reductase chain B	2.23	up	9.61E-06	
D11S_0551	ATP-dependent chaperone ClpB	2.03	up	1.37E-04	
D11S_0597	aspartate ammonia-lyase	6.86	up	7.29E-06	12.4 ± 0.16
D11S_0670	conserved ATP-binding protein	2.89	up	0.021983	
D11S_0810	fumarate reductase subunit C (Fumarate reductase	2.39	up	1.51E-05	3.35 ± 0.07

D11S_0811	fumarate reductase iron-sulfur subunit	2.39	up	2.15E-05	
D11S_0812	fumarate reductase flavoprotein subunit	3.86	up	4.10E-05	
D11S_0838	RecN protein	2.38	up	1.28E-06	
D11S_0887	cystathionine beta-lyase	2.28	up	1.56E-04	
D11S_0922	chaperone protein DnaK	2.1	up	0.001914	3.1 ± 0.1
D11S_0939	ImpA	2.41	up	4.03E-04	
D11S_1049	probable L-ascorbate-6-phosphate lactonase UlaG	2.1	up	8.44E-04	
D11S_1061	fumarate hydratase, class II	2.43	up	4.66E-06	4.18 ± 0.12
D11S_1092	hydrogenase accessory protein HypB	1.81	up	3.50E-05	
D11S_1093	hydrogenase expression/formation protein HypD	1.57	up	0.001163	
D11S_1135	protein YgiW	17.3	up	4.67E-07	13.4 ± 0.29
D11S_1136	protein QseB	4.63	up	4.22E-04	4.0 ± 0.21
D11S_1137	protein QseC	3.63	up	7.24E-04	3.4 ± 0.18
D11S_1269	fructosamine kinase	3.46	up	7.19E-07	
D11S_1299	hypothetical protein	2.6	up	5.83E-05	
D11S_1305	MacA macrolide exporter	2.15	up	0.006983	
D11S_1317	lipoprotein HlpB	2.48	up	3.43E-04	
D11S_1330	nonheme iron-containing ferritin	9.87	up	5.47E-05	
D11S_1331	ferritin	10.59	up	2.38E-04	5.5 ± 0.07
D11S_1343	AcrA protein	5.52	up	5.47E-05	
D11S_1344	CcmA protein	3.73	up	3.83E-04	
D11S_1345	ABC-type multidrug transport	3.21	up	0.019619	
D11S_1346	ABC-2 type transporter	4.77	up	0.005669	
D11S_1347	ToIC protein	2.5	up	8.83E-04	
D11S_1376	hydrogenase assembly chaperone HypC/HupF	1.88	up	6.28E-05	
D11S_1379	oxaloacetate decarboxylase gamma chain 3	4.74	up	3.30E-07	19.8 ± 0.72

D11S_1380	oxaloacetate decarboxylase alpha subunit	4.44	up	3.21E-07	
D11S_1381	oxaloacetate decarboxylase beta chain	4.31	up	2.69E-06	
D11S_1387	hypothetical protein	2.17	up	7.16E-04	
D11S_1399	dethiobiotin synthase	4.08	up	2.98E-07	
D11S_1412	cytochrome c-type protein TorY	7.68	up	6.78E-09	
D11S_1413	trimethylamine-n-oxide reductase 2	4.67	up	1.97E-07	
D11S_1431	cold shock domain protein CspD	2.1	up	0.005718	
D11S_1631	PqqL peptidase	2	up	0.028597	
D11S_1676	cytochrome c peroxidase	5.05	up	5.12E-07	
D11S_1735	[NiFe] hydrogenase maturation protein HypF	2.58	up	8.83E-04	3.6 ± 0.07
D11S_1736	electron transport protein HydN	18.44	up	5.00E-09	
D11S_1737	hydrogenase-4 component B	14.93	up	1.54E-08	
D11S_1738	hydrogenase-4 component B	15.02	up	1.42E-09	
D11S_1739	hydrogenase-4 component C	10.68	up	1.60E-07	
D11S_1740	hydrogenase-4 component D	10.59	up	3.57E-08	
D11S_1741	hydrogenase-4 component E	7.95	up	5.22E-07	
D11S_1742	hydrogenase-4 component F	7.76	up	4.85E-08	
D11S_1743	hydrogenase-4 component G	5.88	up	1.38E-07	
D11S_1744	hydrogenase-4 component H	5.87	up	3.07E-07	
D11S_1745	hydrogenase-4 component I	5.41	up	5.18E-07	
D11S_1746	hydrogenase-4 component J	4.62	up	8.70E-08	
D11S_1747	hydrogenase maturation peptidase Hycl	4.79	up	1.03E-06	
D11S_1748	formate dehydrogenase H	10.42	up	5.29E-09	
D11S_1749	formate dehydrogenase, alpha subunit	10.01	up	5.95E-08	3.83 ± 0.36
D11S_1763	peptidase T	6.62	up	9.97E-08	

D11S_1771	C4-dicarboxylate membrane transporter	1.73	up	1.02E-05	
D11S_1801	ribosomal protein L11 methyltransferase	2.24	up	2.89E-04	
D11S_1811	bifunctional acetaldehyde-CoA/alcohol dehydrogenase	2.72	up	1.04E-06	
D11S_1888	TorCAD operon transcriptional regulatory protein	1.86	up	1.62E-04	
D11S_1981	hypothetical protein	2.08	up	3.86E-04	
D11S_1983	thiol-disulfide interchange protein	3.19	up	1.08E-04	
D11S_1984	cytochrome c-type biogenesis protein CcmF	3.87	up	1.84E-05	8.59 ± 0.5
D11S_1986	NrfD protein	11.59	up	1.14E-07	2.1 ± 0.02
D11S_1987	cytochrome c nitrite reductase, Fe-S protein	13.63	up	4.20E-07	
D11S_1988	cytochrome c nitrite reductase, pentaheme	17.09	up	2.38E-09	
D11S_1989	nitrite reductase (cytochrome; ammonia-forming)	18.44	up	5.00E-09	
D11S_1992	TPR-repeat-containing protein	1.51	up	0.003085	
D11S_1993	cytochrome c-type biogenesis protein CcmH	1.57	up	0.001409	
D11S_1994	thiol-disulfide interchange protein	2.04	up	1.71E-05	
D11S_1995	cytochrome c-type biogenesis protein CcmF	2.39	up	5.05E-05	
D11S_1996	cytochrome c-type biogenesis protein CcmE	2.45	up	3.65E-06	
D11S_1997	Heme exporter protein D (CcmD)	2.66	up	5.69E-07	
D11S_1998	CcmC	3.16	up	7.34E-06	
D11S_1999	heme exporter protein CcmB	2.69	up	1.88E-06	
D11S_2000	heme ABC exporter, ATP-binding protein CcmA	3.31	up	1.80E-05	
D11S_2007	lipoprotein GNA1870	6.73	up	3.00E-07	
D11S_2125	putative long-chain-fatty-acid--CoA ligase-like	2.15	up	0.0183	
D11S_2128	anaerobic ribonucleoside-triphosphate reductase	2.7	up	5.42E-04	
D11S_2148	transporter protein	1.69	up	3.68E-04	

D11S_2165	hypothetical protein	1.87	up	0.007808
D11S_2171	hypothetical protein	1.63	up	0.01497
D11S_0016	YjjP	0.277	down	1.58E-06
D11S_0017	YjjB	0.195	down	1.42E-07
D11S_0018	hypothetical protein	0.332	down	8.55E-04
D11S_0046	multiphosphoryl transfer protein	0.498	down	5.13E-05
D11S_0052	LysR family transcriptional regulator	0.49	down	0.003419
D11S_0083	carbamate kinase	0.493	down	5.91E-04
D11S_0084	ornithine carbamoyltransferase	0.469	down	5.07E-04
D11S_0085	EriC protein	0.469	down	8.86E-05
D11S_0117	LapB	0.356	down	7.35E-04
D11S_0144	lipoprotein VacJ	0.495	down	0.005554
D11S_0152	Low affinity tryptophan permease	0.394	down	0.021582
D11S_0167	biofilm PGA synthesis lipoprotein PgaB	0.469	down	3.95E-06
D11S_0216	DNA transformation protein TfoX (Competence)	0.493	down	1.99E-05
D11S_0231	hypothetical protein	0.459	down	1.19E-04
D11S_0260	molybdopterin biosynthesis mog protein	0.418	down	0.004003
D11S_0283	anhydro-N-acetylmuramic acid kinase	0.413	down	0.005207
D11S_0284	N-acetylmuramic acid 6-phosphate etherase	0.411	down	4.20E-05
D11S_0292	sulfur relay protein TusB/DsrH	0.407	down	0.002779
D11S_0301	shikimate 5-dehydrogenase	0.208	down	4.22E-06
D11S_0302	CydD	0.375	down	1.56E-06
D11S_0341	Na ⁺ /H ⁺ antiporter NhaC	0.463	down	0.014605
D11S_0342	aminotransferase	0.469	down	0.001164

D11S_0343	monosaccharide-transporting ATPase	0.472	down	0.003003
D11S_0344	possible xylose ABC superfamily ATP binding	0.485	down	3.87E-05
D11S_0359	RfaL protein	0.422	down	1.15E-04
D11S_0360	CrcB protein	0.373	down	3.08E-04
D11S_0397	RNA methyltransferase, TrmH family, group 3	0.465	down	2.63E-06
D11S_0415	excinuclease ABC subunit B	0.357	down	0.00117
D11S_0487	TonB-system energizer ExbB	0.208	down	1.30E-05
D11S_0488	TonB system transport protein ExbD	0.223	down	4.29E-06
D11S_0489	protein TonB	0.229	down	6.56E-06
D11S_0621	iron(III)-transport system permease protein FbpB	0.182	down	1.94E-05
D11S_0622	ferric iron binding protein	0.195	down	1.30E-07
D11S_0664	CpxA two component sensor	0.442	down	0.003331
D11S_0671	O-methyltransferase N-terminus family protein	0.341	down	0.001208
D11S_0694	adenylate cyclase, class I	0.426	down	1.43E-04
D11S_0785	cell division protein FtsW	0.422	down	0.007201
D11S_0815	iron(III) dicitrate transport ATP-binding	0.123	down	2.42E-05
D11S_0816	ABC transporter, iron chelate uptake transporter	0.108	down	1.72E-04
D11S_0817	iron(III) dicitrate transport system permease	0.166	down	6.78E-06
D11S_0818	iron(III) dicitrate-binding periplasmic protein	0.157	down	1.05E-06
D11S_0858	citrate lyase, alpha subunit	0.498	down	2.92E-04
D11S_0859	citrate lyase beta chain	0.375	down	0.009593
D11S_0860	citrate lyase acyl carrier protein	0.448	down	0.001633
D11S_0861	[citrate (pro-3S)-lyase] ligase	0.474	down	3.56E-05
D11S_0867	peptidase B (Aminopeptidase B)	0.167	down	2.69E-05
D11S_0868	nucleoside diphosphate kinase	0.325	down	1.15E-05
D11S_0869	Chb protein	0.202	down	7.10E-04

D11S_0873	FeS assembly protein IscX	0.284	down	6.02E-07	
D11S_0874	ferredoxin, 2Fe-2S type, ISC system	0.282	down	2.33E-05	
D11S_0875	Fe-S protein assembly chaperone HscA	0.325	down	2.88E-06	
D11S_0876	Fe-S protein assembly co-chaperone HscB	0.326	down	3.42E-05	
D11S_0877	iron-sulfur cluster assembly protein IscA	0.345	down	1.45E-05	0.59 ± 0.02
D11S_0878	FeS cluster assembly scaffold IscU	0.417	down	7.31E-05	
D11S_0879	cysteine desulfurase IscS	0.444	down	1.03E-04	
D11S_0890	sugar efflux transporter	0.481	down	0.003058	
D11S_0902	relaxase	0.448	down	8.83E-04	
D11S_0916	CDP-diacylglycerol--glycerol-3-phosphate	0.5	down	5.96E-04	
D11S_0930	NlpC cell wall peptidase	0.378	down	4.21E-04	
D11S_0977	hypothetical protein	0.216	down	9.38E-04	
D11S_0993	thiamine-monophosphate kinase	0.5	down	0.001987	
D11S_0994	phosphatidylglycerophosphatase A	0.448	down	0.006652	
D11S_0995	threonine efflux protein	0.449	down	1.64E-04	
D11S_0999	hypothetical protein	0.425	down	0.01952	
D11S_1067	hypothetical protein	0.268	down	9.22E-04	
D11S_1097	5,10-methylenetetrahydrofolate reductase	0.5	down	4.21E-04	
D11S_1125	high-affinity zinc uptake system membrane	0.37	down	0.001867	
D11S_1128	iron(III) dicitrate transport ATP-binding	0.215	down	3.94E-05	
D11S_1129	iron(III) transport system permease protein	0.331	down	0.001976	
D11S_1130	putative iron/heme permease	0.23	down	4.24E-04	
D11S_1131	putative periplasmic siderophore binding protein	0.143	down	5.47E-05	
D11S_1147	CRISPR-associated helicase Cas3	0.418	down	0.027601	
D11S_1179	tRNA(Ile)-lysidine synthase	0.398	down	0.002894	
D11S_1219	3-deoxy-D-manno-octulosonate	0.5	down	0.002824	

D11S_1226	hypothetical protein	0.332	down	3.75E-04
D11S_1227	phosphate acetyltransferase	0.417	down	0.003227
D11S_1235	tellurite resistance protein TehB	0.439	down	0.010619
D11S_1238	dihydrolipoyl dehydrogenase	0.465	down	2.09E-04
D11S_1265	Ndh NADH dehydrogenase	0.379	down	2.17E-04
D11S_1322	chromosome partition protein MukE (Protein	0.402	down	0.002735
D11S_1324	cell division protein MukB	0.412	down	0.005851
D11S_1325	exodeoxyribonuclease I	0.446	down	2.55E-04
D11S_1332	hypothetical protein	0.486	down	0.00174
D11S_1334	UspA universal stress protein	0.476	down	7.38E-04
D11S_1360	DoxX family protein	0.405	down	4.67E-04
D11S_1370	anthranilate synthase component I	0.436	down	0.017378
D11S_1457	ATP-dependent DNA helicase RecG	0.417	down	4.29E-04
D11S_1519	RhaT permease	0.385	down	0.026275
D11S_1557	high-affinity Fe ²⁺ /Pb ²⁺ permease	0.245	down	3.03E-04
D11S_1558	high affinity Fe ²⁺ transporter	0.122	down	1.28E-05
D11S_1559	putative Fe ²⁺ permease	0.138	down	4.81E-05
D11S_1560	FtsX-like permease	0.156	down	3.33E-04
D11S_1561	membrane permease component	0.165	down	2.62E-05
D11S_1562	macrolide export ATP-binding/permease protein	0.069	down	0.001665
D11S_1563	ResA	0.183	down	4.38E-04
D11S_1564	cytochrome c-553	0.157	down	3.79E-05
D11S_1601	hypothetical protein	0.443	down	5.93E-04
D11S_1602	putative translation initiation inhibitor, YjgF	0.357	down	1.23E-04
D11S_1604	hypothetical protein	0.515	down	1.73E-05
D11S_1630	putative TonB-dependent iron receptor	0.48	down	0.008308
D11S_1635	MetR	0.365	down	0.002098

D11S_1636	5-methyltetrahydropteroyltriglutamate--	0.5	down	0.001143
D11S_1643	AfeC periplasmic iron binding protein	0.403	down	8.22E-04
D11S_1644	acyl phosphatase	0.404	down	8.62E-05
D11S_1652	protein-(glutamine-N5) methyltransferase,	0.481	down	0.003915
D11S_1668	lipid A biosynthesis lauroyl acyltransferase	0.362	down	0.003732
D11S_1685	cysteine/glutathione ABC transporter	0.435	down	8.63E-04
D11S_1686	ABC transporter, CydDC cysteine exporter	0.41	down	0.002955
D11S_1694	hypothetical protein	0.213	down	3.94E-05
D11S_1729	formate dehydrogenase, alpha subunit	0.287	down	0.001835
D11S_1730	formate dehydrogenase, alpha subunit	0.467	down	0.001382
D11S_1731	formate dehydrogenase, alpha subunit	0.524	down	0.007025
D11S_1769	Hypothetical protein	0.413	down	0.01957
D11S_1792	histidinol-phosphate aminotransferase	0.319	down	0.004321
D11S_1793	3-phosphoshikimate 1-carboxyvinyltransferase	0.355	down	8.83E-04
D11S_1800	cupin 2, conserved barrel	0.459	down	0.002002
D11S_1809	heme acquisition system receptor	0.463	down	1.04E-04
D11S_1819	LtxA	0.482	down	0.020787
D11s_1820	LtxC	0.48	down	3.43E-04
D11S_1827	ribosomal-protein-alanine acetyltransferase	0.472	down	1.05E-04
D11S_1843	cytochrome D ubiquinol oxidase, subunit II	0.341	down	8.53E-05
D11S_1844	cytochrome D ubiquinol oxidase subunit 1	0.4	down	6.65E-04
D11S_1864	outer membrane protein 64	0.106	down	2.40E-05
D11S_1954	23S rRNA (uracil-5-)-methyltransferase RumB	0.5	down	0.001068
D11S_1973	DNA polymerase III, beta subunit	0.48	down	1.38E-04
D11S_1974	DNA replication and repair protein RecF	0.455	down	0.004321

D11S_1975	methyltransferase domain family	0.305	down	2.48E-04
D11S_2018	menaquinone-specific isochorismate synthase	0.457	down	0.01013
D11S_2029	hypothetical protein	0.471	down	0.004366
D11S_2050	type I modification enzyme	0.442	down	5.17E-06
D11S_2052	YaeB	0.5	down	4.17E-04
D11S_2056	conserved transporter, NadC family	0.271	down	5.47E-05
D11S_2060	glycerate kinase	0.461	down	7.80E-04
D11S_2061	transporter, gluconate:H ⁺ symporter	0.426	down	6.44E-04
D11S_2118	glycosyltransferase sugar-binding region	0.424	down	0.005345
D11S_2154	fatty acid/phospholipid synthesis protein PlsX	0.429	down	2.01E-04

Appendix Table 2: Genes Differentially Regulated in Δ qseB

ID Tag	Product	Fold Change	Direction
D11S_0016	YjjP	3.07	up
D11S_0136	Putative transposase	2.95	up
D11S_0146	heat shock protein HslVU, ATPase subunit HslU	8.24	up
D11S_0147	ATP-dependent protease peptidase subunit	8.15	up
D11S_0171	regulatory protein UhpC	2.29	up
D11S_0204	bifunctional glutathionylspermidine	2.71	up
D11S_0278	transposase	2.88	up
D11S_0279	deoxyribose-phosphate aldolase	2.53	up
D11S_0281	transporter	2.22	up
D11S_0297	hypothetical	2.04	up
D11S_0298	hybrid peroxiredoxin hyPrx5 (Thioredoxin	2.58	up
D11S_0310	fructose-1,6-bisphosphatase, class II	2.43	up
D11S_0361	protein cof	2.16	up
D11S_0420	methyltransferase domain family	2.06	up
D11S_0460	hypothetical	2.23	up
D11S_0461	preprotein translocase subunit SecA	2.15	up
D11S_0480	MerR family transcriptional regulator	2.28	up
D11S_0551	ATP-dependent chaperone ClpB	14.5	up
D11S_0578	hypothetical	2.33	up
D11S_0599	chaperonin GroS	5.36	up
D11S_0600	chaperonin GroEL	7.15	up
D11S_0651	transcriptional repressor protein MetJ	2.03	up

D11S_0656	universal stress protein A	2.17	up
D11S_0687	putative outer membrane protein	2.04	up
D11S_0689	phosphoenolpyruvate carboxykinase	2.49	up
D11S_0738	MclA	4.8	up
D11S_0739	RNA polymerase sigma factor RpoE	4.3	up
D11S_0795	heat shock protein 90	11.32	up
D11S_0812	fumarate reductase	2.14	up
D11S_0824	preprotein translocase subunit SecG	2.15	up
D11S_0840	hypothetical	3.47	up
D11S_0841	heat shock protein GrpE	6.96	up
D11S_0843	5-methylaminomethyl-2-thiouridine methyltransferase	2.28	up

142

D11S_0893	curved DNA-binding protein	3.48	up
D11S_0894	MerR family regulatory protein	2.9	up
D11S_0922	molecular chaperone DnaK	8.91	up
D11S_1049	putative L-ascorbate 6-phosphate lactonase	4.03	up
D11S_1050	transcriptional repressor UlaR	2.45	up
D11S_1051	putative L-xylulose 5-phosphate 3-epimerase	2.01	up
D11S_1061	fumarate hydratase	2.12	up
D11S_1070	HTH-type transcriptional regulator HipB	2.27	up
D11S_1087	putative periplasmic binding protein CbiK	2.2	up
D11S_1104	ModE	2.14	up
D11S_1114	malate dehydrogenase	2.21	up
D11S_1132	bifunctional 2',3'-cyclic nucleotide 2'-phosphodiesterase/3'-nucleotidase periplasmic protein	2.12	up
D11S_1162	protein YegP	4.36	up

D11S_1163	PTS system maltose and glucose-specific transporter subunit IIBC	2.53	up
D11S_1192	putative integrase	2.4	up
D11S_1269	fructosamine kinase	2.18	up
D11S_1331	ferritin	2.52	up
D11S_1387	tryptophan synthase subunit alpha	2.61	up
D11S_1412	cytochrome c-type protein TorY	2.14	up
D11S_1414	MmcQ protein	2.03	up
D11S_1415	CitT protein	2.5	up
D11S_1443	MsmK	2.15	up
D11S_1444	ATP-dependent metalloproteinase HflB	3.1	up
D11S_1445	ribosomal RNA large subunit methyltransferase J	3.37	up
D11S_1447	H-NS histone family	2.82	up
D11S_1480	DNA mismatch repair protein	2.16	up
D11S_1522	ATP-dependent protease La	4.51	up
D11S_1662	hypothetical	2.23	up
D11S_1674	hypothetical	3.12	up
D11S_1676	cytochrome c peroxidase	4.57	up
D11S_1735	hydrogenase maturation protein HypF	2.11	up
D11S_1763	peptidase T	3.94	up
D11S_1770	seryl-tRNA synthetase	2.16	up
D11S_1771	C4-dicarboxylate membrane transporter	2.15	up
D11S_1789	hypothetical	2.04	up
D11S_1798	Stability protein StbD	2.41	up
D11S_1799	putative relE protein	2.13	up
D11S_1800	cupin 2	3.08	up
D11S_1801	hypothetical (? ribosomal protein L11 methyltransferase?)	2.27	up

D11S_1822	lipoprotein	2.32	up
D11S_1870	hypothetical	2.19	up
D11S_1888	TorCAD operon transcriptional regulatory protein	3.43	up
D11S_1911	fructose-1,6-bisphosphatase	2.81	up
D11S_1949	formate acetyltransferase	2.47	up
D11S_1989	nitrite reductase (cytochrome; ammonia-forming)	2.18	up
D11S_2007	lipoprotein	3.28	up
D11S_2022	S-adenosylmethionine synthetase	2.67	up
D11S_2024	serine transporter	2.12	up
D11S_2047	copper-translocating P-type ATPase	2.36	up
D11S_2067	EbgC protein	2.35	up
D11S_2078	sigma 54 modulation protein/ribosomal protein S30EA	3.49	up
D11S_2165	hypothetical	3.39	up
D11S_2175	hypothetical	2.58	up
D11S_2183	I protein	2.71	up
D11S_2184	Mu-like phage G protein 1	2.74	up
D11S_2185	f protein	3.47	up
D11S_0039	DNA Polymerase I	0.327	down
D11S_0040	tRNA (uracil-5-)-methyltransferase	0.435	down
D11S_0046	multiphosphoryl transfer protein	0.278	down
D11S_0047	1-phosphofructokinase	0.354	down
D11S_0060	hypothetical	0.381	down
D11S_0064	DNA-directed RNA polymerase, beta subunit	0.477	down
D11S_0101	Trk system potassium uptake protein TrkA	0.428	down
D11S_0156	tryptophanyl-tRNA synthetase	0.436	down

D11S_0167	biofilm PGA synthesis lipoprotein PgaB	0.404	down
D11S_0180	PnuC transporter	0.478	down
D11S_0192	ATP-dependent DNA helicase Rep	0.344	down
D11S_0250	UDP-3-O-[3-hydroxymyristoyl] glucosamine	0.495	down
D11s_0283	anhydro-N-acetylmuramic acid kinase	0.406	down
D11S_0284	N-acetylmuramic acid 6-phosphate etherase	0.396	down
D11S_0292	sulfur relay protein TusB/DsrH	0.332	down
D11S_0293	sulfur relay protein TusC/DsrF	0.452	down
D11S_0306	glycerol-3-phosphate dehydrogenase (NAD(P)+)	0.402	down
D11S_0323	FOF1 ATP synthase subunit gamma	0.466	down
D11S_0324	FOF1 ATP synthase subunit beta	0.463	down
D11S_0325	ATP synthase F1, epsilon subunit	0.48	down

145

D11S_0370	2-C-methyl-D-erythritol 4-phosphate	0.355	down
D11S_0372	tRNA pseudouridine synthase D	0.366	down
D11S_0415	excinuclease ABC subunit B	0.247	down
D11S_0422	acriflavine resistance protein	0.338	down
D11S_0423	AcrA protein	0.296	down
D11S_0424	AcrR protein	0.254	down
D11S_0434	formamidopyrimidine-DNA glycosylase	0.294	down
D11S_0444	cAMP-regulatory protein	0.494	down
D11S_0455	DNA adenine methylase	0.45	down
D11S_0520	aspartate racemase	0.452	down
D11S_0530	hypothetical	0.362	down
D11S_0531	outer membrane lipoprotein carrier protein LolA	0.485	down
D11S_0532	thioesterase	0.381	down

D11S_0533	glycosyl transferase, family 2	0.25	down
D11S_0534	glycosyl transferase, group 2 family protein	0.242	down
D11S_0535	AMP-binding enzyme family protein	0.286	down
D11S_0536	integral membrane protein	0.402	down
D11S_0588	drug/metabolite exporter family transporter	0.376	down
D11S_0589	drug/metabolite exporter family transporter	0.358	down
D11S_0594	hypothetical	0.487	down
D11S_0607	diacylglycerol kinase	0.433	down
D11S_0608	GTP pyrophosphokinase	0.492	down
D11S_0609	23S rRNA 5-methyluridine methyltransferase	0.121	down
D11S_0619	tRNA-dihydrouridine synthase C	0.358	down
D11S_0623	hypothetical	0.5	down
D11S_0652	UTP-glucose-1-phosphate uridylyltransferase	0.329	down
D11S_0751	hypothetical	0.314	down
D11S_0815	iron-dicitrate transporter ATP-binding subunit	0.177	down
D11S_0816	subunit FecD	0.229	down
D11S_0817	iron-dicitrate transporter permease subunit	0.267	down
D11S_0822	DNA topoisomerase III	0.487	down
D11S_0823	hypothetical	0.418	down
D11S_0831	intracellular septation protein A	0.41	down
D11S_0856	inner membrane protein Ybhl	0.248	down
D11S_0857	citrate lyase subunit alpha	0.257	down
D11S_0858	citrate lyase subunit beta	0.259	down
D11S_0859	gamma	0.176	down
D11S_0891	sugar efflux transporter	0.478	down
D11S_0909	cytolethal distending toxin protein B	0.458	down

D11S_0910	cytolethal distending toxin protein C	0.462	down
D11S_0916	CDP-diacylglycerol--glycerol-3-phosphate 3-phosphatidyltransferase	0.35	down
D11S_0928	protein-(glutamine-N5) methyltransferase	0.386	down
D11S_0951	dipeptide transport system permease DppC	0.442	down
D11S_0960	tRNA delta(2)-isopentenylpyrophosphate transferase	0.478	down
D11S_0964	hypothetical	0.433	down
D11S_0965	hypothetical	0.202	down
D11S_0966	glycosyl transferase, family 2	0.215	down
D11S_0967	putative inner membrane protein	0.197	down
D11S_0968	integral membrane protein	0.13	down
D11S_0985	outer membrane-specific lipoprotein transporter subunit LolE	0.447	down
D11S_0993	thiamine-monophosphate kinase	0.408	down

D11S_0994	phosphatidylglycerophosphatase A	0.341	down
D11S_0995	threonine efflux protein	0.335	down
D11S_1039	sulfate/thiosulfate import ATP-binding protein CysA	0.397	down
D11S_1066	valyl-tRNA synthetase	0.465	down
D11S_1067	hypothetical	0.227	down
D11s_1075	exoribonuclease II	0.418	down
D11S_1096	shikimate 5-dehydrogenase	0.412	down
D11S_1123	endonuclease III	0.486	down
D11S_1128	iron(III) dicitrate transport ATP-binding protein FecE	0.315	down
D11S_1136	QseB	0.059	down
D11S_1179	tRNA(Ile)-lysidine synthase	0.473	down
D11S_1191	putative tail fiber assembly protein	0.465	down
D11S_1210	putative DNA repair ATPase	0.462	down
D11S_1218	excinuclease ABC subunit C	0.411	down

D11S_1219	3-deoxy-manno-octulosonate cytidyltransferase	0.38	down
D11S_1220	hypothetical	0.447	down
D11S_1221	tetraacyldisaccharide 4'-kinase	0.378	down
D11S_1225	poly A polymerase	0.362	down
D11S_1227	phosphate acetyltransferase	0.219	down
D11S_1232	4-alpha-glucanotransferase	0.054	down
D11S_1261	hypothetical	0.493	down
D11S_1304	ABC transporter-like protein	0.393	down
D11S_1307	hypothetical	0.376	down
D11S_1324	cell division protein MukB	0.332	down
D11s_1338	dihydroorotate dehydrogenase 2	0.337	down
D11S_1353	TonB dependent outer membrane siderophore receptor protein	0.471	down
D11S_1389	ribonucleoside-diphosphate reductase subunit beta	0.421	down
D11S_1419	tRNA pseudouridine synthase A	0.303	down
D11S_1423	tellurite resistance protein TehB	0.372	down
D11S_1424	exodeoxyribonuclease V subunit alpha	0.31	down
D11S_1437	two component Fis family transcriptional regulator	0.376	down
D11S_1455	glutamate racemase	0.442	down
D11S_1456	chorismate--pyruvate lyase	0.376	down
D11S_1457	ATP-dependent DNA helicase RecG	0.492	down
D11S_1479	UDP-N-acetylglucosamine 1-carboxyvinyltransferase	0.46	down
D11S_1500	threonine synthase	0.387	down
D11S_1501	putative 4'-phosphopantetheinyl transferase	0.277	down
D11S_1524	DNA primase	0.496	down
D11S_1530	NAD-dependent DNA ligase LigA	0.398	down
D11S_1568	putative inner membrane protein	0.366	down

D11S_1574	FAD linked oxidase	0.398	down
D11S_1575	esterase Ydil	0.288	down
D11S_1598	DNA topoisomerase IV subunit A	0.335	down
D11S_1606	hypothetical	0.389	down
D11S_1607	DNA polymerase III subunit tau	0.342	down
D11S_1608	hypothetical	0.454	down
D11S_1611	inner membrane protein YfcA	0.497	down
D11S_1640	sulfurtransferase TusE	0.398	down
D11S_1653	transketolase, central region	0.363	down
D11S_1654	transketolase, N- subunit	0.36	down
D11S_1664	protein ParB	0.624	down
D11S_1686	cysteine/glutathione ABC transporter membrane/ATP-binding protein	0.395	down
D11S_1700	hypothetical	0.451	down
D11S_1701	glycosyltransferase	0.273	down
D11S_1702	exopolysaccharide production protein EXOZ	0.479	down
D11S_1704	lipopolysaccharide biosynthesis protein	0.417	down
D11S_1709	hypothetical	0.427	down
D11S_1749	formate dehydrogenase subunit alpha	0.44	down
D11S_1758	periplasmic protein	0.455	down
D11S_1780	SH3 domain-containing protein	0.339	down
D11S_1781	multifunctional tRNA nucleotidyl transferase/2'3'-cyclic phosphodiesterase/2'nucleotidase/phosphatase	0.257	down
D11S_1782	outer membrane lipoprotein LolB	0.26	down
D11S_1783	4-diphosphocytidyl-2-C-methyl-D-erythritol kinase	0.231	down
D11S_1809	heme acquisition system receptor	0.387	down
D11S_1860	putative transposase	0.491	down

D11S_1862	hypothetical	0.448	down
D11S_1915	ThiF family protein	0.465	down
D11S_1954	23S rRNA (uracil-5-)-methyltransferase RumB	0.492	down
D11S_1955	23S rRNA methyluridine methyltransferase	0.272	down
D11S_1969	ribonuclease P protein component	0.5	down
D11S_1981	hypothetical	0.431	down
D11S_1982	thiol-disulfide interchange protein	0.498	down
D11S_1983	cytochrome c-type biogenesis protein CcmF	0.443	down
D11S_1992	TPR-repeat-containing protein	0.497	down
D11S_2020	acyl-CoA thioester hydrolase YfbB	0.339	down
D11S_2030	4-hydroxy-3-methylbut-2-en-1-yl diphosphate synthase	0.372	down

150

D11S_2031	histidyl-tRNA synthetase	0.331	down
D11S_2072	PilC	0.44	down
D11S_2082	ribosomal protein L11 methyltransferase	0.459	down
D11S_2083	sodium/panthothenate symporter	0.366	down
D11S_2084	sodium/panthothenate symporter	0.402	down
D11S_2085	acetyl-CoA carboxylase biotin carboxylase subunit	0.448	down
D11S_2086	chromosomal replication initiation protein	0.409	down
D11S_2093	O-succinylbenzoate synthase	0.411	down
D11S_2094	DNA polymerase, beta domain-containing protein	0.468	down
D11S_2102	tRNA-specific adenosine deaminase	0.402	down
D11S_2112	cold-shock DNA-binding domain-containing protein	0.475	down
D11S_2131	anaerobic ribonucleotide reductase-activating protein	0.463	down
D11S_2147	transcription termination factor Rho	0.368	down
D11S_2154	putative glycerol-3-phosphate acyltransferase PlsX	0.469	down

CURRICULUM VITAE

Whitney Weigel
whitney.weigel@gmail.com
Microbiology & Immunology
University of Louisville
501 S. Preston
(502) 852-3806

Education

Ph. D., Microbiology & Immunology, University of Louisville Louisville, Ky Field of Research: Functional characterization of the <i>A. actinomycetemcomitans</i> QseBC: a bacterial adrenergic receptor and global regulator of virulence	2011-2015
M.S., Microbiology & Immunology, University of Louisville Louisville, Ky	2010-2012
B.A., History, Centre College, Danville, Ky	2004-2008

Educational/Teaching Experience

Microbiology & Immunology Student Organization (MISO) Student Mentor 2011-2012 University of Louisville, Department of Microbiology & Immunology	
Research Technician, University of Louisville Louisville, Ky, (for Dr. Maragaret Carreiro, Department of Biology Professor)	2011
Volunteer, University of Louisville Louisville, Ky, (for Micah Worley, Department of Biology Professor)	2010-2011
Assistant Language Teacher, JET Programme Oshima, Japan	2008-2010
Chemistry Lab Assistant, Centre College Danville, Ky	2005-2006

Awards and Grants

Graduated Summa cum Laude from Centre College (2008)
Graduate Student Council Research Grant (2014)
President of MISO (2014-2015)
Finalist for Research! Louisville poster competition (2014)
1st Place Microbiology Oral Presentation Kentucky Academy of Science (2014)
Graduate Student Council Travel Grant (2015)

Presentations/Invited Talks

University of Louisville Graduate Student Research Symposium, 2014, QseBC Mediates *Aggregatibacter actinomycetemcomitans*'s Stress Response

Research! Louisville, 2014, Catecholamine Mediated Acquisition of Iron in *Aggregatibacter actinomycetemcomitans*

Kentucky Academy of Science, 2014, Catecholamines Induce Anaerobic Respiration and Oxidative Stress Genes in *Aggregatibacter actinomycetemcomitans*

International Association of Dental Research, 2015, Catecholamine Mediated Activation of QseBC Induces Genes Involved in Anaerobic Respiration in *Aggregatibacter actinomycetemcomitans*

Helmholtz Center for Infectious Disease, 2015, QseBC: A Bacterial Adrenergic Receptor in *A. actinomycetemcomitans*

Publications

Weigel WA, Demuth DR, Torres-Escobar A, Juarez-Rodriguez MD, A. *actinomycetemcomitans* QseBC is activated by catecholamines and iron and regulates genes encoding proteins associated with anaerobic respiration and metabolism. Mol. Oral Microbiol. 2015

QseBC: a Global Regulator of Virulence in the *Enterobacteriaceae* and *Pasteurellaceae*. Mol. Oral Microbiol. 2015

Catecholamines and Iron Result in Metabolic Changes and the Increase in Biofilm formation in *A. actinomycetemcomitans* (First Author, In preparation)

A RelE like Toxin/Anti-toxin System Regulates Expression of *qseBC* in *Aggregatibacter actinomycetemcomitans* (First Author, In Preparation)

A Putative TonB Dependent Receptor is Essential for Catecholamine and Iron Mediated Changes in Growth in *Aggregatibacter actinomycetemcomitans* (First Author, In preparation)

Mentorship

Hazel Ozuna, M.S. (Microbiology & Immunology Ph.D. candidate) 2014-2015
Project: Characterizing the Interaction between Neutrophils and *Aggregatibacter actinomycetemcomitans*

Taylor Johnston, B.S., (Oral Biology Masters student) 2014-2015
Project: Determining the Role of the Putative Enterobactin Operon on Catecholamine Mediated Iron Acquisition